WAVE MODELS FOR THE FLEXURAL VIBRATIONS OF THIN PLATES

—

Image source method for polygonal plates
&
Vibration damping using the acoustic black hole effect

Jacques Cuenca

supervised by Prof. **François Gautier** and Prof. **Laurent Simon**

Laboratoire d'Acoustique de l'Université du Maine – UMR CNRS 6613

Le Mans, France, 20th October 2009

Introduction: Why flexural vibrations?

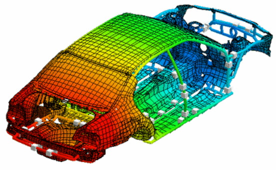

Flexural vibrations:

- arise in **thin structures** (plates, shells)
- are frequent in aerospatial, aeronautical, automotive, rail vehicles, ...
- are related to **radiated noise** and **structural damage**

Amongst the major concerns:

- Accurate and reliable models and methods for vibration analysis
- Efficient vibration damping

Introduction: Models and methods

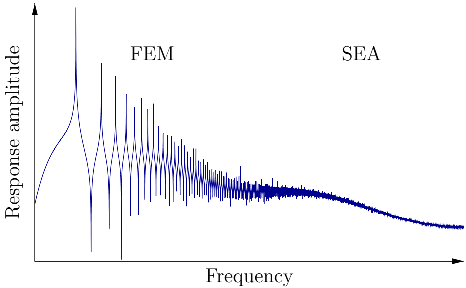

- Analytical modal expansion or other analytical methods
  difficult to generalise to arbitrary geometries and boundary condition sets
- Finite element method (FEM)
  Adapted to **low frequencies** (spatial discretisation)
- Statistical energy analysis (SEA)
  Adapted to **high frequencies** (assumption of high modal overlap)
- New methods show the evolution of needs
  Hybrid FEM-SEA, Wave-FEM, Wave-based methods, Variational theory of complex rays, . . .

$\Rightarrow$ **Contribute to the development of different approaches**

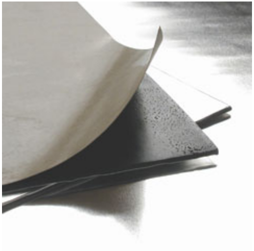

- Vibration damping: necessary for **preventing radiated noise and structural damage**
- Vibration damping often requires large amounts of mass
- Weight reduction ⇒ **reduction of fuel consumption**

⇒ **Develop alternative solutions**

1. Model of the flexural vibrations of polygonal plates by the image source method
   - Introduction
   - Generalisation to arbitrary convex polygonal geometry
   - General boundary conditions
   - Polygonal plates
   - Plate assemblies

2. Acoustic black hole effect for vibration damping in plates and beams
   - Principle
   - Model
   - Experiments
   - Black-hole effect by a thermal gradient

Introduction: Green's function of a polygonal plate

Problem to solve

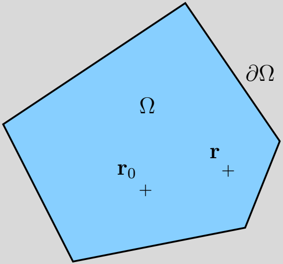

$$\begin{cases} D\left(\nabla^4 - k_f^4\right) G_\Omega(\mathbf{r}, \mathbf{r}_0) = \delta(\mathbf{r} - \mathbf{r}_0) \\ \text{Boundary conditions} \end{cases}$$

Idea

Polygonal thin structures = elementary component of a complex structure

Context

- Arbitrary polygonal shape
- Arbitrary boundary conditions
- Mid- and high-frequency vibrations

Parameters

- Harmonic excitation at $\mathbf{r}_0$ ($\sim e^{-j\omega t}$)
- ω: circular frequency
- $D = \dfrac{Eh^3}{12\left(1 - \nu^2\right)}$ Flexural rigidity
- $k_f = \left(\omega \dfrac{\rho h}{D}\right)^{1/4}$ flexural wavenumber
- $E = E_0(1 - j\eta)$ complex Young's modulus
- η: structural damping ratio

Introduction: Green's function of a polygonal plate

Problem to solve

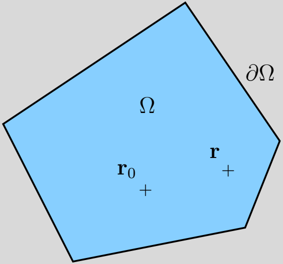

$$\begin{cases} D\left(\nabla^4 - k_f^4\right) G_\Omega(\mathbf{r}, \mathbf{r}_0) = \delta(\mathbf{r} - \mathbf{r}_0) \\ \text{Boundary conditions} \end{cases}$$

Integral formulation

$$G_\Omega(\mathbf{r}, \mathbf{r}_0) =$$

$$G_\infty(\mathbf{r}, \mathbf{r}_0) \qquad \textbf{source}$$

$$+ \sum_{n=1}^{N_v} \int_{v_n}^{v_{n+1}} \Big(G_\infty V_n^{(\Omega)} - G_\Omega V_n^{(\infty)} + \theta_n^{(\infty)} M_n^{(\Omega)} - \theta_n^{(\Omega)} M_n^{(\infty)} \Big)\, d\mathbf{r} \qquad \textbf{edges}$$

$$+ \sum_{n=1}^{N_v} \left[G_\Omega M_{ln}^{(\infty)} \right]_{v_n}^{v_{n+1}} \qquad \textbf{corners}$$

- Pertinent for arbitrary geometries $G_\Omega = G_{\text{source}} + G_{\text{boundaries}}$
- Boundary Element Method presents limitations in high frequencies

Introduction: Green's function of a polygonal plate

Problem to solve

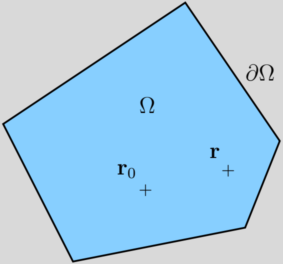

$$\begin{cases} D\left(\nabla^4 - k_f^4\right) G_\Omega(\mathbf{r}, \mathbf{r}_0) = \delta(\mathbf{r} - \mathbf{r}_0) \\ \text{Boundary conditions} \end{cases}$$

$\Rightarrow$

Image source solution

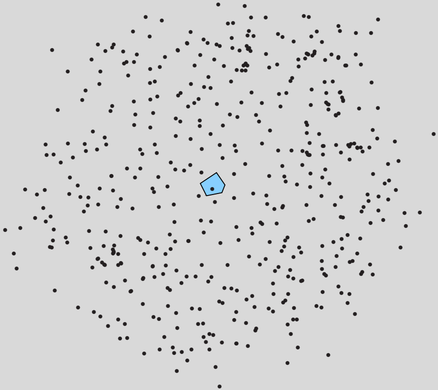

$$G_\Omega(\mathbf{r}, \mathbf{r}_0) = \sum_{s=0}^{\infty} G_s(\mathbf{r}, \mathbf{r}_s)$$

Find the image source contributions $G_s(\mathbf{r}, \mathbf{r}_s)$

Introduction: Previous work on the image source method

Room acoustics

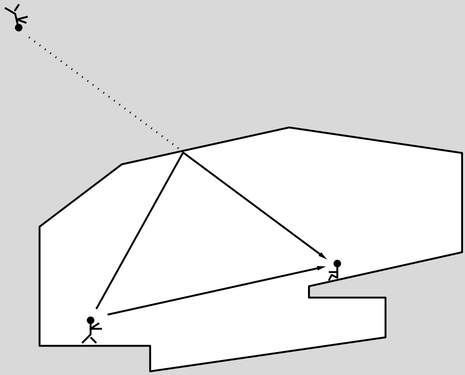

Introduction: Previous work on the image source method

Room acoustics

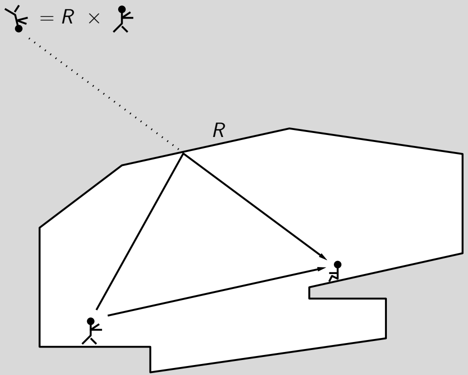

Introduction: Previous work on the image source method

Room acoustics

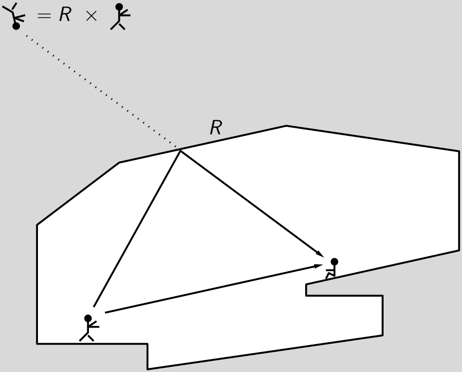

Flexural plate vibration

- Applied to simply supported and roller supported **rectangular plates** ($R=-1$ and $R=1$)
- **Accuracy is improved with frequency and damping**

Gunda et al., J. Sound Vib. 185 (1995)

Introduction: Previous work on the image source method

Room acoustics

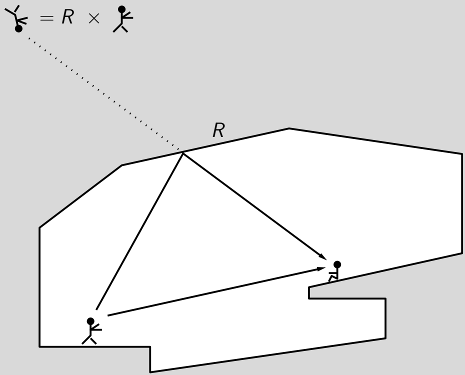

Flexural plate vibration

- Applied to simply supported and roller supported **rectangular plates** ($R = -1$ and $R = 1$)
- **Accuracy is improved with frequency and damping**

Gunda et al., J. Sound Vib. 185 (1995)

What needs to be done?

- Generalise to arbitrary geometries
- Generalise to arbitrary boundary conditions
- Apply to plate assemblies

1. Model of the flexural vibrations of polygonal plates by the image source method
   - Introduction
   - Generalisation to arbitrary convex polygonal geometry
   - General boundary conditions
   - Polygonal plates
   - Plate assemblies

2. Acoustic black hole effect for vibration damping in plates and beams
   - Principle
   - Model
   - Experiments
   - Black-hole effect by a thermal gradient

Generalisation to arbitrary convex polygonal geometry: Problem to solve

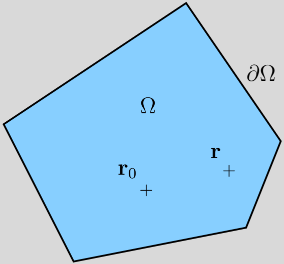

Example: Simply supported plate

$$\begin{cases} D\left(\nabla^4 - k_f^4\right) G_\Omega(\mathbf{r}, \mathbf{r}_0) = \delta(\mathbf{r} - \mathbf{r}_0) \\ G_\Omega(\mathbf{r}, \mathbf{r}_0) = 0 \\ \dfrac{\partial^2 G_\Omega}{\partial n^2}(\mathbf{r}, \mathbf{r}_0) + \nu \dfrac{\partial^2 G_\Omega}{\partial \tau^2}(\mathbf{r}, \mathbf{r}_0) = 0 \end{cases}$$

Reflection coefficient: $R = -1$

Generalisation to arbitrary convex polygonal geometry: Problem to solve

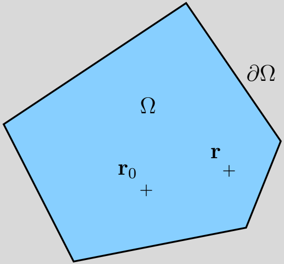

Example: Simply supported plate

$$\begin{cases} D\left(\nabla^4 - k_f^4\right) G_\Omega(\mathbf{r},\mathbf{r}_0) = \delta(\mathbf{r}-\mathbf{r}_0) \\ G_\Omega(\mathbf{r},\mathbf{r}_0) = 0 \\ \dfrac{\partial^2 G_\Omega}{\partial n^2}(\mathbf{r},\mathbf{r}_0) + \nu \dfrac{\partial^2 G_\Omega}{\partial \tau^2}(\mathbf{r},\mathbf{r}_0) = 0 \end{cases}$$

Reflection coefficient: $R = -1$

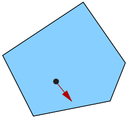

Original source $G_\infty(\mathbf{r},\mathbf{r}_0)$

$$G_\infty(\mathbf{r},\mathbf{r}_0) = \frac{j}{8k_f^2 D}\left(H_0^{(1)}(k_f|\mathbf{r}-\mathbf{r}_0|) - H_0^{(1)}(jk_f|\mathbf{r}-\mathbf{r}_0|)\right)$$

(Infinite plate Green's function)

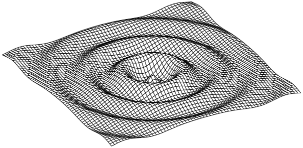

Generalisation to arbitrary convex polygonal geometry: Problem to solve

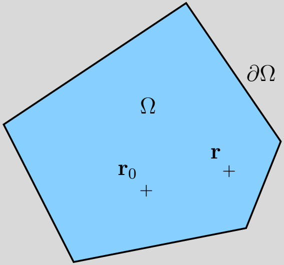

Example: Simply supported plate

$$\begin{cases} D\left(\nabla^4 - k_f^4\right) G_\Omega(\mathbf{r},\mathbf{r}_0) = \delta(\mathbf{r}-\mathbf{r}_0) \\ G_\Omega(\mathbf{r},\mathbf{r}_0) = 0 \\ \dfrac{\partial^2 G_\Omega}{\partial n^2}(\mathbf{r},\mathbf{r}_0) + \nu \dfrac{\partial^2 G_\Omega}{\partial \tau^2}(\mathbf{r},\mathbf{r}_0) = 0 \end{cases}$$

Reflection coefficient: $R = -1$

First reflection

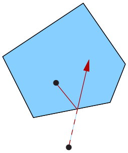

$R \cdot G_\infty(\mathbf{r},\mathbf{r}_1)$

$$G_\infty(\mathbf{r},\mathbf{r}_0) = \frac{j}{8k_f^2 D}\left(H_0^{(1)}(k_f|\mathbf{r}-\mathbf{r}_0|) - H_0^{(1)}(jk_f|\mathbf{r}-\mathbf{r}_0|)\right)$$

(Infinite plate Green's function)

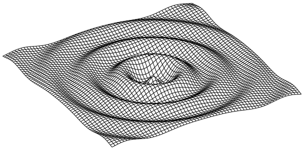

Generalisation to arbitrary convex polygonal geometry: Problem to solve

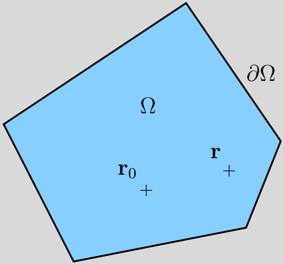

Example: Simply supported plate

$$\begin{cases} D\left(\nabla^4 - k_f^4\right) G_\Omega(\mathbf{r},\mathbf{r}_0) = \delta(\mathbf{r}-\mathbf{r}_0) \\ G_\Omega(\mathbf{r},\mathbf{r}_0) = 0 \\ \dfrac{\partial^2 G_\Omega}{\partial n^2}(\mathbf{r},\mathbf{r}_0) + \nu \dfrac{\partial^2 G_\Omega}{\partial \tau^2}(\mathbf{r},\mathbf{r}_0) = 0 \end{cases}$$

Reflection coefficient: $R = -1$

Second reflection

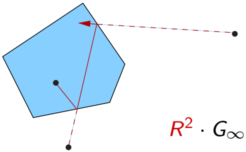

$R^2 \cdot G_\infty(\mathbf{r}, \mathbf{r}_2)$

$$G_\infty(\mathbf{r},\mathbf{r}_0) = \frac{j}{8k_f^2 D}\left(H_0^{(1)}(k_f|\mathbf{r}-\mathbf{r}_0|) - H_0^{(1)}(jk_f|\mathbf{r}-\mathbf{r}_0|)\right)$$

(Infinite plate Green's function)

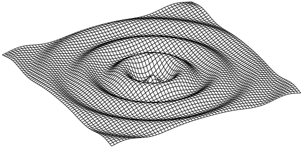

Generalisation to arbitrary convex polygonal geometry: Problem to solve

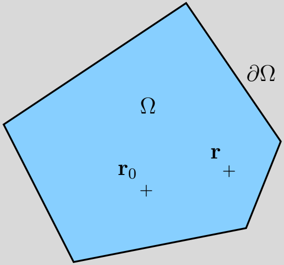

Example: Simply supported plate

$$\begin{cases} D\left(\nabla^4 - k_f^4\right) G_\Omega(\mathbf{r},\mathbf{r}_0) = \delta(\mathbf{r}-\mathbf{r}_0) \\ G_\Omega(\mathbf{r},\mathbf{r}_0) = 0 \\ \dfrac{\partial^2 G_\Omega}{\partial n^2}(\mathbf{r},\mathbf{r}_0) + \nu \dfrac{\partial^2 G_\Omega}{\partial \tau^2}(\mathbf{r},\mathbf{r}_0) = 0 \end{cases}$$

Reflection coefficient: $R = -1$

Third reflection

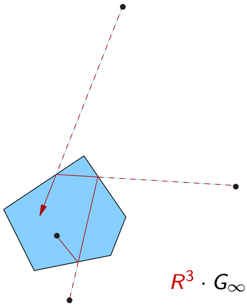

$R^3 \cdot G_\infty(\mathbf{r}, \mathbf{r}_3)$

$$G_\infty(\mathbf{r},\mathbf{r}_0) = \frac{j}{8k_f^2 D}\left(H_0^{(1)}(k_f|\mathbf{r}-\mathbf{r}_0|) - H_0^{(1)}(jk_f|\mathbf{r}-\mathbf{r}_0|)\right)$$

(Infinite plate Green's function)

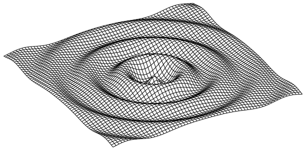

Generalisation to arbitrary convex polygonal geometry: Problem to solve

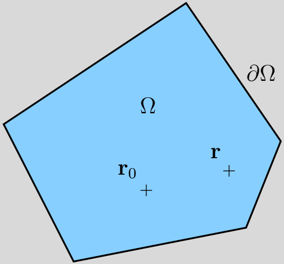

Example: Simply supported plate

$$\begin{cases} D\left(\nabla^4 - k_f^4\right) G_\Omega(\mathbf{r},\mathbf{r}_0) = \delta(\mathbf{r}-\mathbf{r}_0) \\ G_\Omega(\mathbf{r},\mathbf{r}_0) = 0 \\ \dfrac{\partial^2 G_\Omega}{\partial n^2}(\mathbf{r},\mathbf{r}_0) + \nu \dfrac{\partial^2 G_\Omega}{\partial \tau^2}(\mathbf{r},\mathbf{r}_0) = 0 \end{cases}$$

Reflection coefficient: $R = -1$

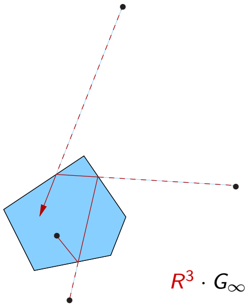

Third reflection $R^3 \cdot G_\infty(\mathbf{r},\mathbf{r}_3)$

$$G_\infty(\mathbf{r},\mathbf{r}_0) = \frac{j}{8k_f^2 D}\left(H_0^{(1)}(k_f|\mathbf{r}-\mathbf{r}_0|) - H_0^{(1)}(jk_f|\mathbf{r}-\mathbf{r}_0|)\right)$$

(Infinite plate Green's function)

Image source pattern:

$$\mathcal{D}_\Omega(\mathbf{r},\mathbf{r}_0) = \sum_{s=0}^{\infty} R^{N(s)}\delta(\mathbf{r}-\mathbf{r}_s)$$

Generalisation to arbitrary convex polygonal geometry: Problem to solve

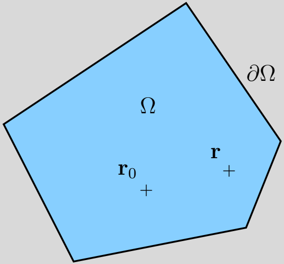

Example: Simply supported plate

$$\begin{cases} D\left(\nabla^4 - k_f^4\right) G_\Omega(\mathbf{r}, \mathbf{r}_0) = \delta(\mathbf{r} - \mathbf{r}_0) \\ G_\Omega(\mathbf{r}, \mathbf{r}_0) = 0 \\ \dfrac{\partial^2 G_\Omega}{\partial n^2}(\mathbf{r}, \mathbf{r}_0) + \nu \dfrac{\partial^2 G_\Omega}{\partial \tau^2}(\mathbf{r}, \mathbf{r}_0) = 0 \end{cases}$$

Reflection coefficient: $R = -1$

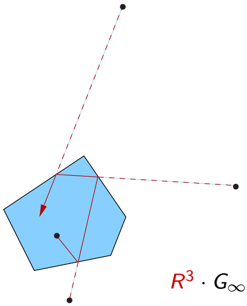

Third reflection $R^3 \cdot G_\infty(\mathbf{r}, \mathbf{r}_3)$

$$G_\infty(\mathbf{r}, \mathbf{r}_0) = \frac{j}{8k_f^2 D}\left(H_0^{(1)}(k_f|\mathbf{r} - \mathbf{r}_0|) - H_0^{(1)}(jk_f|\mathbf{r} - \mathbf{r}_0|)\right)$$

(Infinite plate Green's function)

Image source pattern:

$$\mathcal{D}_\Omega(\mathbf{r}, \mathbf{r}_0) = \sum_{s=0}^{\infty} R^{N(s)} \delta(\mathbf{r} - \mathbf{r}_s)$$

Green's function:

$$\boxed{G_\Omega(\mathbf{r}, \mathbf{r}_0) = \mathcal{D}_\Omega(\mathbf{r}, \mathbf{r}_0) * G_\infty(\mathbf{r}, \mathbf{0})}$$

Plate geometry and image source pattern shape

Periodic source pattern

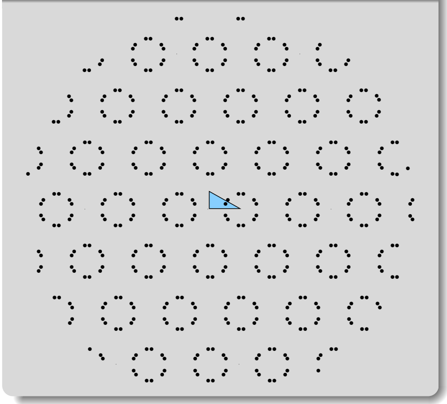

Recurrence relation

⇓

Exact **Green's function**

Aperiodic source pattern

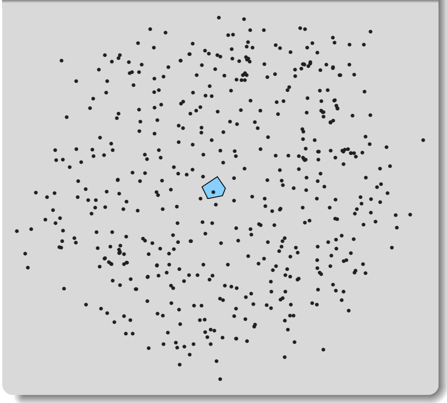

Truncation of the image source series

⇓

Approximate solution

Periodic image source pattern

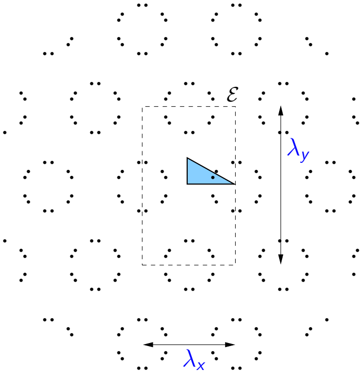

$$\underbrace{\mathcal{D}_\Omega(\mathbf{r},\mathbf{r}_0) = \mathcal{P}_\Omega(\mathbf{r}) * \mathcal{E}(\mathbf{r},\mathbf{r}_0)}$$
$$G_\Omega(\mathbf{r},\mathbf{r}_0) = \mathcal{D}_\Omega(\mathbf{r},\mathbf{r}_0) * G_\infty(\mathbf{r},\mathbf{0})$$
$$\Downarrow$$
$G_\Omega(\mathbf{r},\mathbf{r}_0)$ **is periodic**

$\mathcal{E}$: elementary pattern
$\mathcal{P}_\Omega$: periodisation operator

$$\mathcal{P}_\Omega(x,y) = \sum_{p=-\infty}^{+\infty} \sum_{q=-\infty}^{+\infty} \delta(x-p\lambda_x, y-q\lambda_y)$$

λ_x, λ_y: spatial periods of the pattern

Closed form of the Green's function $\left(k_m = \frac{m2\pi}{\lambda_x},\ k_n = \frac{n2\pi}{\lambda_y}\right)$

$$G_\Omega(x,y;x_0,y_0) = \sum_{p=-\infty}^{+\infty} \sum_{q=-\infty}^{+\infty} \delta(x-p\lambda_x, y-q\lambda_y) * \mathcal{E}(x,y;x_0,y_0) * G_\infty(x,y;0,0)$$

$\Updownarrow$ Fourier Series

$$G_\Omega(x,y;x_0,y_0) = \frac{1}{\lambda_x\lambda_y} \sum_{m=-\infty}^{+\infty} \sum_{n=-\infty}^{+\infty} \mathcal{F}\left[\mathcal{E}(x,y;x_0,y_0)\right]_{(k_m,k_n)} \mathcal{F}\left[G_\infty(x,y;0,0)\right]_{(k_m,k_n)} e^{-j(k_m x + k_n y)}$$

Periodic image source pattern: Exact Green's functions

Rectangle

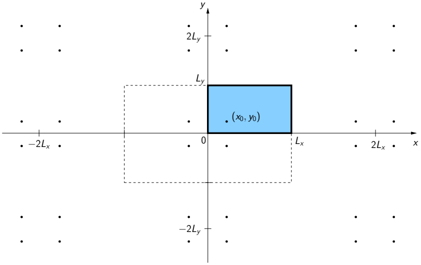

$$\mathcal{P}_\Omega(x,y) = \sum_{p=-\infty}^{+\infty} \sum_{q=-\infty}^{+\infty} \delta(x - p2L_x, y - q2L_y)$$

$$\mathcal{E}(x,y;x_0,y_0) = \begin{cases} \delta(x - x_0, y - y_0) \\ -\delta(x - x_0, y + y_0) \\ -\delta(x + x_0, y - y_0) \\ +\delta(x + x_0, y + y_0) \end{cases}$$

$$G_\Omega(x,y;x_0,y_0) = \frac{4}{L_x L_y} \sum_{m=1}^{\infty} \sum_{n=1}^{\infty} \frac{\sin(k_m x_0)\sin(k_n y_0)\sin(k_m x)\sin(k_n y)}{D\left(\left(k_m^2 + k_n^2\right)^2 - k_f^4\right)}$$

$$\omega_{mn} = \left(\frac{D}{\rho h}\right)^{1/2} \left(\left(\frac{m\pi}{L_x}\right)^2 + \left(\frac{n\pi}{L_y}\right)^2\right)$$

$$G_\Omega(x,y;x_0,y_0) = \frac{4}{L_x L_y} \sum_{m=1}^{\infty} \sum_{n=1}^{\infty} \frac{\sin(k_m x_0)\sin(k_n y_0)\sin(k_m x)\sin(k_n y)}{D\left((k_m^2 + k_n^2)^2 - k_f^4\right)}$$

$$G_\Omega(x,y;x_0,y_0) = \frac{4}{L^2} \sum_{m=1}^{+\infty} \sum_{n=1}^{+\infty} \frac{\sin(k_m x_0)\sin(k_n y_0) - \sin(k_m(L - y_0))\sin(k_n(L - x_0))}{D\left((k_m^2 + k_n^2)^2 - k_f^4\right)} \sin(k_m x)\sin(k_n y)$$

$$G_\Omega(x,y;x_0,y_0) = \frac{4}{\sqrt{3}L^2} \sum_{m=1}^{+\infty} \sum_{n=1}^{+\infty} \frac{\sum_{i=1}^{6} -\xi_i \sin(k_m x_i)\sin(k_n y_i)}{D\left((k_m^2 + k_n^2)^2 - k_f^4\right)} \sin(k_m x)\sin(k_n y)$$

$$G_\Omega(x,y;x_0,y_0) = \frac{1}{3L \cdot \sqrt{3}L} \sum_{m=-\infty}^{+\infty} \sum_{n=-\infty}^{+\infty} \frac{\sum_{i=1}^{12} \xi_i e^{jk_m x_i} e^{jk_n y_i}}{D\left((k_m^2 + k_n^2)^2 - k_f^4\right)} e^{-jk_m x} e^{-jk_n y}$$

Periodic image source pattern: Exact Green's functions

$$G_\Omega(x, y; x_0, y_0) = \frac{4}{L_x L_y} \sum_{m=1}^{\infty} \sum_{n=1}^{\infty} \frac{\sin(k_m x_0)\sin(k_n y_0)\sin(k_m x)\sin(k_n y)}{D\left((k_m^2 + k_n^2)^2 - k_f^4\right)}$$

$$G_\Omega(x, y; x_0, y_0) = \frac{4}{L^2} \sum_{m=1}^{+\infty} \sum_{n=1}^{+\infty} \frac{\sin(k_m x_0)\sin(k_n y_0) - \sin(k_m(L - y_0))\sin(k_n(L - x_0))}{D\left((k_m^2 + k_n^2)^2 - k_f^4\right)} \sin(k_m x)\sin(k_n y)$$

$$G_\Omega(x, y; x_0, y_0) = \frac{4}{\sqrt{3}L^2} \sum_{m=1}^{+\infty} \sum_{n=1}^{+\infty} \frac{\sum_{i=1}^{6} -\xi_i \sin(k_m x_i)\sin(k_n y_i)}{D\left((k_m^2 + k_n^2)^2 - k_f^4\right)} \sin(k_m x)\sin(k_n y)$$

$$G_\Omega(x, y; x_0, y_0) = \frac{1}{3L \cdot \sqrt{3}L} \sum_{m=-\infty}^{+\infty} \sum_{n=-\infty}^{+\infty} \frac{\sum_{i=1}^{12} \xi_i e^{jk_m x_i} e^{jk_n y_i}}{D\left((k_m^2 + k_n^2)^2 - k_f^4\right)} e^{-jk_m x} e^{-jk_n y}$$

Periodic image source pattern: Exact Green's functions

Isosceles right triangle

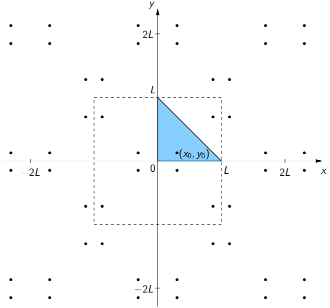

$$\mathcal{E}(x,y,x_0,y_0)=\begin{cases}\delta(x-x_0,y-y_0)\\-\delta(x-x_0,y+y_0)\\-\delta(x+x_0,y-y_0)\\+\delta(x+x_0,y+y_0)\end{cases}+\begin{cases}-\delta(x-(L-y_0),y-(L-x_0))\\+\delta(x-(L-y_0),y+(L-x_0))\\+\delta(x+(L-y_0),y-(L-x_0))\\-\delta(x+(L-y_0),y+(L-x_0))\end{cases}$$

$$\mathcal{P}_\Omega(x,y)=\sum_{p=-\infty}^{+\infty}\sum_{q=-\infty}^{+\infty}\delta(x-p2L,y-q2L)$$

$$G_\Omega(x,y,x_0,y_0)=$$

$$\frac{4}{L^2}\sum_{m=1}^{+\infty}\sum_{n=1}^{+\infty}\frac{\sin(k_m x_0)\sin(k_n y_0)-\sin(k_m(L-y_0))\sin(k_n(L-x_0))}{D\left((k_m^2+k_n^2)^2-k_f^4\right)}\sin(k_m x)\sin(k_n y)$$

$$\omega_{mn}=\left(\frac{D}{\rho h}\right)^{1/2}\left(\left(\frac{m\pi}{L}\right)^2+\left(\frac{n\pi}{L}\right)^2\right)$$

$$G_\Omega(x,y;x_0,y_0)=\frac{4}{L_xL_y}\sum_{m=1}^{\infty}\sum_{n=1}^{\infty}\frac{\sin(k_m x_0)\sin(k_n y_0)\sin(k_m x)\sin(k_n y)}{D\left((k_m^2+k_n^2)^2-k_f^4\right)}$$

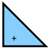

$$G_\Omega(x,y;x_0,y_0)=\frac{4}{L^2}\sum_{m=1}^{+\infty}\sum_{n=1}^{+\infty}\frac{\sin(k_m x_0)\sin(k_n y_0)-\sin(k_m(L-y_0))\sin(k_n(L-x_0))}{D\left((k_m^2+k_n^2)^2-k_f^4\right)}\sin(k_m x)\sin(k_n y)$$

$$G_\Omega(x,y;x_0,y_0)=\frac{4}{\sqrt{3}L^2}\sum_{m=1}^{+\infty}\sum_{n=1}^{+\infty}\frac{\sum_{i=1}^{6}-\xi_i\sin(k_m x_i)\sin(k_n y_i)}{D\left((k_m^2+k_n^2)^2-k_f^4\right)}\sin(k_m x)\sin(k_n y)$$

$$G_\Omega(x,y;x_0,y_0)=\frac{1}{3L\cdot\sqrt{3}L}\sum_{m=-\infty}^{+\infty}\sum_{n=-\infty}^{+\infty}\frac{\sum_{i=1}^{12}\xi_i e^{jk_m x_i}e^{jk_n y_i}}{D\left((k_m^2+k_n^2)^2-k_f^4\right)}e^{-jk_m x}e^{-jk_n y}$$

Periodic image source pattern: Exact Green's functions

$$G_\Omega(x, y; x_0, y_0) = \frac{4}{L_x L_y} \sum_{m=1}^{\infty} \sum_{n=1}^{\infty} \frac{\sin(k_m x_0) \sin(k_n y_0) \sin(k_m x) \sin(k_n y)}{D\left((k_m^2 + k_n^2)^2 - k_f^4\right)}$$

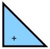

$$G_\Omega(x, y; x_0, y_0) = \frac{4}{L^2} \sum_{m=1}^{+\infty} \sum_{n=1}^{+\infty} \frac{\sin(k_m x_0) \sin(k_n y_0) - \sin(k_m(L - y_0)) \sin(k_n(L - x_0))}{D\left((k_m^2 + k_n^2)^2 - k_f^4\right)} \sin(k_m x) \sin(k_n y)$$

$$G_\Omega(x, y; x_0, y_0) = \frac{4}{\sqrt{3}L^2} \sum_{m=1}^{+\infty} \sum_{n=1}^{+\infty} \frac{\sum_{i=1}^{6} -\xi_i \sin(k_m x_i) \sin(k_n y_i)}{D\left((k_m^2 + k_n^2)^2 - k_f^4\right)} \sin(k_m x) \sin(k_n y)$$

$$G_\Omega(x, y; x_0, y_0) = \frac{1}{3L \cdot \sqrt{3}L} \sum_{m=-\infty}^{+\infty} \sum_{n=-\infty}^{+\infty} \frac{\sum_{i=1}^{12} \xi_i e^{jk_m x_i} e^{jk_n y_i}}{D\left((k_m^2 + k_n^2)^2 - k_f^4\right)} e^{-jk_m x} e^{-jk_n y}$$

Periodic image source pattern: Exact Green's functions

Half-equilateral triangle

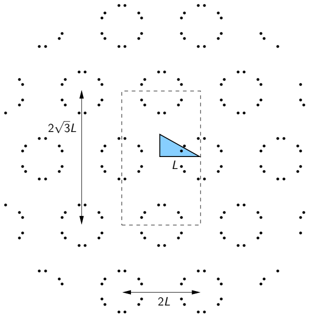

$$\mathcal{E}(x, y, x_0, y_0) = \sum_{i=1}^{6} \xi_i \begin{cases} \delta(x - x_i, y - y_i) \\ -\delta(x - x_i, y + y_i) \\ -\delta(x + x_i, y - y_i) \\ +\delta(x + x_i, y + y_i) \end{cases}$$

$$\mathcal{P}_\Omega(x, y) = \sum_{p=-\infty}^{+\infty} \sum_{q=-\infty}^{+\infty} \delta(x - p2L, y - q2\sqrt{3}L)$$

$$G_\Omega(x, y, x_0, y_0) = \frac{4}{\sqrt{3}L^2} \sum_{m=1}^{+\infty} \sum_{n=1}^{+\infty} \frac{\sum_{i=1}^{6} -\xi_i \sin(k_m x_i) \sin(k_n y_i)}{D\left((k_m^2 + k_n^2)^2 - k_f^4\right)} \sin(k_m x) \sin(k_n y)$$

$$\omega_{mn} = \left(\frac{D}{\rho h}\right)^{1/2} \left(\left(\frac{m\pi}{L}\right)^2 + \left(\frac{n\pi}{\sqrt{3}L}\right)^2\right)$$

$$G_\Omega(x, y; x_0, y_0) = \frac{4}{L_x L_y} \sum_{m=1}^{\infty} \sum_{n=1}^{\infty} \frac{\sin(k_m x_0) \sin(k_n y_0) \sin(k_m x) \sin(k_n y)}{D\left((k_m^2 + k_n^2)^2 - k_f^4\right)}$$

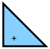

$$G_\Omega(x, y; x_0, y_0) = \frac{4}{L^2} \sum_{m=1}^{+\infty} \sum_{n=1}^{+\infty} \frac{\sin(k_m x_0) \sin(k_n y_0) - \sin(k_m(L - y_0)) \sin(k_n(L - x_0))}{D\left((k_m^2 + k_n^2)^2 - k_f^4\right)} \sin(k_m x) \sin(k_n y)$$

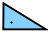

$$G_\Omega(x, y; x_0, y_0) = \frac{4}{\sqrt{3}L^2} \sum_{m=1}^{+\infty} \sum_{n=1}^{+\infty} \frac{\sum_{i=1}^{6} -\xi_i \sin(k_m x_i) \sin(k_n y_i)}{D\left((k_m^2 + k_n^2)^2 - k_f^4\right)} \sin(k_m x) \sin(k_n y)$$

$$G_\Omega(x, y; x_0, y_0) = \frac{1}{3L \cdot \sqrt{3}L} \sum_{m=-\infty}^{+\infty} \sum_{n=-\infty}^{+\infty} \frac{\sum_{i=1}^{12} \xi_i e^{jk_m x_i} e^{jk_n y_i}}{D\left((k_m^2 + k_n^2)^2 - k_f^4\right)} e^{-jk_m x} e^{-jk_n y}$$

Periodic image source pattern: Exact Green's functions

$$G_\Omega(x, y; x_0, y_0) = \frac{4}{L_x L_y} \sum_{m=1}^{\infty} \sum_{n=1}^{\infty} \frac{\sin(k_m x_0) \sin(k_n y_0) \sin(k_m x) \sin(k_n y)}{D\left((k_m^2 + k_n^2)^2 - k_f^4\right)}$$

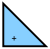

$$G_\Omega(x, y; x_0, y_0) = \frac{4}{L^2} \sum_{m=1}^{+\infty} \sum_{n=1}^{+\infty} \frac{\sin(k_m x_0) \sin(k_n y_0) - \sin(k_m (L - y_0)) \sin(k_n (L - x_0))}{D\left((k_m^2 + k_n^2)^2 - k_f^4\right)} \sin(k_m x) \sin(k_n y)$$

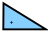

$$G_\Omega(x, y; x_0, y_0) = \frac{4}{\sqrt{3}L^2} \sum_{m=1}^{+\infty} \sum_{n=1}^{+\infty} \frac{\sum_{i=1}^{6} -\xi_i \sin(k_m x_i) \sin(k_n y_i)}{D\left((k_m^2 + k_n^2)^2 - k_f^4\right)} \sin(k_m x) \sin(k_n y)$$

$$G_\Omega(x, y; x_0, y_0) = \frac{1}{3L \cdot \sqrt{3}L} \sum_{m=-\infty}^{+\infty} \sum_{n=-\infty}^{+\infty} \frac{\sum_{i=1}^{12} \xi_i e^{jk_m x_i} e^{jk_n y_i}}{D\left((k_m^2 + k_n^2)^2 - k_f^4\right)} e^{-jk_m x} e^{-jk_n y}$$

Periodic image source pattern: Exact Green's functions

Equilateral triangle

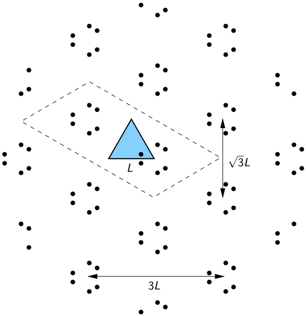

$$\mathcal{E}(x, y, x_0, y_0) = \sum_{i=1}^{12} \xi_i \delta(x - x_i, y - y_i)$$

$$\mathcal{P}_\Omega(x, y) = \sum_{p=-\infty}^{+\infty} \sum_{q=-\infty}^{+\infty} \delta(x - p3L, y - q\sqrt{3}L)$$

$$G_\Omega(x, y, x_0, y_0) = \frac{1}{3L \cdot \sqrt{3}L} \sum_{m=-\infty}^{+\infty} \sum_{n=-\infty}^{+\infty} \frac{\sum_{i=1}^{12} \xi_i e^{\mathrm{j}k_m x_i} e^{\mathrm{j}k_n y_i}}{D\left((k_m^2 + k_n^2)^2 - k_f^4\right)} e^{-\mathrm{j}k_m x} e^{-\mathrm{j}k_n y}$$

$$\omega_{mn} = \left(\frac{D}{\rho h}\right)^{1/2} \left(\left(\frac{m2\pi}{3L}\right)^2 + \left(\frac{n2\pi}{\sqrt{3}L}\right)^2\right)$$

$$G_\Omega(x, y; x_0, y_0) = \frac{4}{L_x L_y} \sum_{m=1}^{\infty} \sum_{n=1}^{\infty} \frac{\sin(k_m x_0)\sin(k_n y_0)\sin(k_m x)\sin(k_n y)}{D\left((k_m^2 + k_n^2)^2 - k_f^4\right)}$$

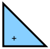

$$G_\Omega(x, y; x_0, y_0) = \frac{4}{L^2} \sum_{m=1}^{+\infty} \sum_{n=1}^{+\infty} \frac{\sin(k_m x_0)\sin(k_n y_0) - \sin(k_m(L - y_0))\sin(k_n(L - x_0))}{D\left((k_m^2 + k_n^2)^2 - k_f^4\right)} \sin(k_m x)\sin(k_n y)$$

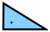

$$G_\Omega(x, y; x_0, y_0) = \frac{4}{\sqrt{3}L^2} \sum_{m=1}^{+\infty} \sum_{n=1}^{+\infty} \frac{\sum_{i=1}^{6} -\xi_i \sin(k_m x_i)\sin(k_n y_i)}{D\left((k_m^2 + k_n^2)^2 - k_f^4\right)} \sin(k_m x)\sin(k_n y)$$

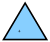

$$G_\Omega(x, y; x_0, y_0) = \frac{1}{3L \cdot \sqrt{3}L} \sum_{m=-\infty}^{+\infty} \sum_{n=-\infty}^{+\infty} \frac{\sum_{i=1}^{12} \xi_i e^{\mathrm{j}k_m x_i} e^{\mathrm{j}k_n y_i}}{D\left((k_m^2 + k_n^2)^2 - k_f^4\right)} e^{-\mathrm{j}k_m x} e^{-\mathrm{j}k_n y}$$

Periodic image source pattern: Exact Green's functions

$$G_\Omega(x, y; x_0, y_0) = \frac{4}{L_x L_y} \sum_{m=1}^{\infty} \sum_{n=1}^{\infty} \frac{\sin(k_m x_0)\sin(k_n y_0)\sin(k_m x)\sin(k_n y)}{D\left((k_m^2 + k_n^2)^2 - k_f^4\right)}$$

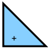

$$G_\Omega(x, y; x_0, y_0) = \frac{4}{L^2} \sum_{m=1}^{+\infty} \sum_{n=1}^{+\infty} \frac{\sin(k_m x_0)\sin(k_n y_0) - \sin(k_m(L - y_0))\sin(k_n(L - x_0))}{D\left((k_m^2 + k_n^2)^2 - k_f^4\right)} \sin(k_m x)\sin(k_n y)$$

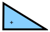

$$G_\Omega(x, y; x_0, y_0) = \frac{4}{\sqrt{3}L^2} \sum_{m=1}^{+\infty} \sum_{n=1}^{+\infty} \frac{\sum_{i=1}^{6} -\xi_i \sin(k_m x_i)\sin(k_n y_i)}{D\left((k_m^2 + k_n^2)^2 - k_f^4\right)} \sin(k_m x)\sin(k_n y)$$

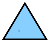

$$G_\Omega(x, y; x_0, y_0) = \frac{1}{3L \cdot \sqrt{3}L} \sum_{m=-\infty}^{+\infty} \sum_{n=-\infty}^{+\infty} \frac{\sum_{i=1}^{12} \xi_i e^{\mathrm{j}k_m x_i} e^{\mathrm{j}k_n y_i}}{D\left((k_m^2 + k_n^2)^2 - k_f^4\right)} e^{-\mathrm{j}k_m x} e^{-\mathrm{j}k_n y}$$

Periodic image source pattern: Exact Green's functions

- Analytically obtained Green's functions
  Fourier series $\Rightarrow$ modal expansions
- New closed forms of Green's functions for triangular plates
- Only 4 geometries yield a periodic image source pattern

$$G_\Omega(x,y;x_0,y_0) = \frac{4}{L_x L_y}\sum_{m=1}^{\infty}\sum_{n=1}^{\infty}\frac{\sin(k_m x_0)\sin(k_n y_0)\sin(k_m x)\sin(k_n y)}{D\left((k_m^2+k_n^2)^2-k_f^4\right)}$$

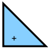

$$G_\Omega(x,y;x_0,y_0) = \frac{4}{L^2}\sum_{m=1}^{+\infty}\sum_{n=1}^{+\infty}\frac{\sin(k_m x_0)\sin(k_n y_0)-\sin(k_m(L-y_0))\sin(k_n(L-x_0))}{D\left((k_m^2+k_n^2)^2-k_f^4\right)}\sin(k_m x)\sin(k_n y)$$

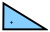

$$G_\Omega(x,y;x_0,y_0) = \frac{4}{\sqrt{3}L^2}\sum_{m=1}^{+\infty}\sum_{n=1}^{+\infty}\frac{\sum_{i=1}^{6}-\xi_i\sin(k_m x_i)\sin(k_n y_i)}{D\left((k_m^2+k_n^2)^2-k_f^4\right)}\sin(k_m x)\sin(k_n y)$$

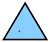

$$G_\Omega(x,y;x_0,y_0) = \frac{1}{3L\cdot\sqrt{3}L}\sum_{m=-\infty}^{+\infty}\sum_{n=-\infty}^{+\infty}\frac{\sum_{i=1}^{12}\xi_i e^{\mathrm{j}k_m x_i}e^{\mathrm{j}k_n y_i}}{D\left((k_m^2+k_n^2)^2-k_f^4\right)}e^{-\mathrm{j}k_m x}e^{-\mathrm{j}k_n y}$$

Truncation of the image source pattern

Image source series truncation

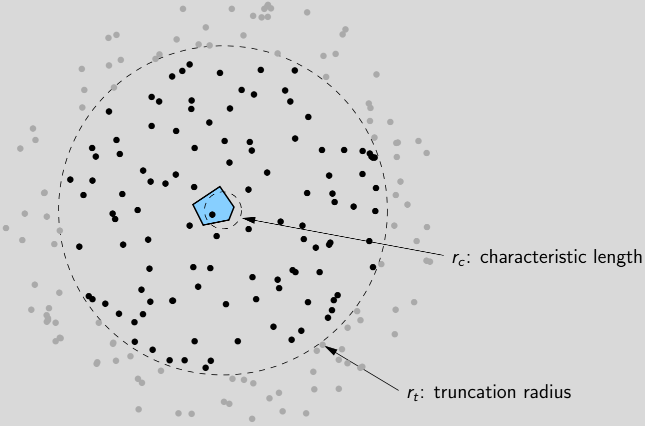

Non-dimensional truncation parameter:

$$\gamma = \frac{r_t}{r_c}$$

Controls the precision of the simulation.

Low, medium and high frequency ranges: Modal Overlap Factor (MOF)

Modal Overlap Factor (MOF)

$$MOF = \frac{\Delta\omega_\mu}{\delta\omega_\mu} = 2\eta\omega n$$

- $\Delta\omega_\mu$: -3dB bandwidth of a resonance
- $\delta\omega_\mu$: frequency interval between two successive resonances
- n: modal density

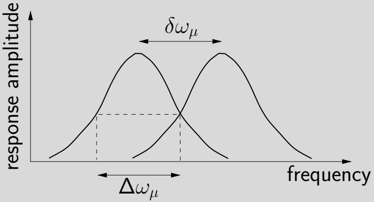

Low, medium and high frequency ranges: Modal Overlap Factor (MOF)

Modal Overlap Factor (MOF)

$$MOF = \frac{\Delta\omega_\mu}{\delta\omega_\mu} = 2\eta\omega n$$

- $\Delta\omega_\mu$: -3dB bandwidth of a resonance
- $\delta\omega_\mu$: frequency interval between two successive resonances
- n: modal density

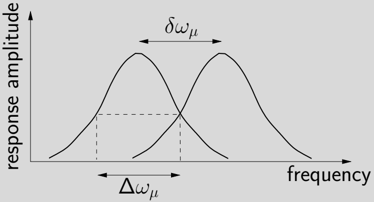

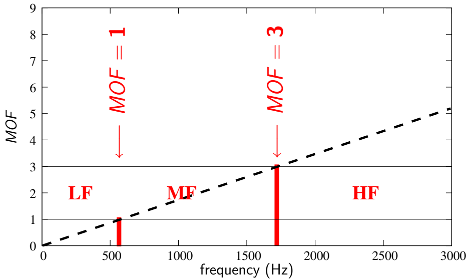

$\eta = 3 \cdot 10^{-2}$

MOF=3: Schroeder frequency

Convergence of the image source method

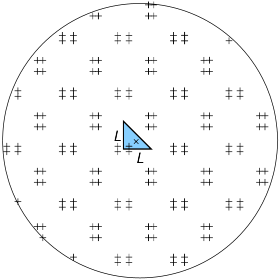

Isosceles right triangular plate
(steel; thickness = 2mm)
$\gamma = 10 \Rightarrow$ (154 sources)
Simply supported edges

$\eta =$ **0.015**

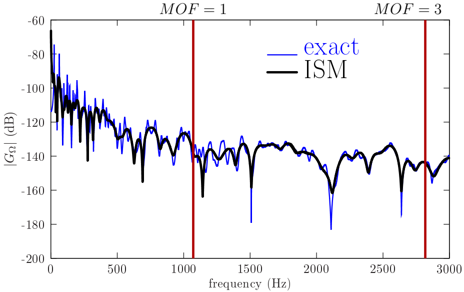

Modulus of G_Ω

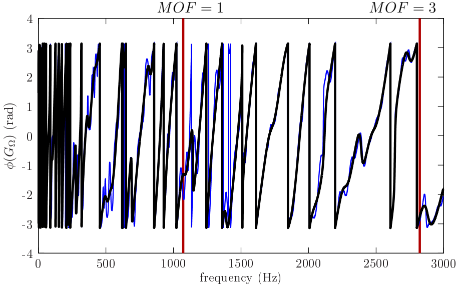

Phase of G_Ω

Convergence of the image source method

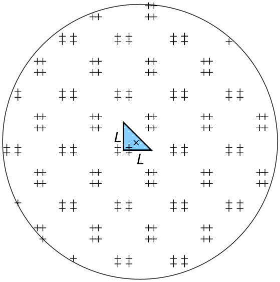

Isosceles right triangular plate
(steel; thickness = 2mm)
$\gamma = 10 \Rightarrow$ (154 sources)
Simply supported edges

$\eta = \mathbf{0.05}$

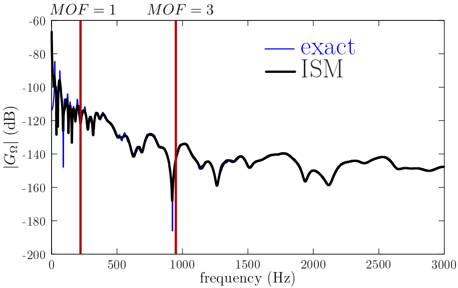

Modulus of G_Ω

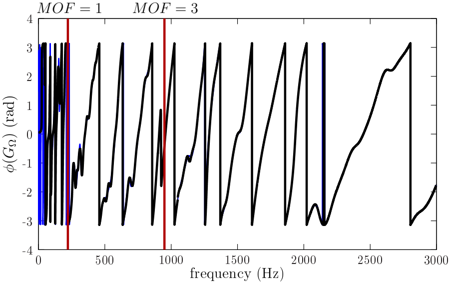

Phase of G_Ω

Convergence of the image source method

Convergence

- Damping ↗
- Frequency ↗

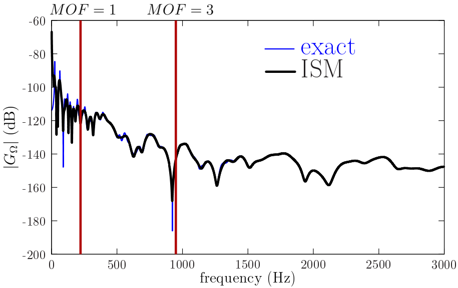

Modulus of G_Ω

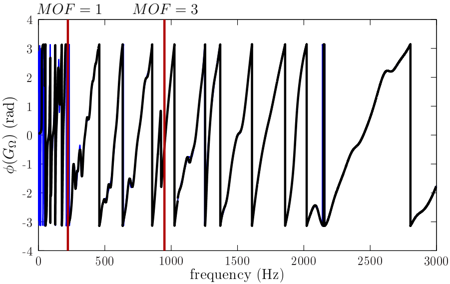

Phase of G_Ω

Convergence of the image source method

Convergence

- Damping $\nearrow$
- Frequency $\nearrow$

Precision control

Mean error in HF

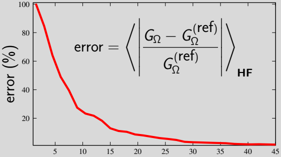

γ

Precision control using the truncation parameter

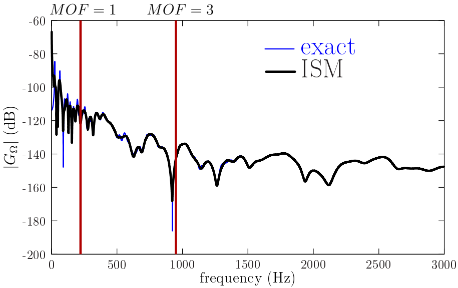

Modulus of G_Ω

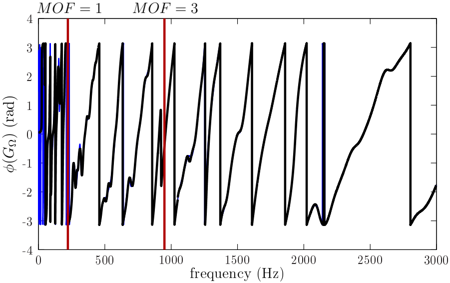

Phase of G_Ω

1. Model of the flexural vibrations of polygonal plates by the image source method
   - Introduction
   - Generalisation to arbitrary convex polygonal geometry
   - General boundary conditions
   - Polygonal plates
   - Plate assemblies

2. Acoustic black hole effect for vibration damping in plates and beams
   - Principle
   - Model
   - Experiments
   - Black-hole effect by a thermal gradient

General boundary conditions

Semi-infinite plate

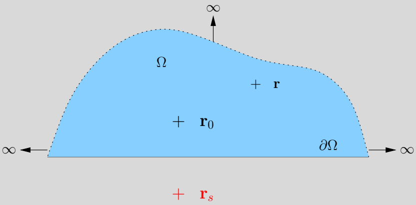

$$G_\Omega(\mathbf{r},\mathbf{r}_0) = G_\infty(\mathbf{r},\mathbf{r}_0) + G_s(\mathbf{r},\mathbf{r}_s)$$

$G_\infty(\mathbf{r},\mathbf{r}_0)$ incident field (original source)
$G_s(\mathbf{r},\mathbf{r}_s)$ reflected field (image source)

General boundary conditions

Semi-infinite plate

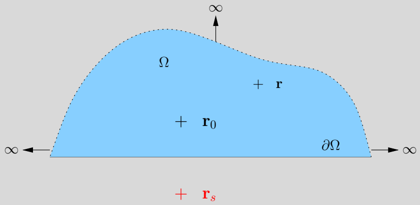

$$G_\Omega(\mathbf{r},\mathbf{r}_0) = G_\infty(\mathbf{r},\mathbf{r}_0) + G_s(\mathbf{r},\mathbf{r}_s)$$

$G_\infty(\mathbf{r},\mathbf{r}_0)$ incident field (original source)
$G_s(\mathbf{r},\mathbf{r}_s)$ reflected field (image source)

$G_s(\mathbf{r},\mathbf{r}_s) = ?$

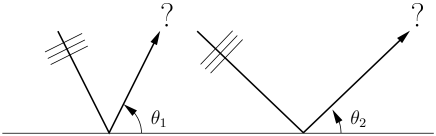

The reflection properties of the boundary depend on the angle of incidence of waves

General boundary conditions

Semi-infinite plate

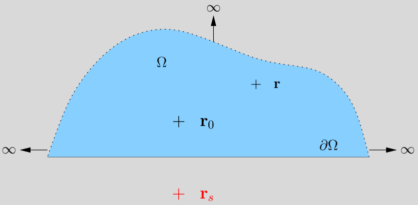

$$G_\Omega(\mathbf{r},\mathbf{r}_0) = G_\infty(\mathbf{r},\mathbf{r}_0) + G_s(\mathbf{r},\mathbf{r}_s)$$

$G_\infty(\mathbf{r},\mathbf{r}_0)$	incident field (original source)
$G_s(\mathbf{r},\mathbf{r}_s)$	reflected field (image source)

$G_s(\mathbf{r},\mathbf{r}_s) = ?$

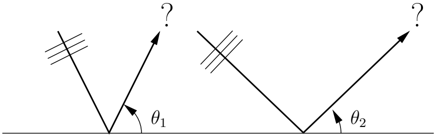

The reflection properties of the boundary depend on the angle of incidence of waves

Simply supported edge

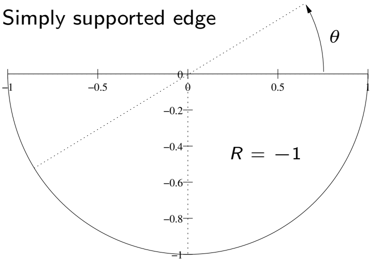

General boundary conditions

Semi-infinite plate

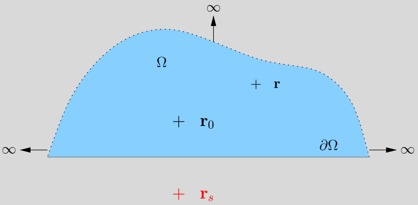

$$G_\Omega(\mathbf{r},\mathbf{r}_0) = G_\infty(\mathbf{r},\mathbf{r}_0) + G_s(\mathbf{r},\mathbf{r}_s)$$

$G_\infty(\mathbf{r},\mathbf{r}_0)$	incident field (original source)
$G_s(\mathbf{r},\mathbf{r}_s)$	reflected field (image source)

$G_s(\mathbf{r},\mathbf{r}_s) = ?$

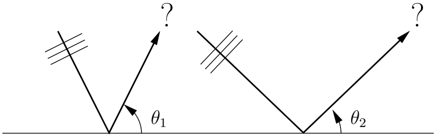

The reflection properties of the boundary depend on the angle of incidence of waves

Clamped edge

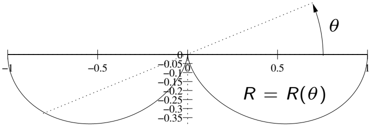

General boundary conditions

Semi-infinite plate

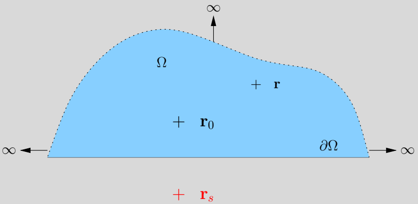

$$G_\Omega(\mathbf{r},\mathbf{r}_0) = G_\infty(\mathbf{r},\mathbf{r}_0) + G_s(\mathbf{r},\mathbf{r}_s)$$

$G_\infty(\mathbf{r},\mathbf{r}_0)$ incident field (original source)
$G_s(\mathbf{r},\mathbf{r}_s)$ reflected field (image source)

$G_s(\mathbf{r},\mathbf{r}_s) = ?$

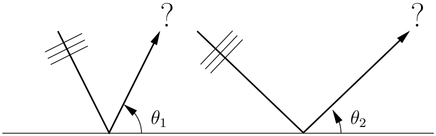

The reflection properties of the boundary depend on the angle of incidence of waves

$$G_\infty(\mathbf{r},\mathbf{r}_0) = \int \text{incident plane waves}$$

$$\Rightarrow G_s(\mathbf{r},\mathbf{r}_s) = \int \text{reflected plane waves}$$

General boundary conditions: Green's function of a semi-infinite plate

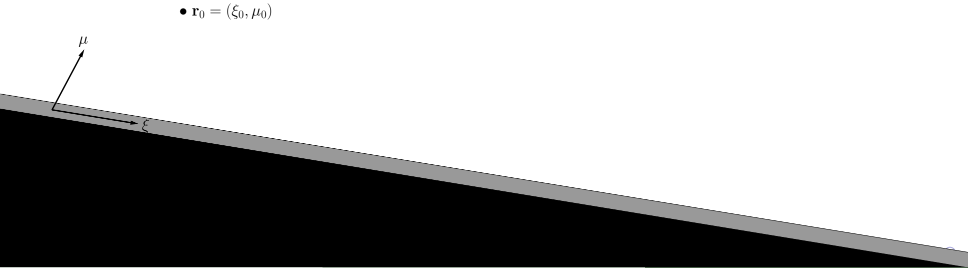

General boundary conditions: Green's function of a semi-infinite plate

Incident field as a continuous sum of **incident** plane waves:

$$G_\infty(\mathbf{r}, \mathbf{r}_0) = \int_{-\infty}^{+\infty} e^{jk_\xi(\xi-\xi_0)} \left(Ae^{-j\sqrt{k_f^2-k_\xi^2}(\mu-\mu_b)} + Be^{\sqrt{k_f^2+k_\xi^2}(\mu-\mu_b)} \right) dk_\xi$$

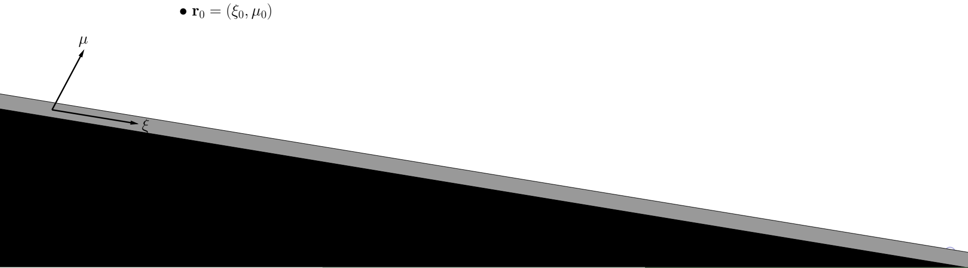

General boundary conditions: Green's function of a semi-infinite plate

Incident field as a continuous sum of **incident** plane waves:

$$G_\infty(\mathbf{r},\mathbf{r}_0) = \int_{-\infty}^{+\infty} e^{jk_\xi(\xi-\xi_0)} \left(Ae^{-j\sqrt{k_f^2-k_\xi^2}(\mu-\mu_b)} + Be^{\sqrt{k_f^2+k_\xi^2}(\mu-\mu_b)} \right) dk_\xi$$

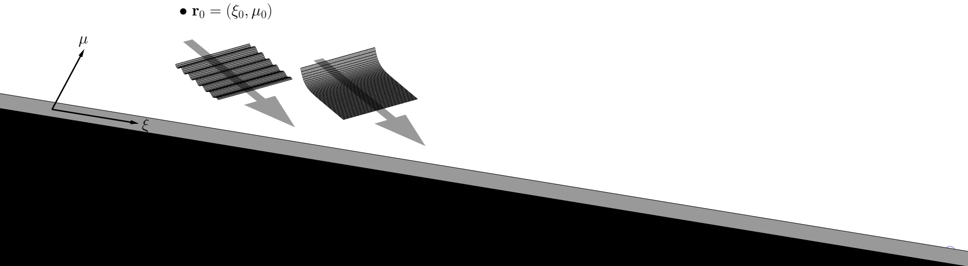

General boundary conditions: Green's function of a semi-infinite plate

Incident field as a continuous sum of **incident** plane waves:

$$G_\infty(\mathbf{r}, \mathbf{r}_0) = \int_{-\infty}^{+\infty} e^{jk_\xi(\xi-\xi_0)} \left(Ae^{-j\sqrt{k_f^2-k_\xi^2}(\mu-\mu_b)} + Be^{\sqrt{k_f^2+k_\xi^2}(\mu-\mu_b)} \right) dk_\xi$$

Reflected field as a continuous sum of **reflected** plane waves:

$$G_s(\mathbf{r}, \mathbf{r}_s) = \int_{-\infty}^{+\infty} e^{jk_\xi(\xi-\xi_0)} \left(Ce^{j\sqrt{k_f^2-k_\xi^2}(\mu-\mu_b)} + De^{-\sqrt{k_f^2+k_\xi^2}(\mu-\mu_b)} \right) dk_\xi$$

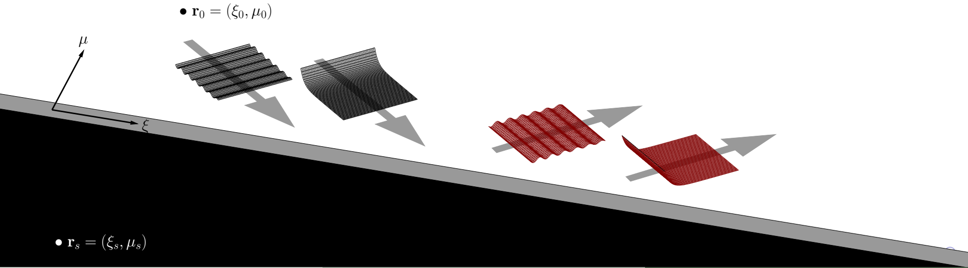

General boundary conditions: Green's function of a semi-infinite plate

Incident field as a continuous sum of **incident** plane waves:

$$G_\infty(\mathbf{r},\mathbf{r}_0) = \int_{-\infty}^{+\infty} e^{jk_\xi(\xi-\xi_0)} \left(Ae^{-j\sqrt{k_f^2-k_\xi^2}(\mu-\mu_b)} + Be^{\sqrt{k_f^2+k_\xi^2}(\mu-\mu_b)} \right) dk_\xi$$

Reflected field as a continuous sum of **reflected** plane waves:

$$G_s(\mathbf{r},\mathbf{r}_s) = \int_{-\infty}^{+\infty} e^{jk_\xi(\xi-\xi_0)} \left(Ce^{j\sqrt{k_f^2-k_\xi^2}(\mu-\mu_b)} + De^{-\sqrt{k_f^2+k_\xi^2}(\mu-\mu_b)} \right) dk_\xi$$

Reflection law:

$$\begin{bmatrix} C \\ D \end{bmatrix} = \begin{bmatrix} R_{pp}(k_\xi,k_f) & R_{ep}(k_\xi,k_f) \\ R_{pe}(k_\xi,k_f) & R_{ee}(k_\xi,k_f) \end{bmatrix} \begin{bmatrix} A \\ B \end{bmatrix}$$

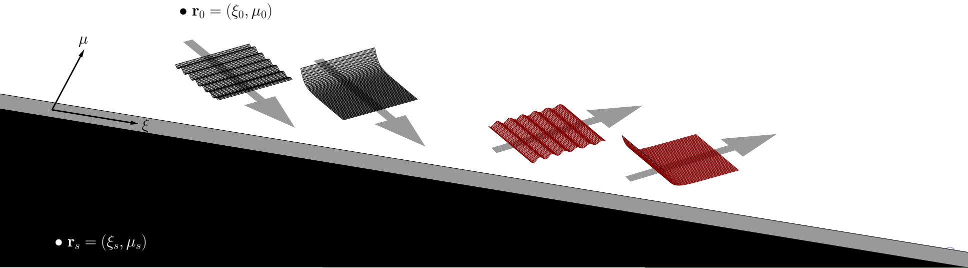

General boundary conditions: Green's function of a semi-infinite plate

Reflected field = **image source contribution**

$$G_s(\mathbf{r},\mathbf{r}_s) = \frac{j}{8\pi k_f^2 D}\int_{-\infty}^{+\infty} e^{jk_\xi(\xi-\xi_s)} \begin{bmatrix} e^{j\sqrt{k_f^2-k_\xi^2}(\mu-\mu_b)} & e^{-\sqrt{k_f^2+k_\xi^2}(\mu-\mu_b)} \end{bmatrix} \begin{bmatrix} R_{pp}(k_\xi,k_f) & R_{ep}(k_\xi,k_f) \\ R_{pe}(k_\xi,k_f) & R_{ee}(k_\xi,k_f) \end{bmatrix} \begin{bmatrix} \dfrac{e^{j\sqrt{k_f^2-k_\xi^2}(\mu_b-\mu_s)}}{\sqrt{k_f^2-k_\xi^2}} \\ j\dfrac{e^{-\sqrt{k_f^2+k_\xi^2}(\mu_b-\mu_s)}}{\sqrt{k_f^2+k_\xi^2}} \end{bmatrix} dk_\xi$$

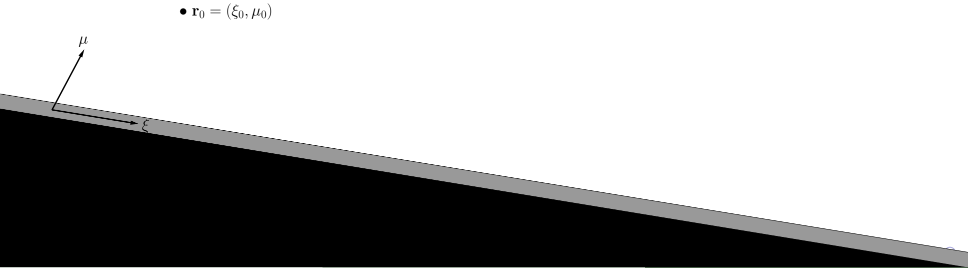

General boundary conditions: Green's function of a semi-infinite plate

Reflected field = **image source contribution**

$$G_s(\mathbf{r},\mathbf{r}_s) = \frac{j}{8\pi k_f^2 D}\int_{-\infty}^{+\infty} e^{jk_\xi(\xi-\xi_s)}$$

$$\begin{bmatrix} e^{j\sqrt{k_f^2-k_\xi^2}(\mu-\mu_b)} & e^{-\sqrt{k_f^2+k_\xi^2}(\mu-\mu_b)} \end{bmatrix} \begin{bmatrix} R_{pp}(k_\xi,k_f) & R_{ep}(k_\xi,k_f) \\ R_{pe}(k_\xi,k_f) & R_{ee}(k_\xi,k_f) \end{bmatrix} \begin{bmatrix} \dfrac{e^{j\sqrt{k_f^2-k_\xi^2}(\mu_b-\mu_s)}}{\sqrt{k_f^2-k_\xi^2}} \\ j\dfrac{e^{-\sqrt{k_f^2+k_\xi^2}(\mu_b-\mu_s)}}{\sqrt{k_f^2+k_\xi^2}} \end{bmatrix} dk_\xi$$

waves travelling in the virtual space

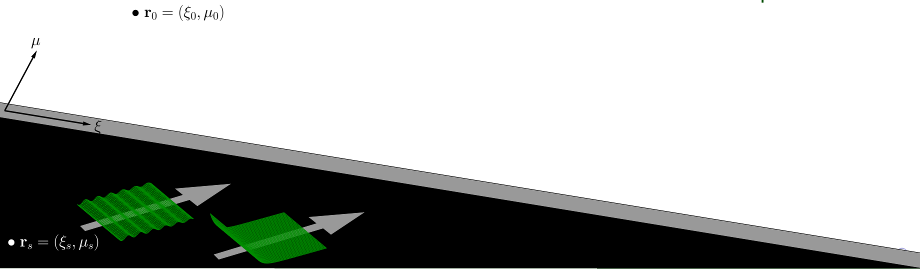

General boundary conditions: Green's function of a semi-infinite plate

Reflected field = **image source contribution**

$$G_s(\mathbf{r},\mathbf{r}_s) = \frac{j}{8\pi k_f^2 D}\int_{-\infty}^{+\infty} e^{jk_\xi(\xi-\xi_s)} \begin{bmatrix} e^{j\sqrt{k_f^2-k_\xi^2}(\mu-\mu_b)} & e^{-\sqrt{k_f^2+k_\xi^2}(\mu-\mu_b)} \end{bmatrix} \begin{bmatrix} R_{pp}(k_\xi,k_f) & R_{ep}(k_\xi,k_f) \\ R_{pe}(k_\xi,k_f) & R_{ee}(k_\xi,k_f) \end{bmatrix} \begin{bmatrix} \dfrac{e^{j\sqrt{k_f^2-k_\xi^2}(\mu_b-\mu_s)}}{\sqrt{k_f^2-k_\xi^2}} \\ j\dfrac{e^{-\sqrt{k_f^2+k_\xi^2}(\mu_b-\mu_s)}}{\sqrt{k_f^2+k_\xi^2}} \end{bmatrix} dk_\xi$$

wave reflection: propagating↔evanescent conversion

waves travelling in the virtual space

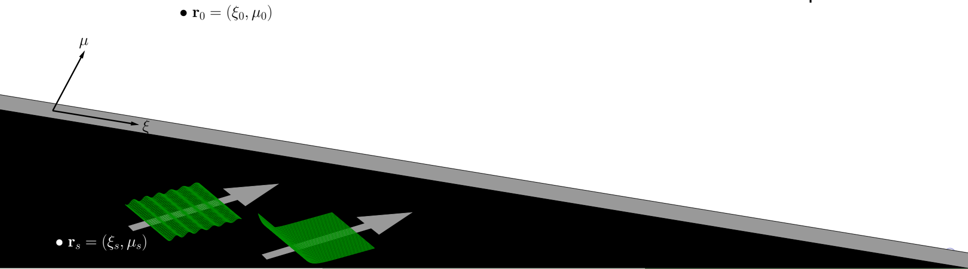

General boundary conditions: Green's function of a semi-infinite plate

Reflected field = **image source contribution**

$$G_s(\mathbf{r},\mathbf{r}_s) = \frac{j}{8\pi k_f^2 D}\int_{-\infty}^{+\infty} e^{jk_\xi(\xi-\xi_s)} \begin{bmatrix} e^{j\sqrt{k_f^2-k_\xi^2}(\mu-\mu_b)} & e^{-\sqrt{k_f^2+k_\xi^2}(\mu-\mu_b)} \end{bmatrix} \begin{bmatrix} R_{pp}(k_\xi,k_f) & R_{ep}(k_\xi,k_f) \\ R_{pe}(k_\xi,k_f) & R_{ee}(k_\xi,k_f) \end{bmatrix} \begin{bmatrix} \dfrac{e^{j\sqrt{k_f^2-k_\xi^2}(\mu_b-\mu_s)}}{\sqrt{k_f^2-k_\xi^2}} \\ j\dfrac{e^{-\sqrt{k_f^2+k_\xi^2}(\mu_b-\mu_s)}}{\sqrt{k_f^2+k_\xi^2}} \end{bmatrix} dk_\xi$$

waves travelling in the real space

wave reflection: propagating↔evanescent conversion

waves travelling in the virtual space

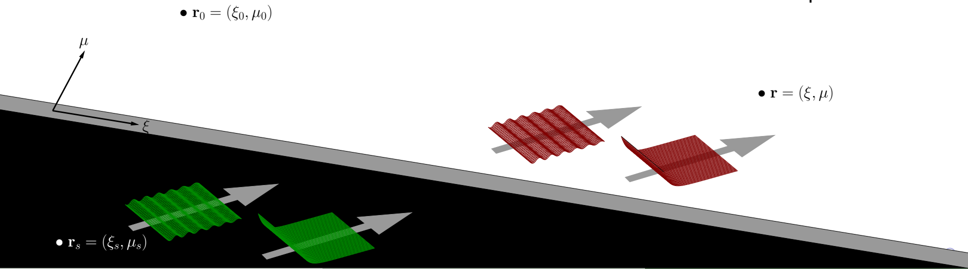

1. Model of the flexural vibrations of polygonal plates by the image source method
   - Introduction
   - Generalisation to arbitrary convex polygonal geometry
   - General boundary conditions
   - Polygonal plates
   - Plate assemblies

2. Acoustic black hole effect for vibration damping in plates and beams
   - Principle
   - Model
   - Experiments
   - Black-hole effect by a thermal gradient

Green's function of a polygonal plate

Image source method

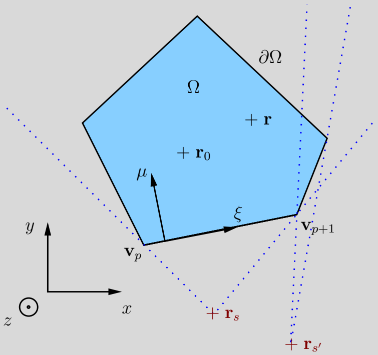

(x, y): global coordinate system
(ξ, μ): local coordinate system

$$\begin{cases} D\left(\nabla^4 - k_f^4\right) G_\Omega(\mathbf{r}, \mathbf{r}_0) = \delta(\mathbf{r} - \mathbf{r}_0) \\ \text{Boundary conditions (reflection matrices)} \end{cases}$$

Green's function of the polygonal plate

$$G_\Omega(\mathbf{r}, \mathbf{r}_0) = \underbrace{G_\infty(\mathbf{r}, \mathbf{r}_0)}_{\text{original source}} + \underbrace{\sum_{s=1}^{\infty} G_s(\mathbf{r}, \mathbf{r}_s)}_{\text{image sources}}$$

Contribution of each image source:

$$g_s(\mathbf{r}, \mathbf{r}_s) = \underbrace{V(\mathbf{r}, \mathbf{r}_s)}_{\text{geometrical validity function}} \; \underbrace{G_s(\mathbf{r}, \mathbf{r}_s)}_{\text{image source contribution for the equivalent semi-infinite plate}}$$

G_Ω is an approximation:

Image sources represent **specular reflection**.
Diffraction by the plate corners is ignored.

Green's function of a polygonal plate

$$G_\Omega(\mathbf{r},\mathbf{r}_0) = \underbrace{G_\infty(\mathbf{r},\mathbf{r}_0)}_{\text{original source}} + \underbrace{\sum_{s=1}^{N} g_s(\mathbf{r},\mathbf{r}_s)}_{\text{image sources}}$$

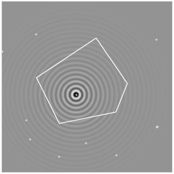

$G_\infty(\mathbf{r},\mathbf{r}_0)$

Original source

Green's function of a polygonal plate

$$G_\Omega(\mathbf{r},\mathbf{r}_0) = \underbrace{G_\infty(\mathbf{r},\mathbf{r}_0)}_{\text{original source}} + \underbrace{\sum_{s=1}^{N} {\color{red} g_s(\mathbf{r},\mathbf{r}_s)}}_{\text{image sources}}$$

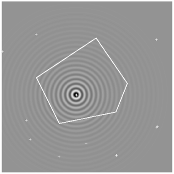

$G_\infty(\mathbf{r},\mathbf{r}_0)$

+

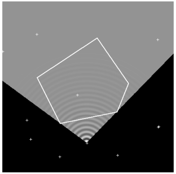

${\color{red} g_s'(\mathbf{r},\mathbf{r}_s)}$

${\color{red} g_s'(\mathbf{r},\mathbf{r}_s)} =$

$$\frac{j{\color{blue} V(\mathbf{r},\mathbf{r}_s)}}{8\pi k_f^2 D}\int_{-\infty}^{+\infty} e^{jk_\xi(\xi-\xi_s)} \begin{bmatrix} e^{j\sqrt{k_f^2-k_\xi^2}(\mu-\mu_b)} & e^{-\sqrt{k_f^2+k_\xi^2}(\mu-\mu_b)}\end{bmatrix}\begin{bmatrix}R_{pp} & R_{ep}\\ R_{pe} & R_{ee}\end{bmatrix}\begin{bmatrix}\dfrac{e^{j\sqrt{k_f^2-k_\xi^2}(\mu_b-\mu_s)}}{\sqrt{k_f^2-k_\xi^2}}\\ j\dfrac{e^{-\sqrt{k_f^2+k_\xi^2}(\mu_b-\mu_s)}}{\sqrt{k_f^2+k_\xi^2}}\end{bmatrix} dk_\xi$$

1$^{\text{st}}$ reflection on boundaries: image sources directly generated from the original source.

Green's function of a polygonal plate

$$G_\Omega(\mathbf{r},\mathbf{r}_0) = \underbrace{G_\infty(\mathbf{r},\mathbf{r}_0)}_{\text{original source}} + \underbrace{\sum_{s=1}^{N} g_s(\mathbf{r},\mathbf{r}_s)}_{\text{image sources}}$$

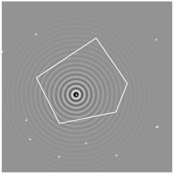

$G_\infty(\mathbf{r},\mathbf{r}_0)$

$+$

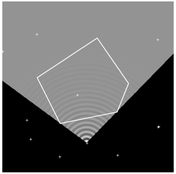

$g_s'(\mathbf{r},\mathbf{r}_s)$

$+$

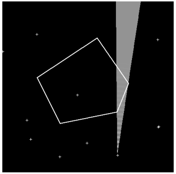

$g_s''(\mathbf{r},\mathbf{r}_s)$

$$g_s''(\mathbf{r},\mathbf{r}_s) \simeq \frac{jV(\mathbf{r},\mathbf{r}_s)}{8\pi k_f^2 D} \int_{-|k_f|}^{|k_f|} \underbrace{e^{jk_\xi(\xi-\xi_s)} A_{pp}^{(s)}(k_\xi,k_f) \frac{e^{j\sqrt{k_f^2-k_\xi^2}(\mu-\mu_s)}}{\sqrt{k_f^2-k_\xi^2}}}_{\text{propagating plane wave}} dk_\xi$$

$$A_{pp}^{(s)}(\theta) = \prod_{n=1}^{N(s)} R_n^{(s)}(\theta,\alpha_n)$$

(n = number of reflecting edge in source history)

($k_\xi = |k_f|\cos(\theta)$ for propagating waves)

2$^{\text{nd}}$ and subsequent reflections: "images of images". Evanescent waves are ignored.

Green's function of a polygonal plate

$$G_\Omega(\mathbf{r},\mathbf{r}_0) = \underbrace{G_\infty(\mathbf{r},\mathbf{r}_0)}_{\text{original source}} + \underbrace{\sum_{s=1}^{N} g_s(\mathbf{r},\mathbf{r}_s)}_{\text{image sources}}$$

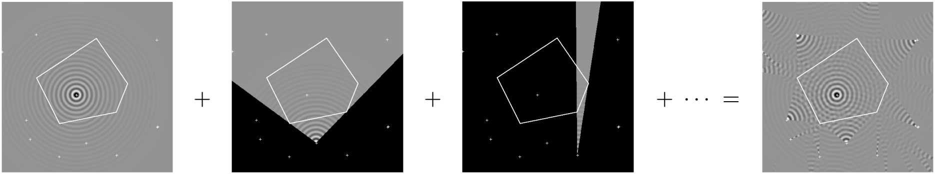

$G_\infty(\mathbf{r},\mathbf{r}_0) + g'_s(\mathbf{r},\mathbf{r}_s) + g''_s(\mathbf{r},\mathbf{r}_s) + \cdots = G_\Omega(\mathbf{r},\mathbf{r}_0)$

Estimated Green's function of the polygonal plate

Green's function of a polygonal plate: Validation (1/2)

Tested plate: **SS-C-SS-SS Levy square plate**

Steel, 2 mm thick, 1 m $\times$ 1 m, frequency: 3 kHz

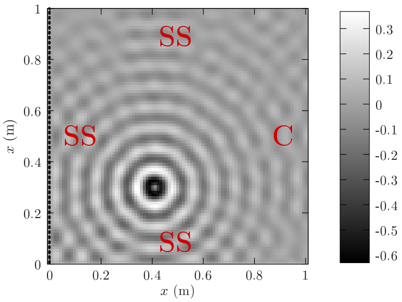

$\gamma = 4.5 \;\Rightarrow$ 126 sources

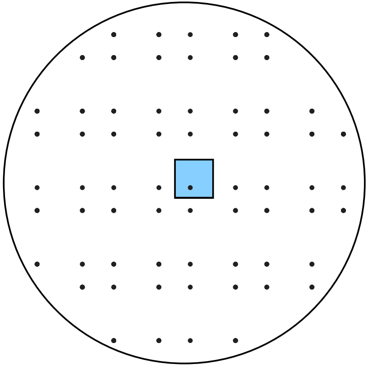

Green's function of a polygonal plate: Validation (1/2)

Tested plate: **SS-C-SS-SS Levy square plate**

Steel, 2 mm thick, 1 m $\times$ 1 m, frequency: 3 kHz

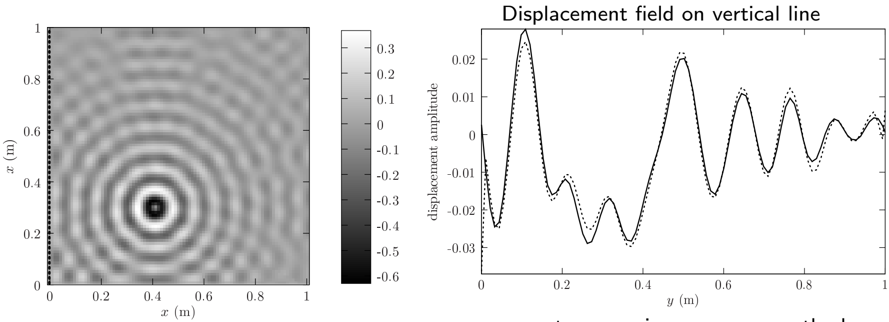

—— exact; ······ image source method

Green's function of a polygonal plate: Validation (1/2)

Tested plate: **SS-C-SS-SS Levy square plate**

Steel, 2 mm thick, 1 m $\times$ 1 m, frequency: 3 kHz

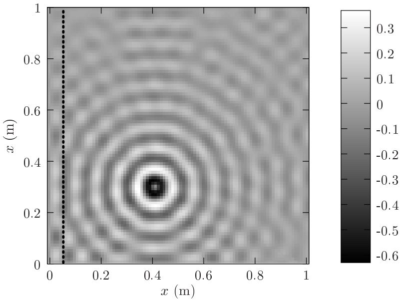

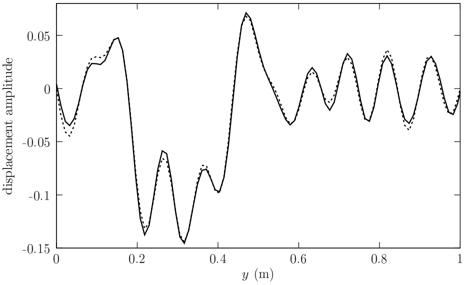

—— exact; ······ image source method

Green's function of a polygonal plate: Validation (1/2)

Tested plate: **SS-C-SS-SS Levy square plate**

Steel, 2 mm thick, 1 m $\times$ 1 m, frequency: 3 kHz

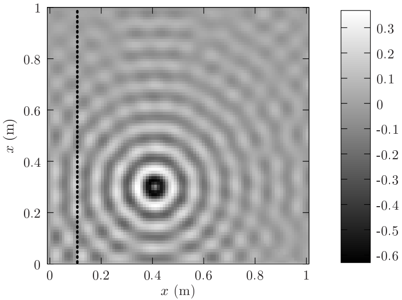

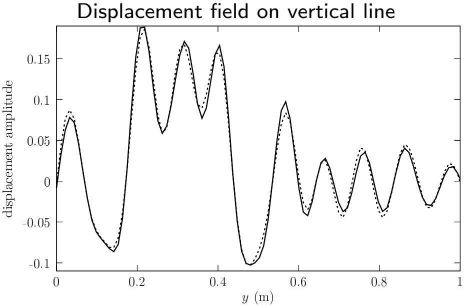

—— exact; · · · · · · image source method

Green's function of a polygonal plate: Validation (1/2)

Tested plate: **SS-C-SS-SS Levy square plate**

Steel, 2 mm thick, 1 m $\times$ 1 m, frequency: 3 kHz

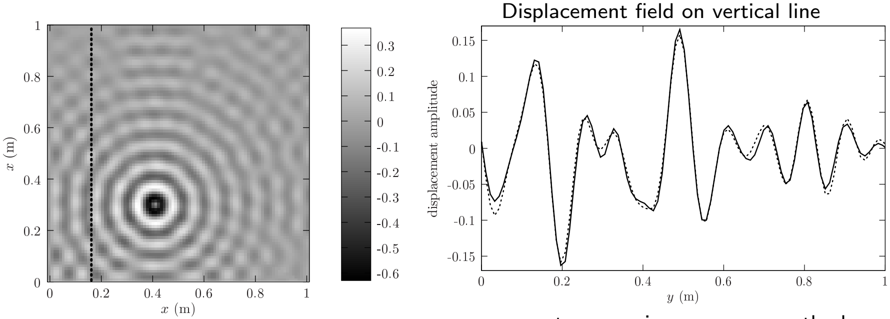

—— exact; ······ image source method

Green's function of a polygonal plate: Validation (1/2)

Tested plate: **SS-C-SS-SS Levy square plate**

Steel, 2 mm thick, 1 m $\times$ 1 m, frequency: 3 kHz

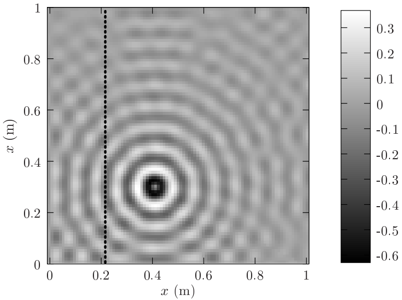

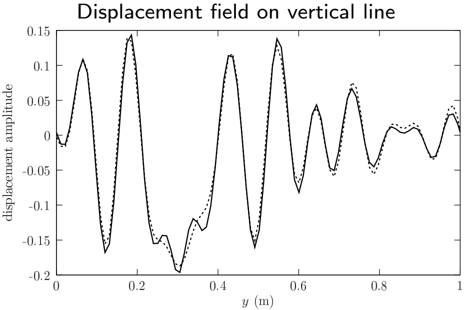

—— exact; $\cdots\cdots$ image source method

Green's function of a polygonal plate: Validation (1/2)

Tested plate: **SS-C-SS-SS Levy square plate**

Steel, 2 mm thick, 1 m $\times$ 1 m, frequency: 3 kHz

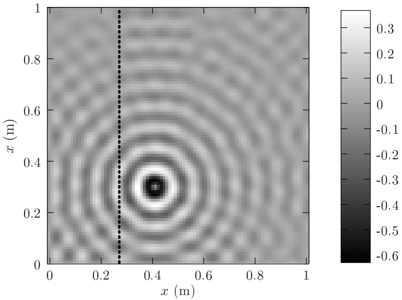

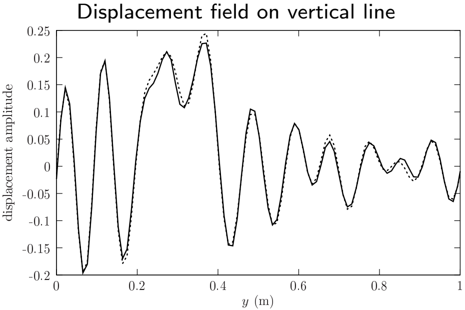

—— exact; ······ image source method

Green's function of a polygonal plate: Validation (1/2)

Tested plate: **SS-C-SS-SS Levy square plate**

Steel, 2 mm thick, 1 m $\times$ 1 m, frequency: 3 kHz

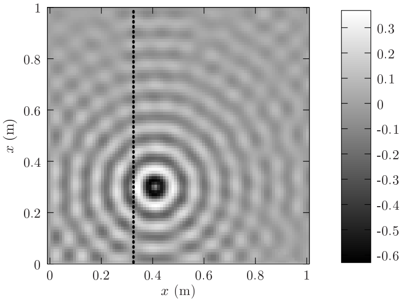

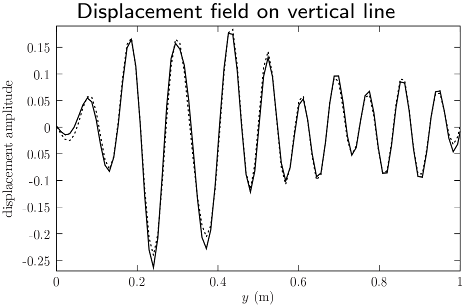

—— exact; ······ image source method

Green's function of a polygonal plate: Validation (1/2)

Tested plate: **SS-C-SS-SS Levy square plate**

Steel, 2 mm thick, 1 m $\times$ 1 m, frequency: 3 kHz

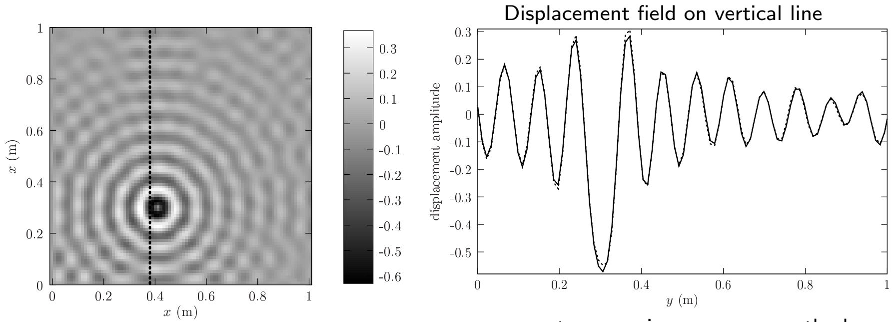

—— exact; $\cdots\cdots$ image source method

Green's function of a polygonal plate: Validation (1/2)

Tested plate: **SS-C-SS-SS Levy square plate**

Steel, 2 mm thick, 1 m $\times$ 1 m, frequency: 3 kHz

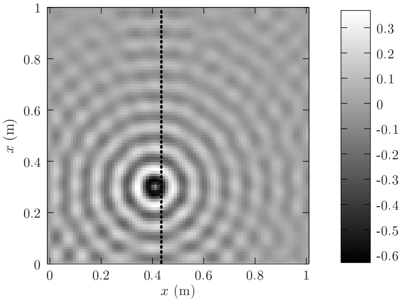

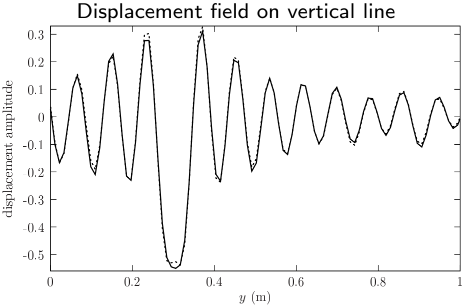

—— exact; ······ image source method

Green's function of a polygonal plate: Validation (1/2)

Tested plate: **SS-C-SS-SS Levy square plate**

Steel, 2 mm thick, 1 m $\times$ 1 m, frequency: 3 kHz

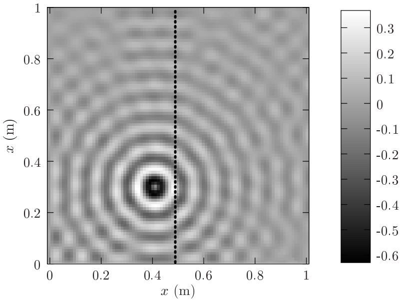

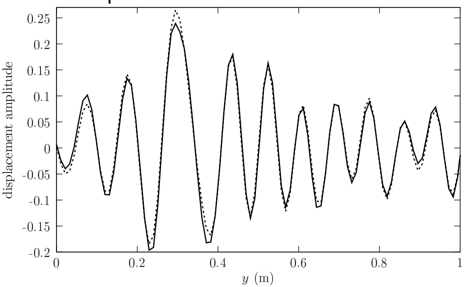

—— exact; · · · · · · image source method

Green's function of a polygonal plate: Validation (1/2)

Tested plate: **SS-C-SS-SS Levy square plate**

Steel, 2 mm thick, 1 m $\times$ 1 m, frequency: 3 kHz

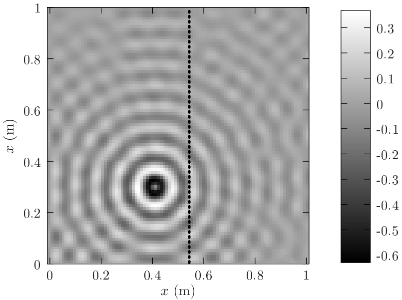

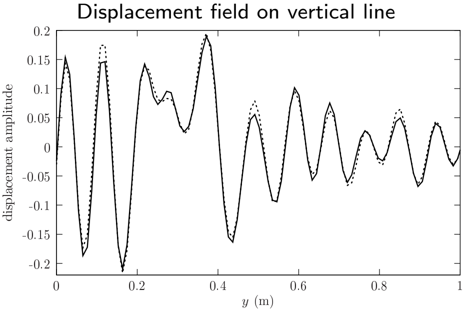

—— exact; ······ image source method

Green's function of a polygonal plate: Validation (1/2)

Tested plate: **SS-C-SS-SS Levy square plate**

Steel, 2 mm thick, 1 m $\times$ 1 m, frequency: 3 kHz

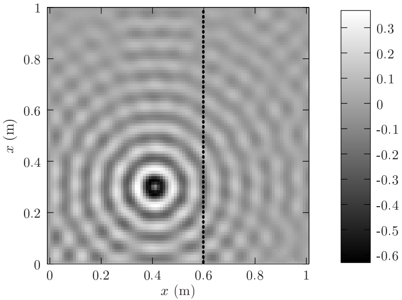

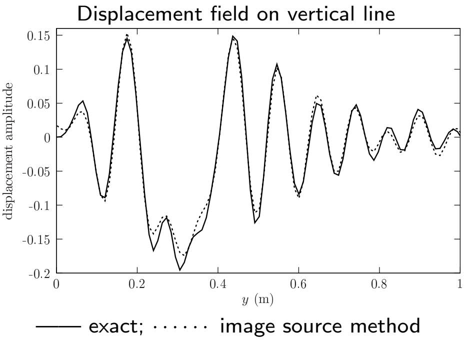

Green's function of a polygonal plate: Validation (1/2)

Tested plate: **SS-C-SS-SS Levy square plate**

Steel, 2 mm thick, 1 m $\times$ 1 m, frequency: 3 kHz

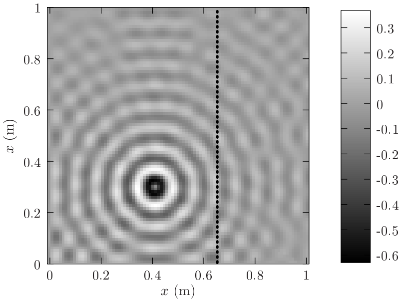

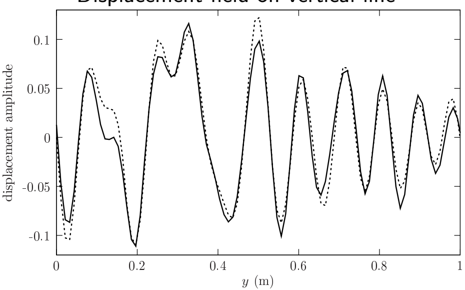

—— exact; · · · · · · image source method

Green's function of a polygonal plate: Validation (1/2)

Tested plate: **SS-C-SS-SS Levy square plate**

Steel, 2 mm thick, 1 m $\times$ 1 m, frequency: 3 kHz

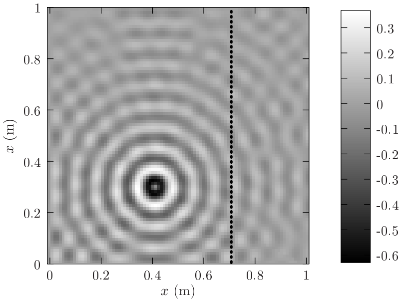

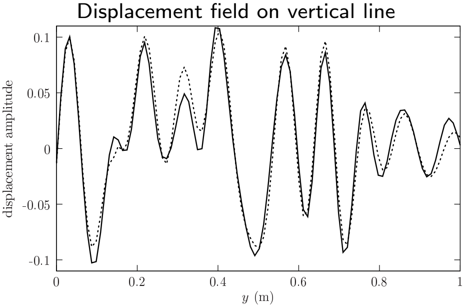

—— exact; ······ image source method

Green's function of a polygonal plate: Validation (1/2)

Tested plate: **SS-C-SS-SS Levy square plate**

Steel, 2 mm thick, 1 m $\times$ 1 m, frequency: 3 kHz

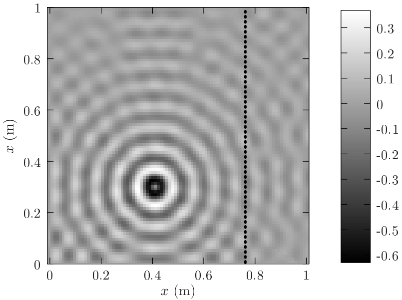

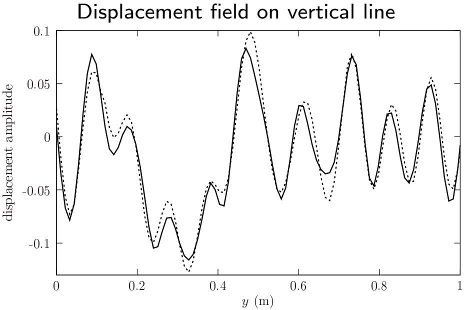

—— exact; · · · · · · image source method

Green's function of a polygonal plate: Validation (1/2)

Tested plate: **SS-C-SS-SS Levy square plate**

Steel, 2 mm thick, 1 m $\times$ 1 m, frequency: 3 kHz

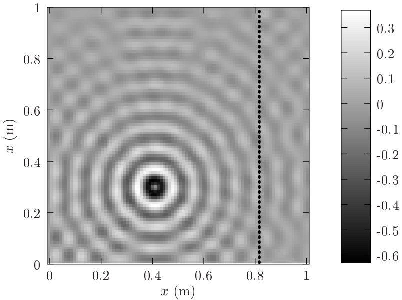

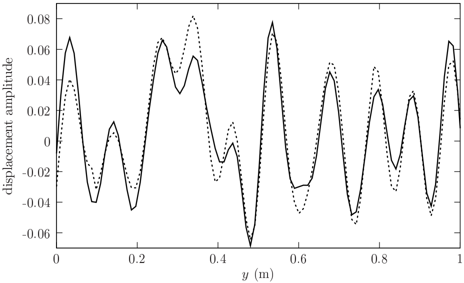

—— exact; ······ image source method

Green's function of a polygonal plate: Validation (1/2)

Tested plate: **SS-C-SS-SS Levy square plate**

Steel, 2 mm thick, 1 m $\times$ 1 m, frequency: 3 kHz

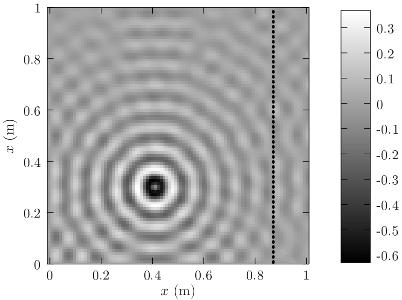

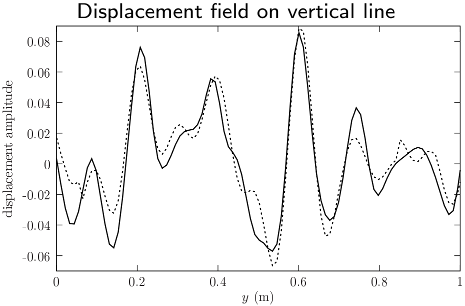

—— exact; ······ image source method

Green's function of a polygonal plate: Validation (1/2)

Tested plate: **SS-C-SS-SS Levy square plate**

Steel, 2 mm thick, 1 m × 1 m, frequency: 3 kHz

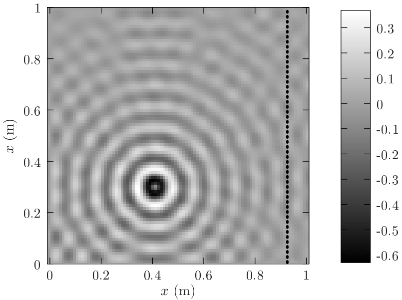

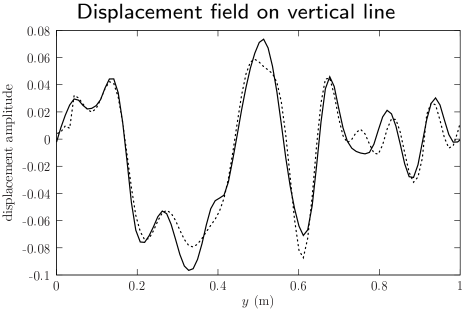

—— exact; ······ image source method

Green's function of a polygonal plate: Validation (1/2)

Tested plate: **SS-C-SS-SS Levy square plate**

Steel, 2 mm thick, 1 m $\times$ 1 m, frequency: 3 kHz

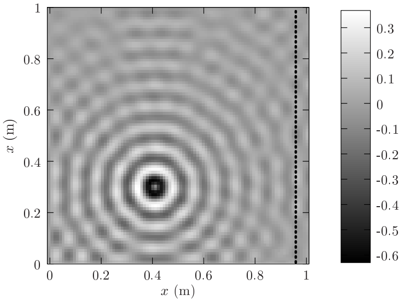

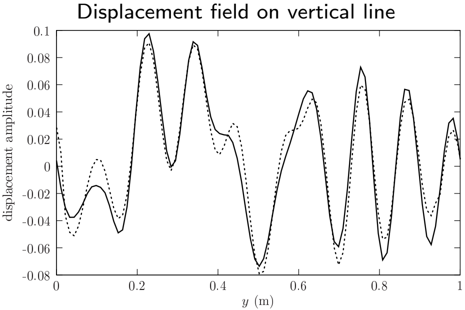

—— exact; ······ image source method

Green's function of a polygonal plate: Validation (1/2)

Tested plate: **SS-C-SS-SS Levy square plate**

Steel, 2 mm thick, 1 m $\times$ 1 m, frequency: 3 kHz

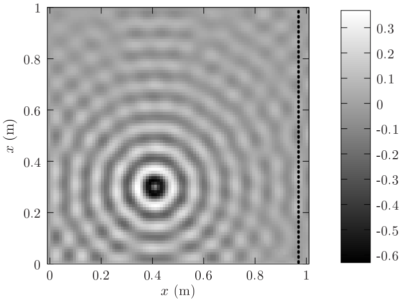

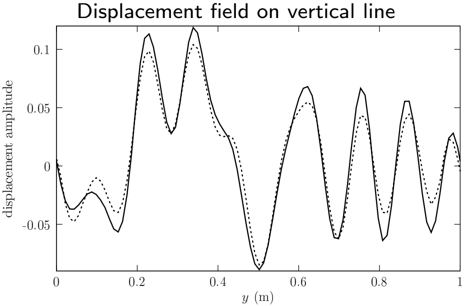

—— exact; $\cdots\cdots$ image source method

Green's function of a polygonal plate: Validation (1/2)

Tested plate: **SS-C-SS-SS Levy square plate**

Steel, 2 mm thick, 1 m × 1 m, frequency: 3 kHz

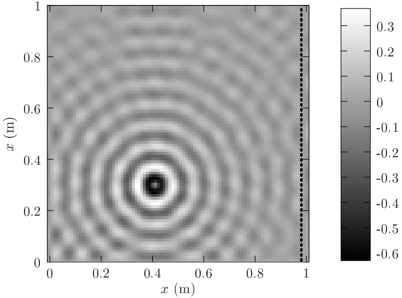

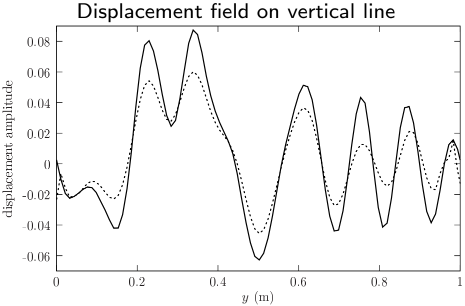

—— exact; ······ image source method

Green's function of a polygonal plate: Validation (1/2)

Tested plate: **SS-C-SS-SS Levy square plate**

Steel, 2 mm thick, 1 m $\times$ 1 m, frequency: 3 kHz

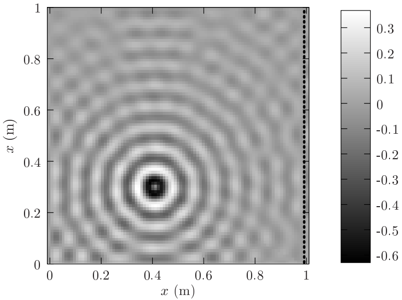

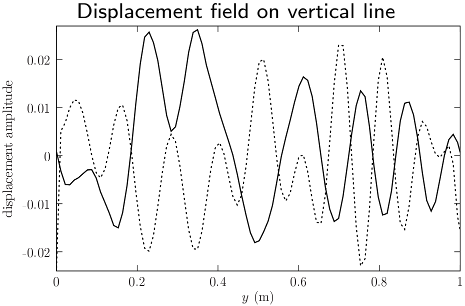

—— exact; ······ image source method

Green's function of a polygonal plate: Validation (1/2)

Tested plate: **SS-C-SS-SS Levy square plate**

Steel, 2 mm thick, 1 m $\times$ 1 m, frequency: 3 kHz

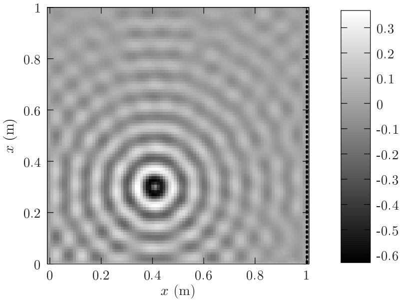

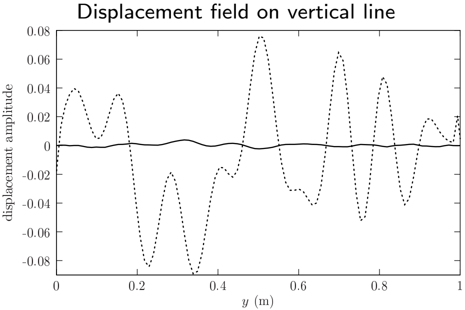

—— exact; ······ image source method

Green's function of a polygonal plate: Validation (1/2)

Tested plate: **SS-C-SS-SS Levy square plate**

Steel, 2 mm thick, 1 m $\times$ 1 m, frequency: 3 kHz

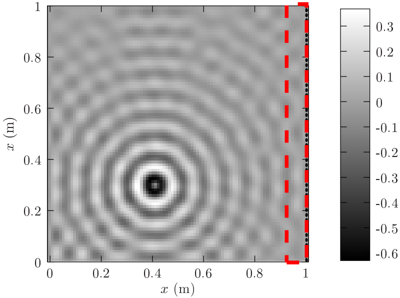

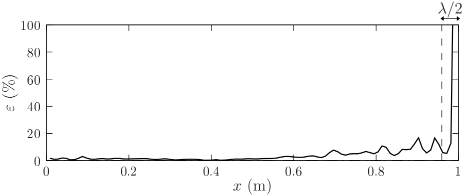

Discrepancies appear in the nearfield of the edges due to the ignored evanescent components.

The displacement field is accurately predicted elsewhere.

Green's function of a polygonal plate: Validation (1/2)

Tested plate: **SS-C-SS-SS Levy square plate**

Steel, 2 mm thick, 1 m × 1 m, frequency: 3 kHz

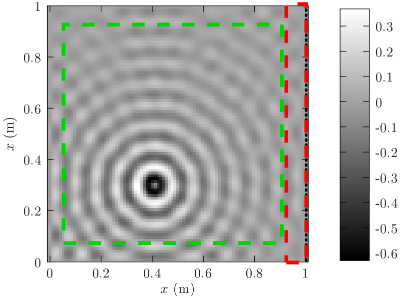

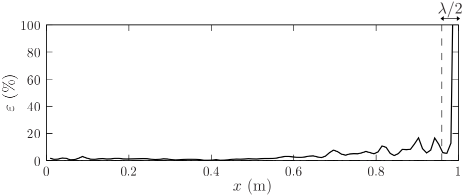

Discrepancies appear in the nearfield of the edges due to the ignored evanescent components.

The displacement field is accurately predicted elsewhere.

Green's function of a polygonal plate: Validation (2/2)

Tested plate: **C-SS-SS-SS-SS arbitrary polygonal plate** Steel, 2 mm thick, 1 m $\times$ 1 m

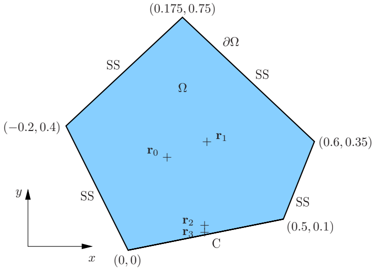

Green's function of a polygonal plate: Validation (2/2)

Tested plate: **C-SS-SS-SS-SS arbitrary polygonal plate** Steel, 2 mm thick, 1 m × 1 m

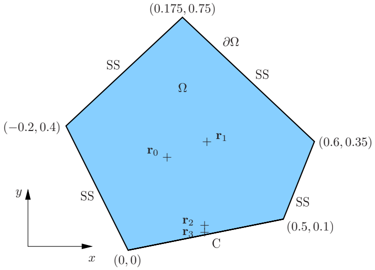

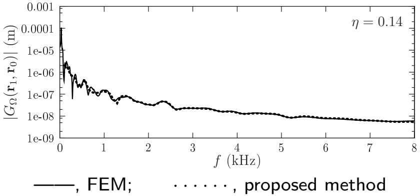

Green's function at $\mathbf{r}_1$

Green's function of a polygonal plate: Validation (2/2)

Tested plate: **C-SS-SS-SS-SS arbitrary polygonal plate** Steel, 2 mm thick, 1 m $\times$ 1 m

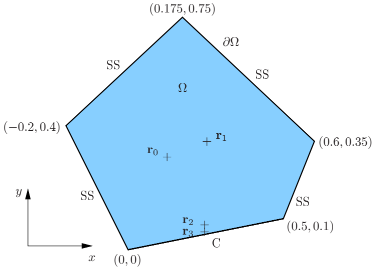

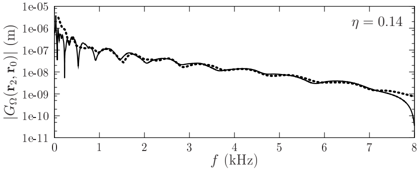

——, FEM; · · · · · ·, proposed method

Green's function at $\mathbf{r}_2$

Green's function of a polygonal plate: Validation (2/2)

Tested plate: **C-SS-SS-SS-SS arbitrary polygonal plate** Steel, 2 mm thick, 1 m × 1 m

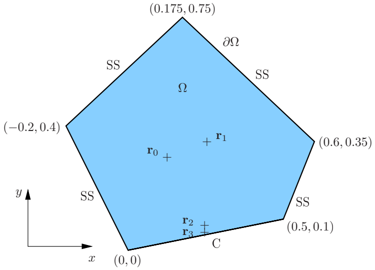

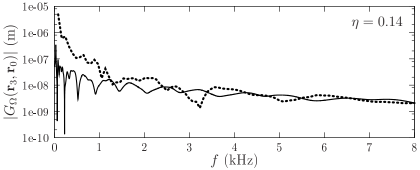

——, FEM; · · · · · ·, proposed method

Green's function at $\mathbf{r}_3$

The error increases in the nearfield of the boundary.
The accuracy is improved with frequency and damping.

1. Model of the flexural vibrations of polygonal plates by the image source method
   - Introduction
   - Generalisation to arbitrary convex polygonal geometry
   - General boundary conditions
   - Polygonal plates
   - Plate assemblies

2. Acoustic black hole effect for vibration damping in plates and beams
   - Principle
   - Model
   - Experiments
   - Black-hole effect by a thermal gradient

Green's function of a plate assembly

Problem to solve

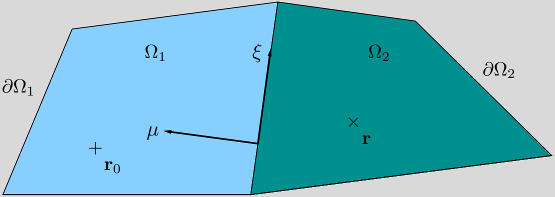

- Plane assembly
- Arbitrary convex geometry
- Arbitrary boundary conditions

$$\begin{cases} D\left(\nabla^4 - k_f^4\right) G_\Omega(\mathbf{r}, \mathbf{r}_0; k_f) = \delta(\mathbf{r} - \mathbf{r}_0) & \text{(plate } \Omega_1\text{)} \\ D\left(\nabla^4 - k_f^4\right) G_\Omega(\mathbf{r}, \mathbf{r}_0; k_f) = 0 & \text{(plate } \Omega_2\text{)} \\ \text{Boundary conditions} & \text{(edges of } \Omega_1\text{)} \\ \text{Boundary conditions} & \text{(edges of } \Omega_2\text{)} \\ \text{Boundary conditions} & \text{(junction)} \end{cases}$$

Model of the junction:
Scattering matrix

Green's function of a plate assembly: Construction of image sources

The original source in Ω_1 ...

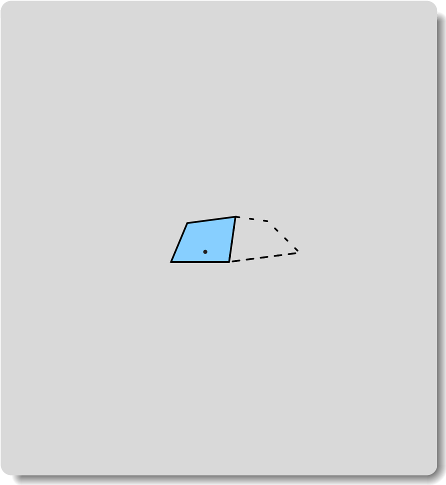

Green's function of a plate assembly: Construction of image sources

The original source in Ω_1 ...

generates some image sources for plate Ω_1.

Internal reflections in plate Ω_1

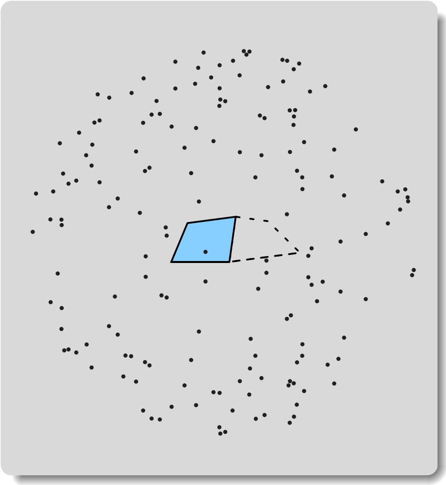

Green's function of a plate assembly: Construction of image sources

Transmission to plate Ω_2

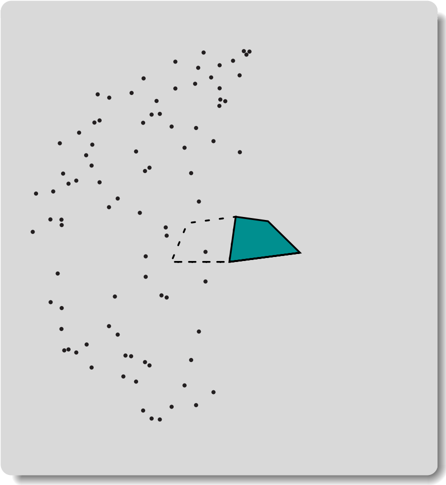

A subset of those new sources is visible from plate Ω_2, ...

Green's function of a plate assembly: Construction of image sources

Internal reflections in plate Ω_2

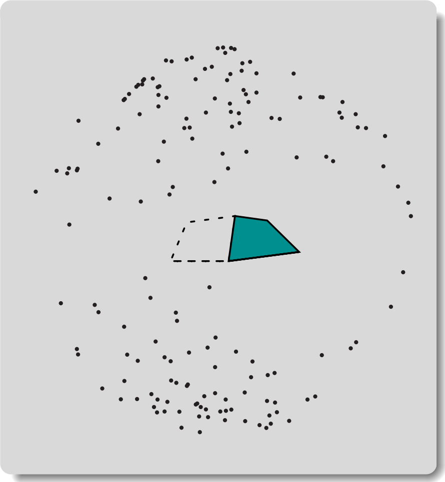

A subset of those new sources is visible from plate Ω_2, ...

which generates new image sources for plate Ω_2.

Green's function of a plate assembly: Construction of image sources

Transmission to plate Ω_1

A subset of those new sources is visible from plate Ω_1, ...

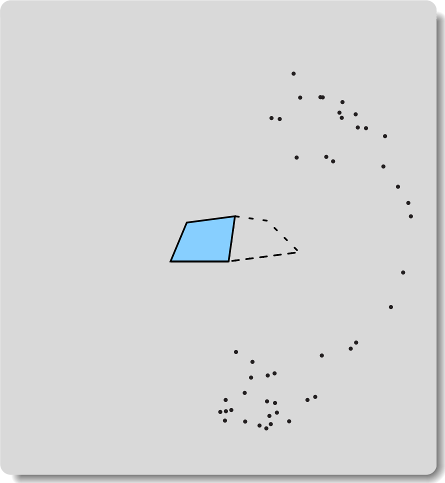

Green's function of a plate assembly: Construction of image sources

Internal reflections in plate Ω_1

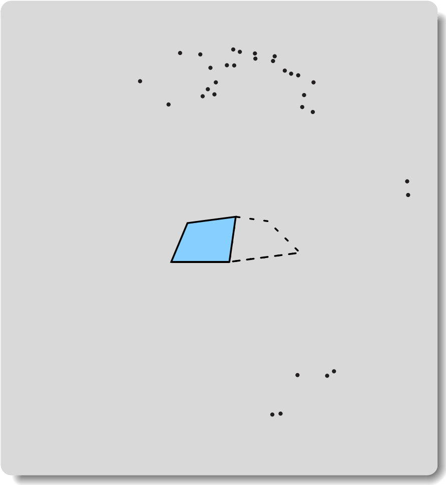

A subset of those new sources is visible from plate Ω_1, ...

which generates new image sources for plate Ω_1.

Green's function of a plate assembly: Construction of image sources

Transmission to plate Ω_2

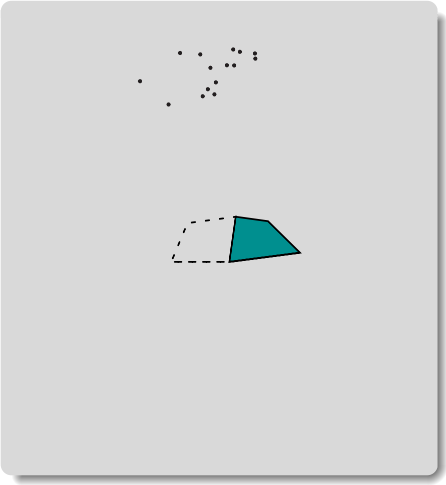

A subset of those new sources is visible from plate Ω_2.

Green's function of a plate assembly: Construction of image sources

Internal reflections in plate Ω_2

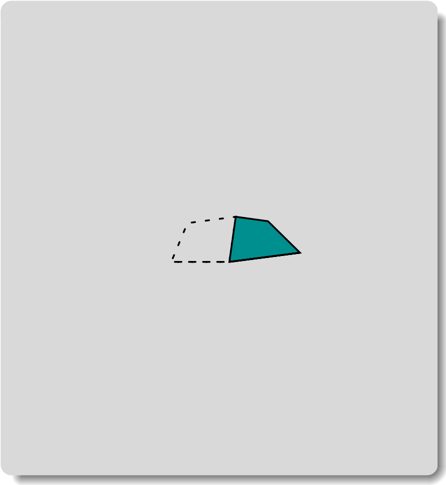

A subset of those new sources is visible from plate Ω_2.

The next iteration does not generate new image sources in the chosen truncation radius.

Green's function of a plate assembly: Construction of image sources

Evanescent waves are ignored for the second and subsequent reflections and transmissions

Green's function of a plate assembly: Examples

Tested junction: **continuity between two rectangular plates**

Aluminium, 2 mm thick, 1 m × 0.7 m, simply supported edges

$G_\Omega(\mathbf{r}, \mathbf{r}_0; k_f)$ at 3 kHz

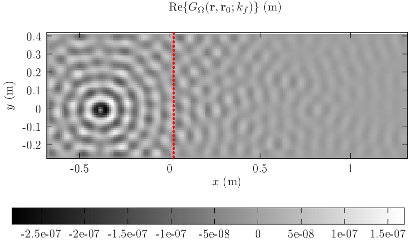

Displacement field

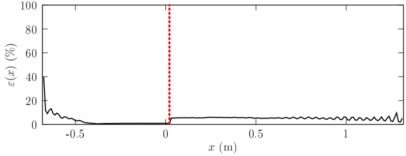

Error on vertical lines

Green's function of a plate assembly: Examples

Tested junction: **continuity between two rectangular plates**

Aluminium, 2 mm thick, 1 m $\times$ 0.7 m, simply supported edges

$G_\Omega(\mathbf{r}, \mathbf{r}_0; k_f)$ at 3 kHz

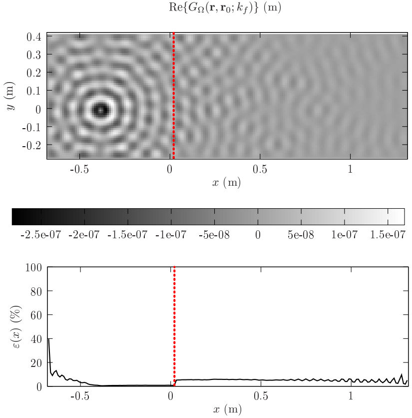

$G_\Omega(\mathbf{r}, \mathbf{r}_0; k_f)$ at 7 kHz

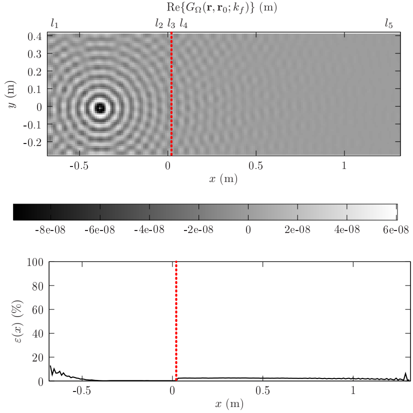

Green's function of a plate assembly: Examples

Tested junction: **continuity between two rectangular plates**

Aluminium, 2 mm thick, $\sim$ 2 m $\times$ $\sim$ 0.7 m, simply supported edges

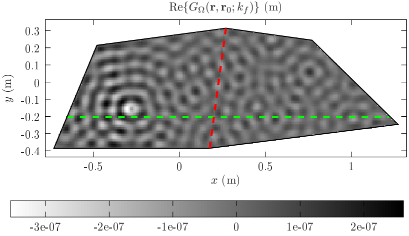

Displacement field

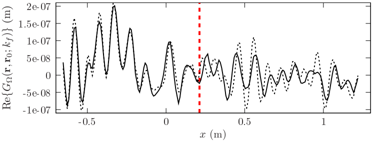

Displacement field along the green line

1. Model of the flexural vibrations of polygonal plates by the image source method
   - Introduction
   - Generalisation to arbitrary convex polygonal geometry
   - General boundary conditions
   - Polygonal plates
   - Plate assemblies

2. Acoustic black hole effect for vibration damping in plates and beams
   - Principle
   - Model
   - Experiments
   - Black-hole effect by a thermal gradient

Principle of the acoustic black hole effect in plates

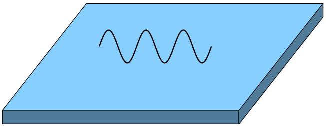

Uniform thickness

$$c_\varphi = \left(\frac{E\omega^2}{12\rho\,(1-\nu^2)} \right)^{1/4} \sqrt{h}$$

Principle of the acoustic black hole effect in plates

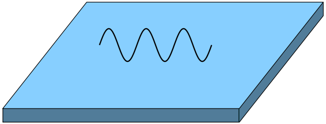

Uniform thickness

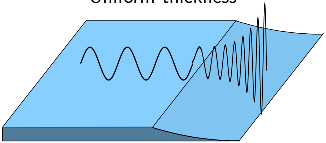

Power-law thickness

$$c_\varphi = \left(\frac{E\omega^2}{12\rho\left(1-\nu^2\right)} \right)^{1/4} \sqrt{h}$$

$$c_\varphi(x) = \left(\frac{E\omega^2}{12\rho\left(1-\nu^2\right)} \right)^{1/4} \sqrt{h(x)}$$

Principle of the acoustic black hole effect in plates

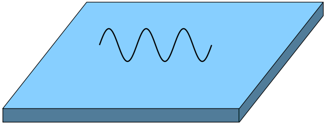

Uniform thickness

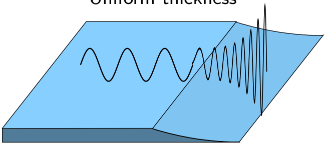

Power-law thickness

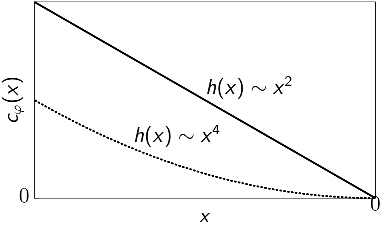

Phase velocity

$$c_\varphi = \left(\frac{E\omega^2}{12\rho\,(1-\nu^2)} \right)^{1/4} \sqrt{h}$$

$$c_\varphi(x) = \left(\frac{E\omega^2}{12\rho\,(1-\nu^2)} \right)^{1/4} \sqrt{h(x)}$$

A flexural wave travelling towards the edge slows down and stops at $x = 0$.

Previous work

Ideal situation

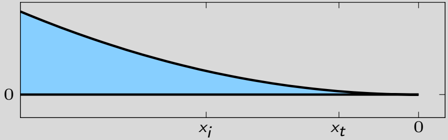

Mironov, Soviet Physics – Acoustics 34 (1988)

$$T = \int_{x_i}^{x_t} \frac{dx}{c_\gamma(x)} \xrightarrow{x_t \to 0} \infty$$

$$R = \exp\left(-2\int_{x_i}^{x_t} \mathrm{Im}\left\{k_f(x)\right\} dx\right) \xrightarrow{x_t \to 0} 0$$

Previous work

Ideal situation

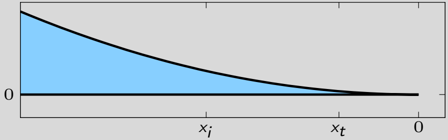

Mironov, Soviet Physics – Acoustics 34 (1988)

Practical situation

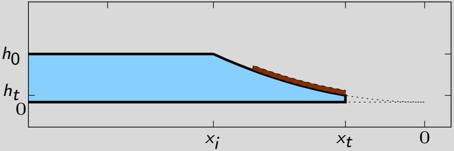

Krylov, A. Acustica united with Acustica. 90 (2004)
Krylov and Tilman, J. Sound Vib. 274 (2004)
Krylov and Winward, J. Sound Vib. 300 (2007)

$$T = \int_{x_i}^{x_t} \frac{dx}{c_\gamma(x)} \xrightarrow{x_t \to 0} \infty$$

$$R = \exp\left(-2 \int_{x_i}^{x_t} \mathrm{Im}\left\{k_f(x)\right\} dx\right) \xrightarrow{x_t \to 0} 0$$

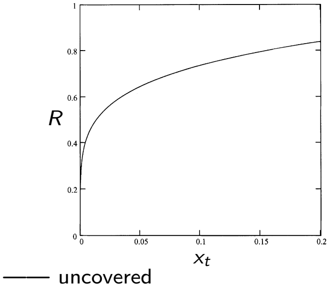

Previous work

Ideal situation

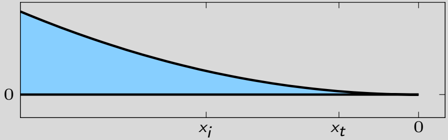

Mironov, Soviet Physics – Acoustics 34 (1988)

Practical situation

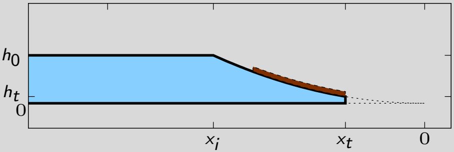

Krylov, A. Acustica united with Acustica. 90 (2004)
Krylov and Tilman, J. Sound Vib. 274 (2004)
Krylov and Winward, J. Sound Vib. 300 (2007)

$$T = \int_{x_i}^{x_t} \frac{dx}{c_\gamma(x)} \xrightarrow{x_t \to 0} \infty$$

$$R = \exp\left(-2\int_{x_i}^{x_t} \mathrm{Im}\left\{k_f(x)\right\} dx\right) \xrightarrow{x_t \to 0} 0$$

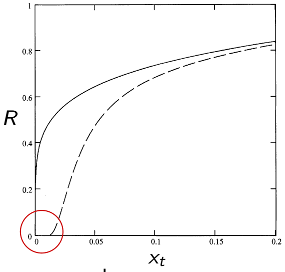

Previous work

Ideal situation

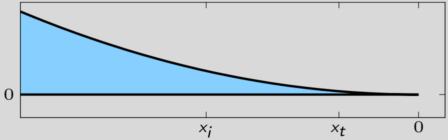

Mironov, Soviet Physics – Acoustics 34 (1988)

Practical situation

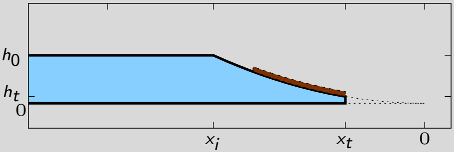

Krylov, A. Acustica united with Acustica. 90 (2004)
Krylov and Tilman, J. Sound Vib. 274 (2004)
Krylov and Winward, J. Sound Vib. 300 (2007)

$$T = \int_{x_i}^{x_t} \frac{dx}{c_\gamma(x)} \xrightarrow{x_t \to 0} \infty$$

$$R = \exp\left(-2\int_{x_i}^{x_t} \mathrm{Im}\left\{k_f(x)\right\} dx\right) \xrightarrow{x_t \to 0} 0$$

- The geometrical acoustics approximation ignores evanescent waves
- The approach is limited to relatively simple variations of geometrical and material parameters

Aims

Aims

- Include the total wave field in the model
- Optimise geometrical and material parameters
- Include in non-academic plate geometries
- Explore other configurations for achieving the black hole effect

Model

Modelled beam

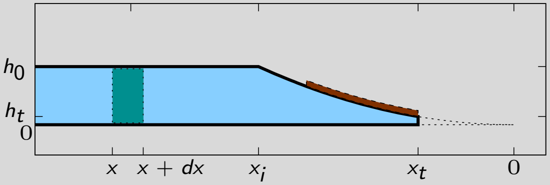

State equation:

$$\frac{\partial \mathbf{W}}{\partial x} = \mathbf{H}\mathbf{W}$$

State vector:

$$\mathbf{W}(x) = \begin{bmatrix} w(x) \\ \theta(x) \\ V(x) \\ M(x) \end{bmatrix}$$

Impedance matrix **Z** given by:

$$\begin{bmatrix} V(x) \\ M(x) \end{bmatrix} = j\omega \mathbf{Z}(x) \begin{bmatrix} w(x) \\ \theta(x) \end{bmatrix}$$

Riccati equation and boundary condition:

$$\begin{cases} \dfrac{\partial \mathbf{Z}}{\partial x} = -\mathbf{Z}\mathbf{H}_1 - j\omega \mathbf{Z}\mathbf{H}_2\mathbf{Z} + \dfrac{\mathbf{H}_3}{j\omega} + \mathbf{H}_4\mathbf{Z} \\ \mathbf{Z}(x_t) = 0 \end{cases} \longrightarrow \boxed{\text{iterative solution (adaptive spatial step)}} \longrightarrow \mathbf{Z}(x)$$

$$\mathbf{Z}(x) \Longrightarrow \mathbf{R}(x) = \begin{bmatrix} R_{pp} & R_{ep} \\ R_{pe} & R_{ee} \end{bmatrix}$$

The model includes

- Arbitrary thickness variations
- Arbitrary material properties

Model

Modelled beam

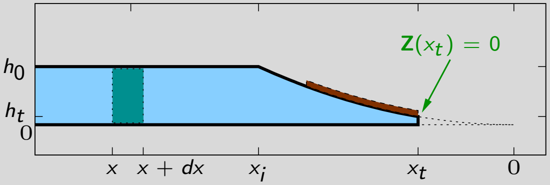

State equation:

$$\frac{\partial \mathbf{W}}{\partial x} = \mathbf{HW}$$

State vector:

$$\mathbf{W}(x) = \begin{bmatrix} w(x) \\ \theta(x) \\ V(x) \\ M(x) \end{bmatrix}$$

Impedance matrix **Z** given by:

$$\begin{bmatrix} V(x) \\ M(x) \end{bmatrix} = j\omega \mathbf{Z}(x) \begin{bmatrix} w(x) \\ \theta(x) \end{bmatrix}$$

Riccati equation and boundary condition:

$$\begin{cases} \dfrac{\partial \mathbf{Z}}{\partial x} = -\mathbf{ZH}_1 - j\omega \mathbf{ZH}_2\mathbf{Z} + \dfrac{\mathbf{H}_3}{j\omega} + \mathbf{H}_4\mathbf{Z} \\ \mathbf{Z}(x_t) = 0 \end{cases} \longrightarrow \boxed{\begin{array}{c}\text{iterative solution} \\ \text{(adaptive spatial step)}\end{array}} \longrightarrow \mathbf{Z}(x)$$

$$\mathbf{Z}(x) \Longrightarrow \mathbf{R}(x) = \begin{bmatrix} R_{pp} & R_{ep} \\ R_{pe} & R_{ee} \end{bmatrix}$$

The model includes

- Arbitrary thickness variations
- Arbitrary material properties

Model

Modelled beam

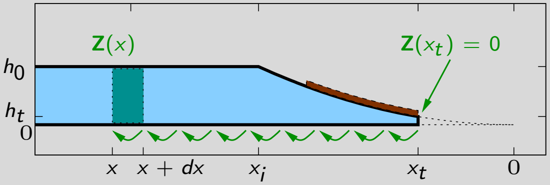

State equation:

$$\frac{\partial \mathbf{W}}{\partial x} = \mathbf{H}\mathbf{W}$$

State vector:

$$\mathbf{W}(x) = \begin{bmatrix} w(x) \\ \theta(x) \\ V(x) \\ M(x) \end{bmatrix}$$

Impedance matrix $\mathbf{Z}$ given by:

$$\begin{bmatrix} V(x) \\ M(x) \end{bmatrix} = j\omega \mathbf{Z}(x) \begin{bmatrix} w(x) \\ \theta(x) \end{bmatrix}$$

Riccati equation and boundary condition:

$$\begin{cases} \dfrac{\partial \mathbf{Z}}{\partial x} = -\mathbf{Z}\mathbf{H}_1 - j\omega \mathbf{Z}\mathbf{H}_2\mathbf{Z} + \dfrac{\mathbf{H}_3}{j\omega} + \mathbf{H}_4\mathbf{Z} \\ \mathbf{Z}(x_t) = 0 \end{cases} \longrightarrow \boxed{\text{iterative solution (adaptive spatial step)}} \longrightarrow \mathbf{Z}(x)$$

$$\mathbf{Z}(x) \Longrightarrow \mathbf{R}(x) = \begin{bmatrix} R_{pp} & R_{ep} \\ R_{pe} & R_{ee} \end{bmatrix}$$

The model includes

- Arbitrary thickness variations
- Arbitrary material properties

Model

Modelled beam

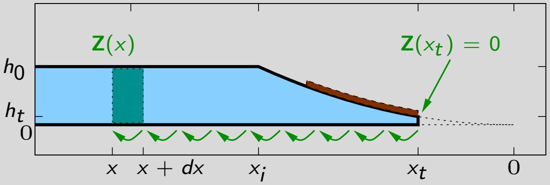

State equation:

$$\frac{\partial \mathbf{W}}{\partial x} = \mathbf{H}\mathbf{W}$$

State vector:

$$\mathbf{W}(x) = \begin{bmatrix} w(x) \\ \theta(x) \\ V(x) \\ M(x) \end{bmatrix}$$

Impedance matrix $\mathbf{Z}$ given by:

$$\begin{bmatrix} V(x) \\ M(x) \end{bmatrix} = j\omega \mathbf{Z}(x) \begin{bmatrix} w(x) \\ \theta(x) \end{bmatrix}$$

Riccati equation and boundary condition:

$$\begin{cases} \dfrac{\partial \mathbf{Z}}{\partial x} = -\mathbf{Z}\mathbf{H}_1 - j\omega \mathbf{Z}\mathbf{H}_2\mathbf{Z} + \dfrac{\mathbf{H}_3}{j\omega} + \mathbf{H}_4\mathbf{Z} \\ \mathbf{Z}(x_t) = 0 \end{cases} \longrightarrow \boxed{\begin{array}{c}\text{iterative solution} \\ \text{(adaptive spatial step)}\end{array}} \longrightarrow \mathbf{Z}(x)$$

$$\mathbf{Z}(x) \Longrightarrow \mathbf{R}(x) = \begin{bmatrix} R_{pp} & R_{ep} \\ R_{pe} & R_{ee} \end{bmatrix}$$

The model includes

- Arbitrary thickness variations
- Arbitrary material properties

Model: Optimisation rules

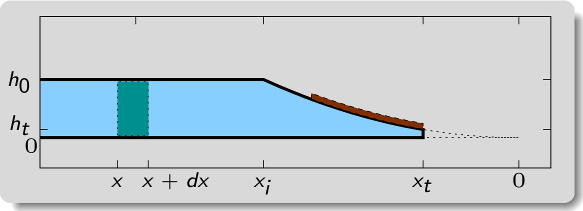

Parameters of the damping layer:

- E_l : Young's modulus
- η_l : loss factor
- l : length
- h_l : thickness

Model: Optimisation rules

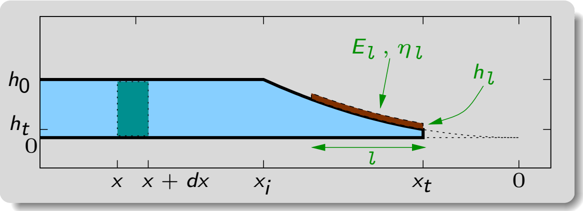

Parameters of the damping layer:

- E_l : Young's modulus
- η_l : loss factor
- l : length
- h_l : thickness

Model: Optimisation rules

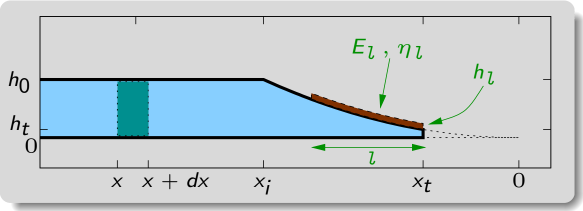

Parameters of the damping layer:

- E_l : Young's modulus
- η_l : loss factor
- l : length
- h_l : thickness

Parametric study

"Rules" for the design of acoustic black hole plates:

- **Truncation distance** x_t of the profile: **as short as possible**
- **Young's modulus** E_l of the damping layer: **as low as possible**
- **Loss factor** η_l of the damping layer: **as high as possible**
- **Length** l of the damping layer: intermediate value
- **Thickness** h_l of the damping layer: intermediate value

Model: Optimisation rules

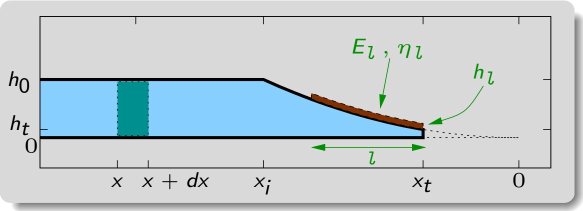

Parameters of the damping layer:

- E_l : Young's modulus
- η_l : loss factor
- l : length
- h_l : thickness

Parametric study

"Rules" for the design of acoustic black hole plates:

- **Truncation distance** x_t of the profile: **as short as possible**
- **Young's modulus** E_l of the damping layer: **as low as possible**
- **Loss factor** η_l of the damping layer: **as high as possible**
- **Length** l of the damping layer: intermediate value
- **Thickness** h_l of the damping layer: intermediate value

Model: Optimisation rules

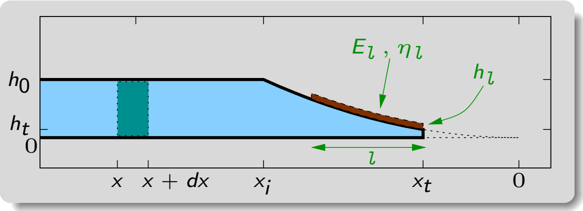

Parameters of the damping layer:

- E_l : Young's modulus
- η_l : loss factor
- l : length
- h_l : thickness

Parametric study

"Rules" for the design of acoustic black hole plates:

- **Truncation distance** x_t of the profile: **as short as possible**
- **Young's modulus** E_l of the damping layer: **as low as possible**
- **Loss factor** η_l of the damping layer: **as high as possible**
- **Length** l of the damping layer: intermediate value
- **Thickness** h_l of the damping layer: intermediate value

Model: Optimisation rules

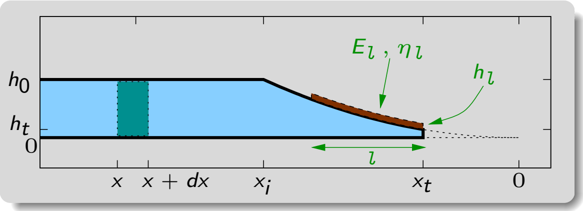

Parameters of the damping layer:

- E_l : Young's modulus
- η_l : loss factor
- l : length
- h_l : thickness

Parametric study

"Rules" for the design of acoustic black hole plates:

- **Truncation distance** x_t of the profile: **as short as possible**
- **Young's modulus** E_l of the damping layer: **as low as possible**
- **Loss factor** η_l of the damping layer: **as high as possible**
- **Length** l of the damping layer: intermediate value
- **Thickness** h_l of the damping layer: intermediate value

Model: Optimisation rules

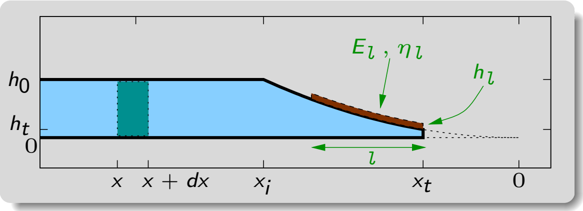

Parameters of the damping layer:

- E_l : Young's modulus
- η_l : loss factor
- l : length
- h_l : thickness

Parametric study

"Rules" for the design of acoustic black hole plates:

- **Truncation distance** x_t of the profile: **as short as possible**
- **Young's modulus** E_l of the damping layer: **as low as possible**
- **Loss factor** η_l of the damping layer: **as high as possible**
- **Length** l of the damping layer: intermediate value
- **Thickness** h_l of the damping layer: intermediate value

Model: Optimisation rules

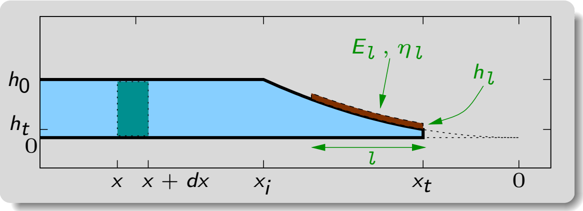

Parameters of the damping layer:

- E_l : Young's modulus
- η_l : loss factor
- l : length
- h_l : thickness

Parametric study

"Rules" for the design of acoustic black hole plates:

- **Truncation distance** x_t of the profile: **as short as possible**
- **Young's modulus** E_l of the damping layer: **as low as possible**
- **Loss factor** η_l of the damping layer: **as high as possible**
- **Length** l of the damping layer: intermediate value
- **Thickness** h_l of the damping layer: intermediate value

Model: Optimisation rules

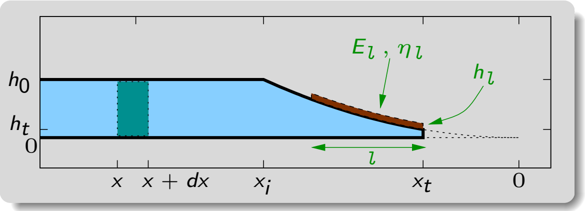

Parameters of the damping layer:

- E_l : Young's modulus
- η_l : loss factor
- l : length
- h_l : thickness

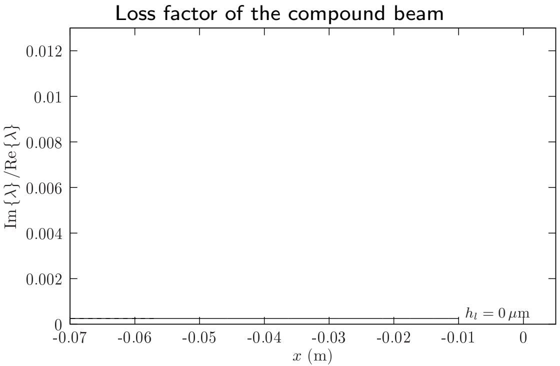

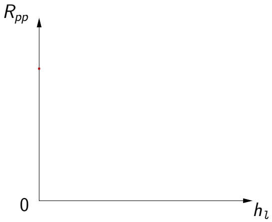

Model: Optimisation rules

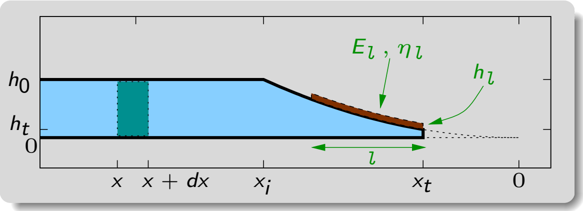

Parameters of the damping layer:

- E_l : Young's modulus
- η_l : loss factor
- l : length
- h_l : thickness

Loss factor of the compound beam

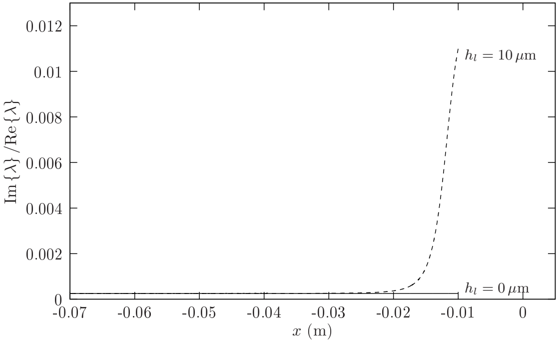

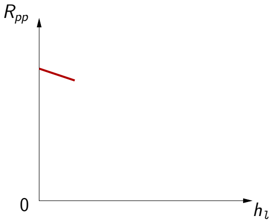

Model: Optimisation rules

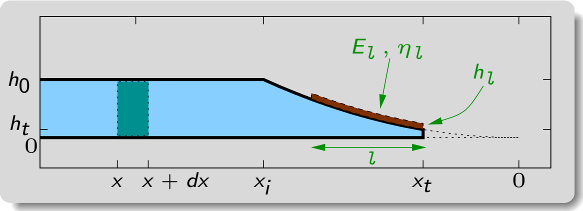

Parameters of the damping layer:

- E_l : Young's modulus
- η_l : loss factor
- l : length
- h_l : thickness

Loss factor of the compound beam

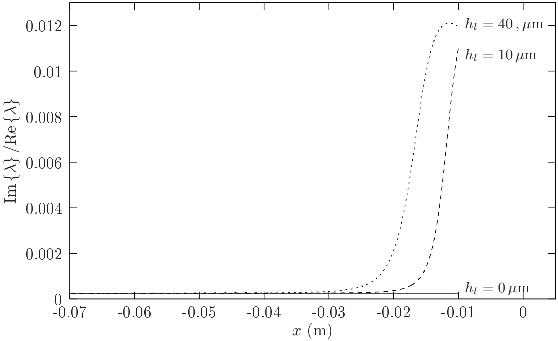

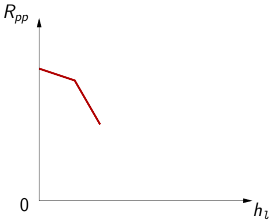

Model: Optimisation rules

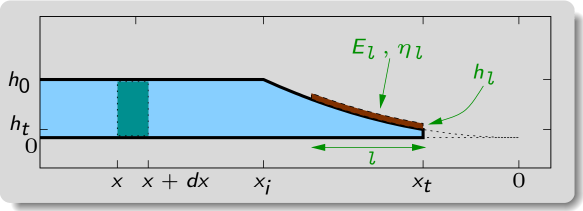

Parameters of the damping layer:

- E_l : Young's modulus
- η_l : loss factor
- l : length
- h_l : thickness

Loss factor of the compound beam

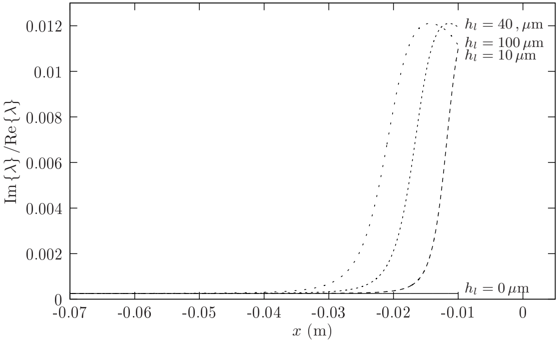

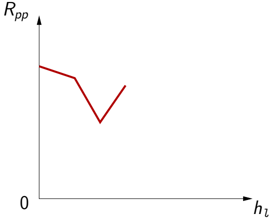

Model: Optimisation rules

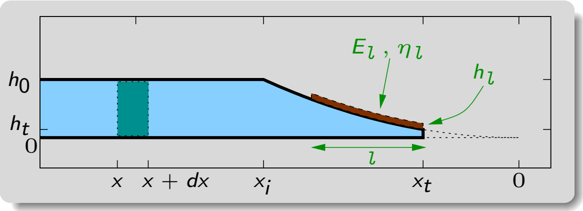

Parameters of the damping layer:

- E_l : Young's modulus
- η_l : loss factor
- l : length
- h_l : thickness

Loss factor of the compound beam

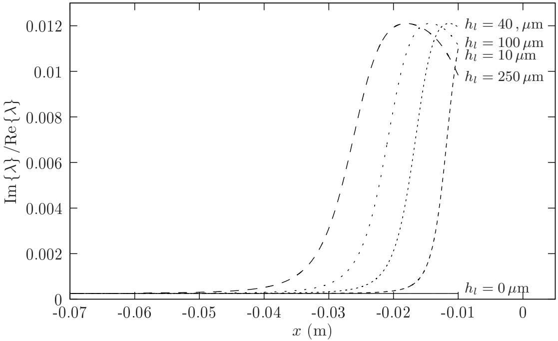

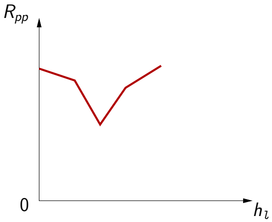

Model: Optimisation rules

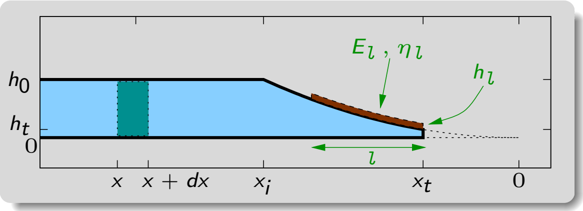

Parameters of the damping layer:

- E_l : Young's modulus
- η_l : loss factor
- l : length
- h_l : thickness

Loss factor of the compound beam

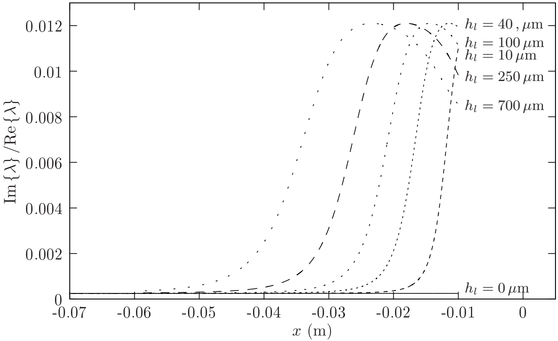

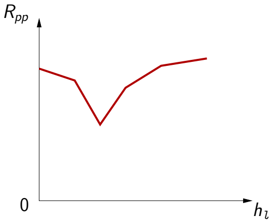

Model: Optimisation rules

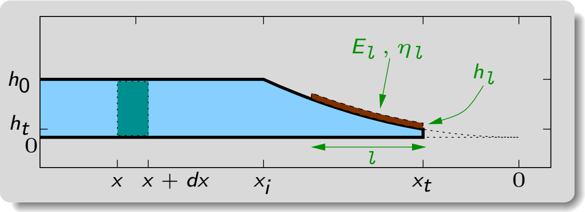

Parameters of the damping layer:

- E_l : Young's modulus
- η_l : loss factor
- l : length
- h_l : thickness

Parametric study

"Rules" for the design of acoustic black hole plates:

- **Truncation distance** x_t of the profile: **as short as possible**
- **Young's modulus** E_l of the damping layer: **as low as possible**
- **Loss factor** η_l of the damping layer: **as high as possible**
- **Length** l of the damping layer: intermediate value
- **Thickness** h_l of the damping layer: intermediate value

Model: Simulated input mobilities

Simulations with the optimised parameters
in a realistic situation

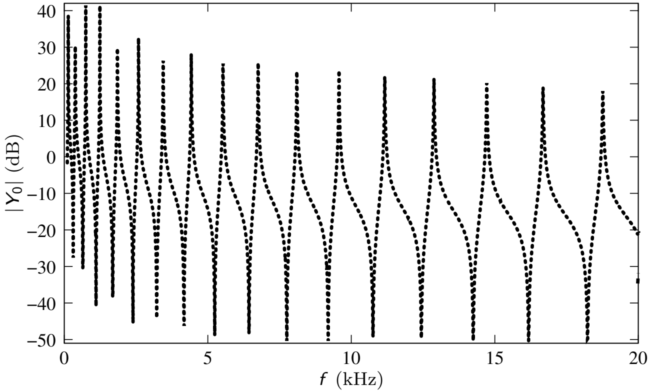

- Uncovered uniform beam
- Totally covered uniform beam
- Black hole beam
  Small amount of covering material

-20 dB

Model: Simulated input mobilities

Simulations with the optimised parameters
in a realistic situation

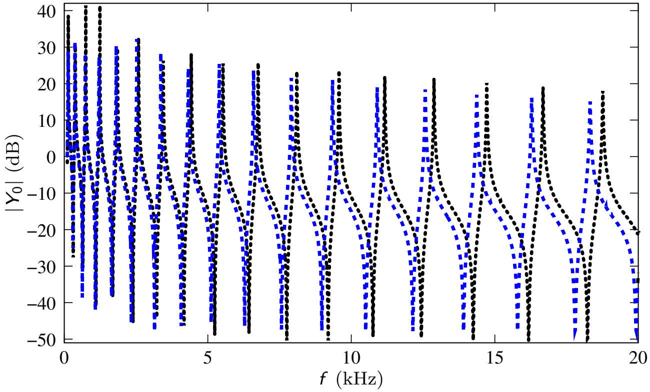

- Uncovered uniform beam
- Totally covered uniform beam
- Black hole beam
  Small amount of covering material

-20 dB

Model: Simulated input mobilities

Simulations with the optimised parameters
in a realistic situation

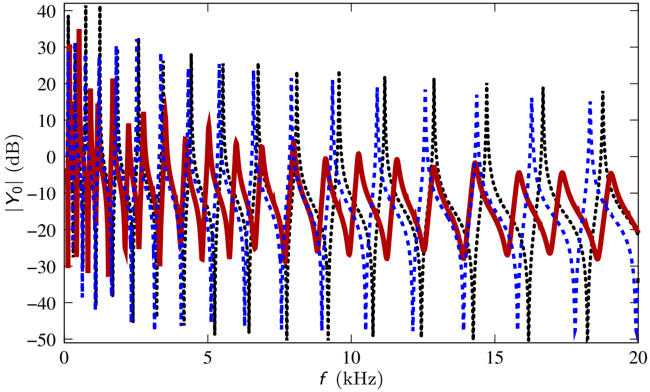

- Uncovered uniform beam
- Totally covered uniform beam
- Black hole beam
  Small amount of covering material

-20 dB

1. Model of the flexural vibrations of polygonal plates by the image source method
   - Introduction
   - Generalisation to arbitrary convex polygonal geometry
   - General boundary conditions
   - Polygonal plates
   - Plate assemblies

2. Acoustic black hole effect for vibration damping in plates and beams
   - Principle
   - Model
   - Experiments
   - Black-hole effect by a thermal gradient

Experiments: Manufactured plates

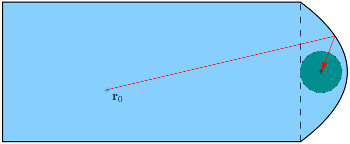

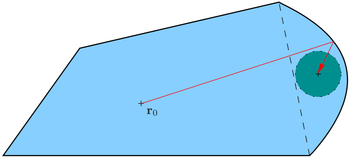

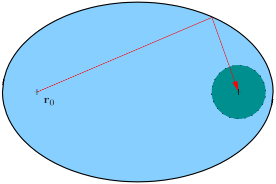

Plates manufactured at
IUT Université du Maine, Le Mans
by S. Renard, A. Aragot, S. Collin

Wave "trap"

- Focusing ellipse or parabola
- Black hole thickness profile of circular symmetry

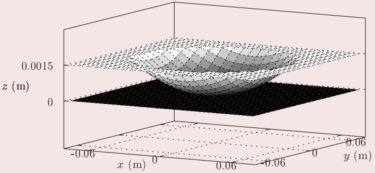

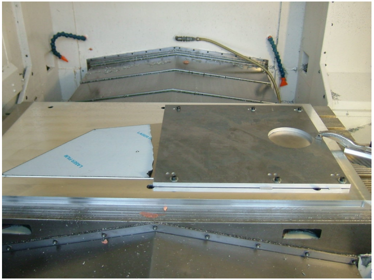

Experiments: Manufactured plates

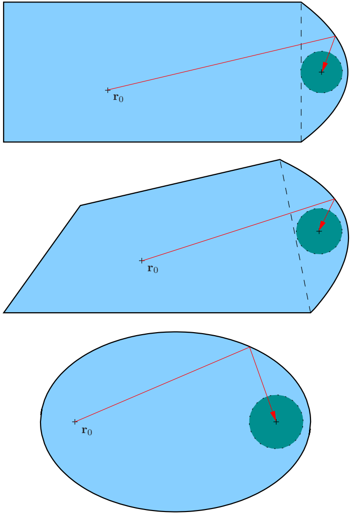

Plates manufactured at
IUT Université du Maine, Le Mans
by S. Renard, A. Aragot, S. Collin

Wave "trap"

- Focusing ellipse or parabola
- Black hole thickness profile of circular symmetry

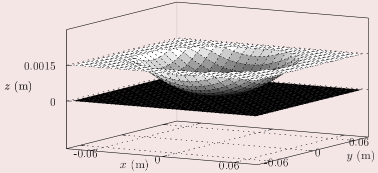

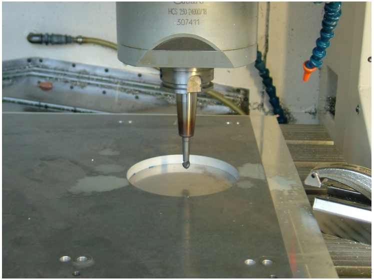

Experiments: Manufactured plates

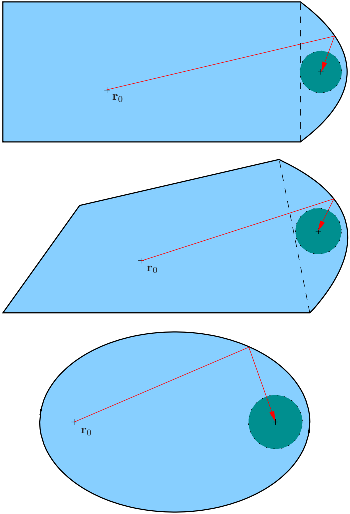

Plates manufactured at
IUT Université du Maine, Le Mans
by S. Renard, A. Aragot, S. Collin

Wave "trap"

- Focusing ellipse or parabola
- Black hole thickness profile of circular symmetry

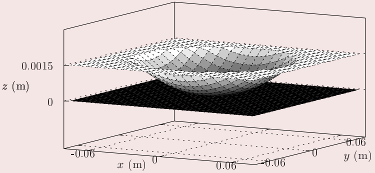

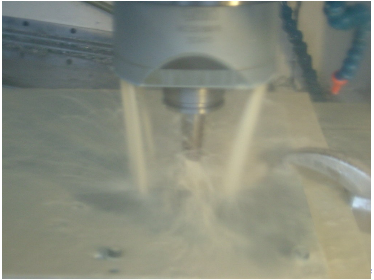

Experiments: Manufactured plates

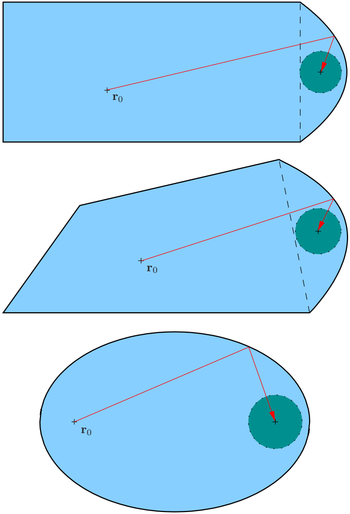

Plates manufactured at
IUT Université du Maine, Le Mans
by S. Renard, A. Aragot, S. Collin

Wave "trap"

- Focusing ellipse or parabola
- Black hole thickness profile of circular symmetry

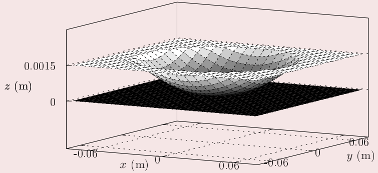

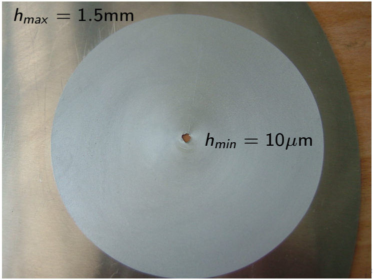

Experiments: Focusing and damping

Mobility $(m \cdot s^{-1} \cdot N^{-1})$

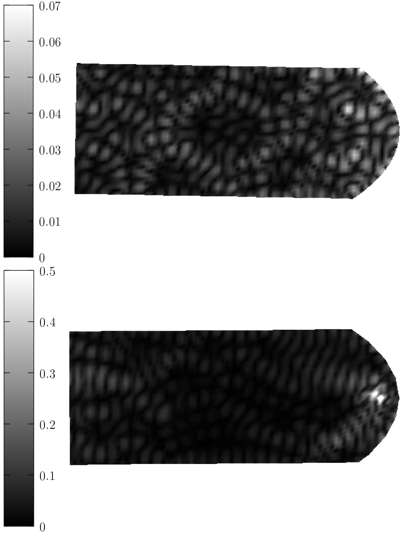

Experiments: Focusing and damping

Mobility ($m \cdot s^{-1} \cdot N^{-1}$)

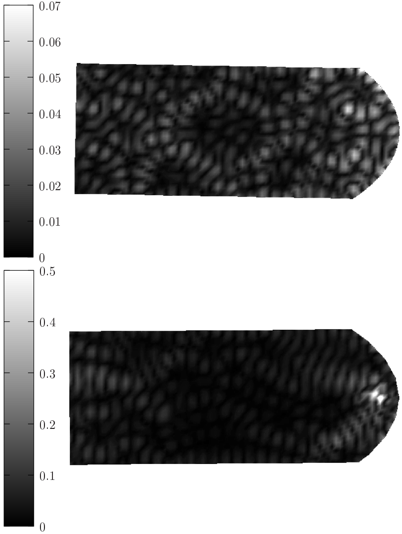

Input mobility (dB)

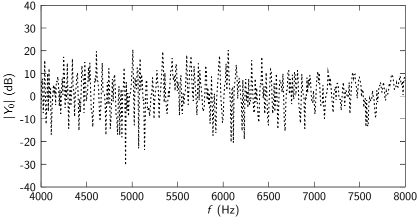

Without black hole thickness profile

Experiments: Focusing and damping

Mobility (m·s^{-1}·N^{-1})

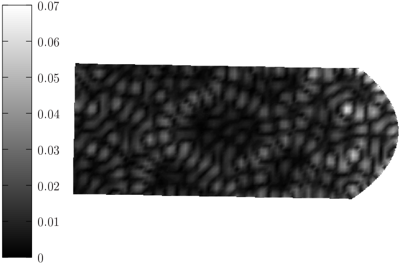

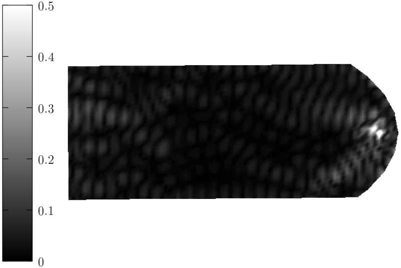

Input mobility (dB)

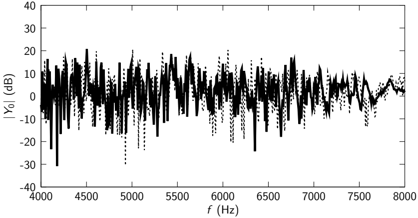

With black hole thickness profile

Experiments: Focusing and damping

Mobility ($m \cdot s^{-1} \cdot N^{-1}$)

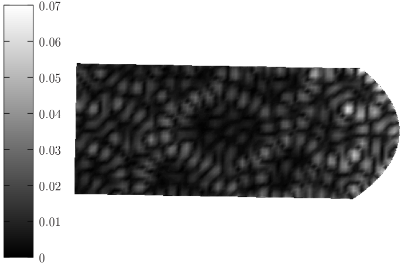

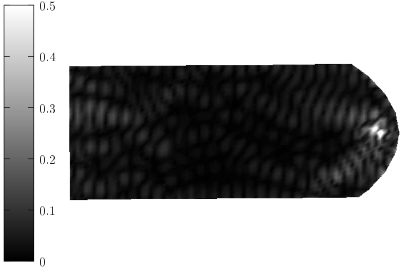

Input mobility (dB)

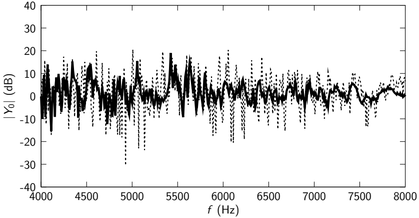

With black hole thickness profile and thin absorbing film

-10 dB

Experiments: Focusing and damping

Mobility (m·s^{-1}·N^{-1})

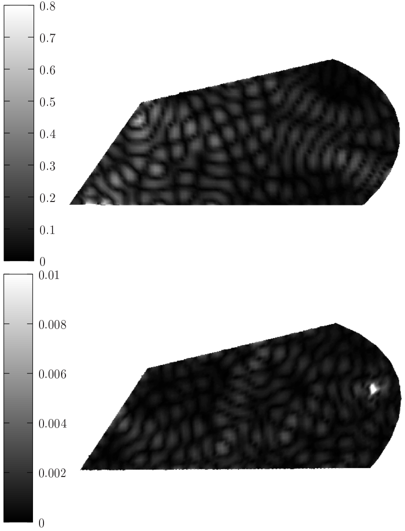

Experiments: Focusing and damping

Mobility (m·s^{-1}·N^{-1})

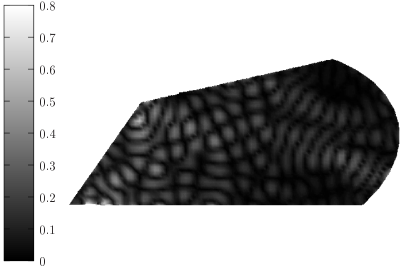

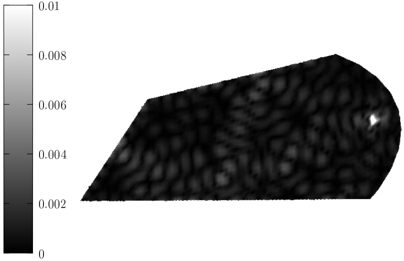

Input mobility (dB)

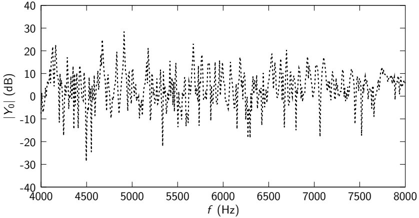

Without black hole thickness profile

Experiments: Focusing and damping

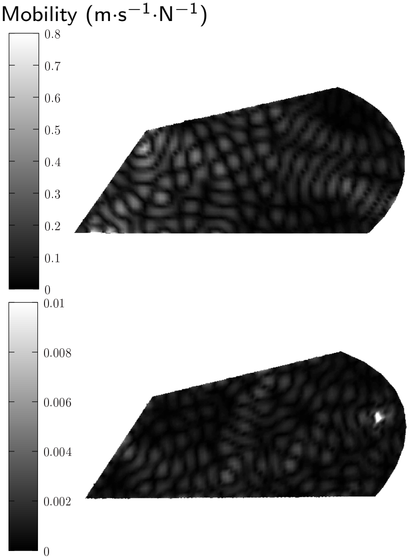

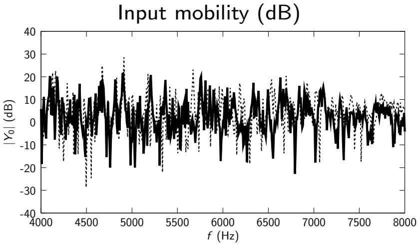

With black hole thickness profile

Experiments: Focusing and damping

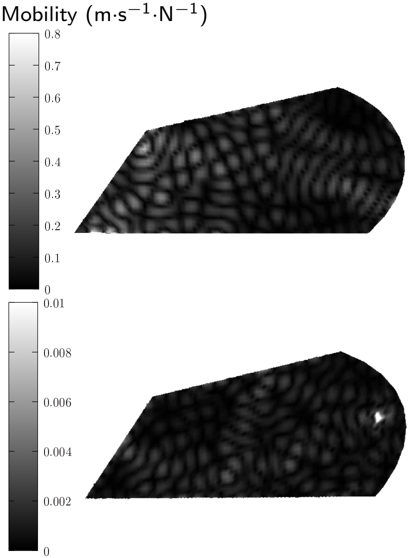

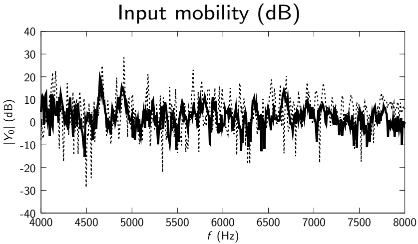

With black hole thickness profile and thin absorbing film

-10 dB

Experiments: Focusing and damping

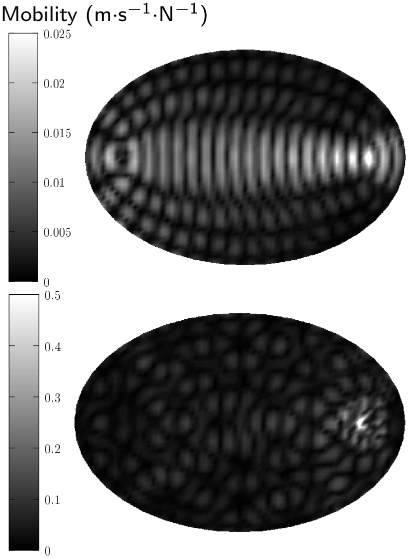

Experiments: Focusing and damping

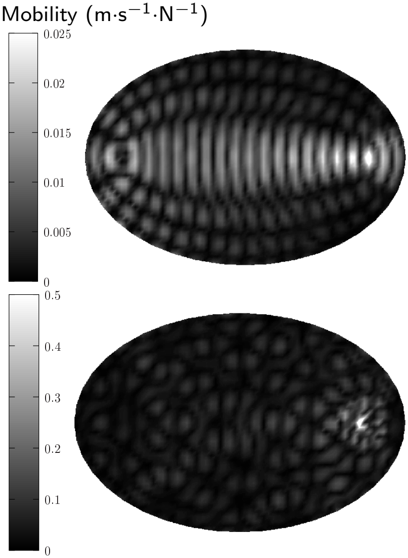

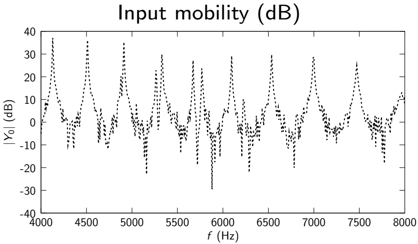

Without black hole thickness profile

Experiments: Focusing and damping

Mobility (m·s^{-1}·N^{-1})

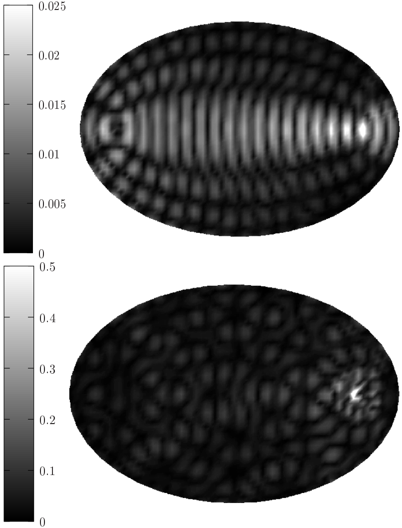

Input mobility (dB)

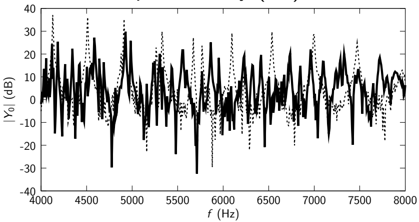

With black hole thickness profile

Experiments: Focusing and damping

Mobility (m·s^{-1}·N^{-1})

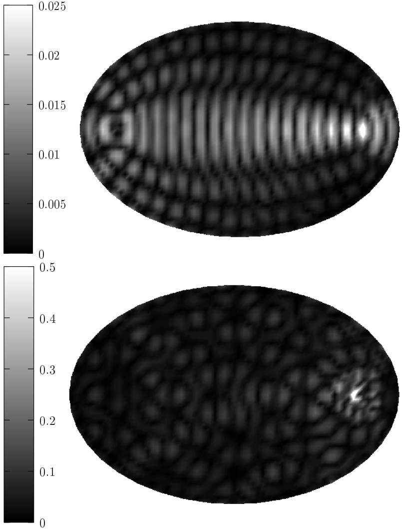

Input mobility (dB)

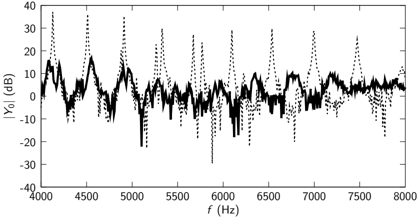

With black hole thickness profile and thin absorbing film

Experiments: Focusing and damping

Mobility ($m \cdot s^{-1} \cdot N^{-1}$)

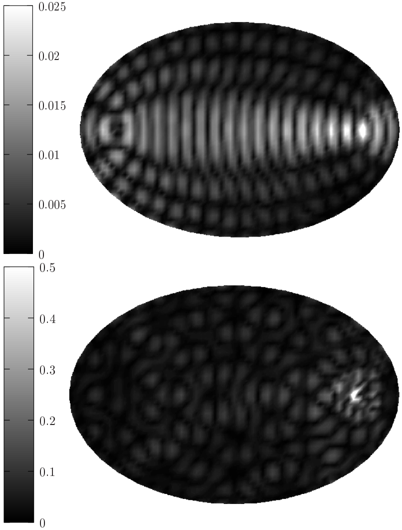

Input mobility (dB)

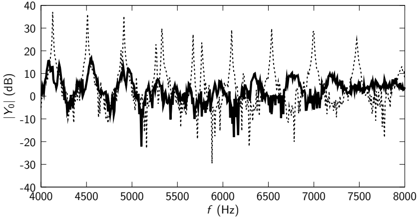

With black hole thickness profile and thin absorbing film

Up to 20 dB of vibration level reduction

(similar to the theoretical results for beams)

Black-hole effect by a thermal gradient: Principle

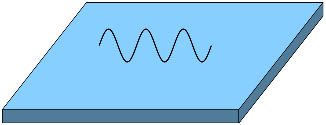

Uniform temperature

$$c_\varphi = \left(\frac{E\omega^2 h^2}{12\rho\left(1-\nu^2\right)} \right)^{1/4}$$

Black-hole effect by a thermal gradient: Principle

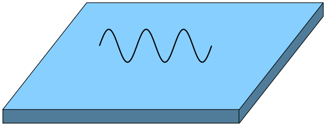

Uniform temperature

$$c_\varphi = \left(\frac{E\omega^2 h^2}{12\rho\,(1-\nu^2)} \right)^{1/4}$$

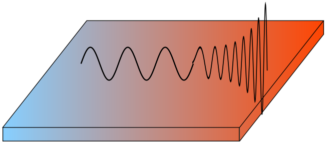

Varying temperature

$$c_\varphi(x) = \left(\frac{E(x)\omega^2 h^2}{12\rho\,(1-\nu^2)} \right)^{1/4}$$

Black-hole effect by a thermal gradient: Principle

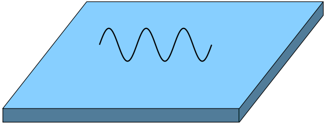

Uniform temperature

$$c_\varphi = \left(\frac{E \omega^2 h^2}{12\rho\,(1-\nu^2)} \right)^{1/4}$$

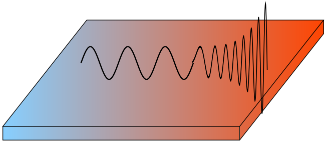

Varying temperature

$$c_\varphi(x) = \left(\frac{E(x) \omega^2 h^2}{12\rho\,(1-\nu^2)} \right)^{1/4}$$

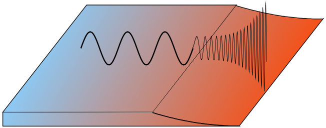

Varying temperature and thickness

$$c_\varphi(x) = \left(\frac{E(x) \omega^2 h(x)^2}{12\rho\,(1-\nu^2)} \right)^{1/4}$$

Black-hole effect by a thermal gradient: Material properties

Shape-memory polymer (Veriflex®, CRG Ind.)

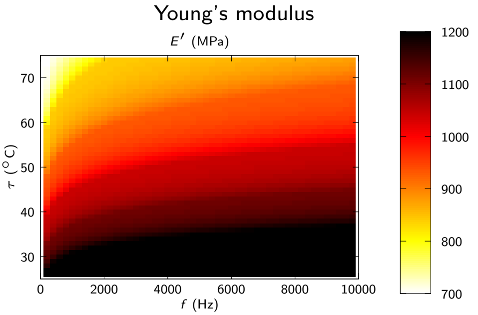

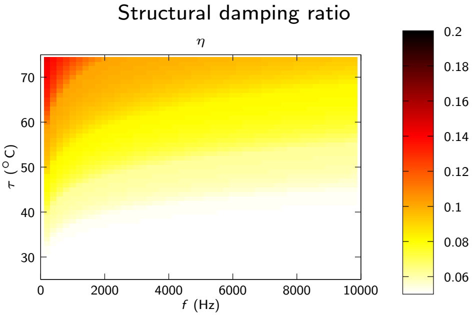

(Measurements done within the Williams-Landel-Ferry (WLF) approximation, by E. Foltête et al., FEMTO-ST)

Black-hole effect by a thermal gradient: Experimental setup

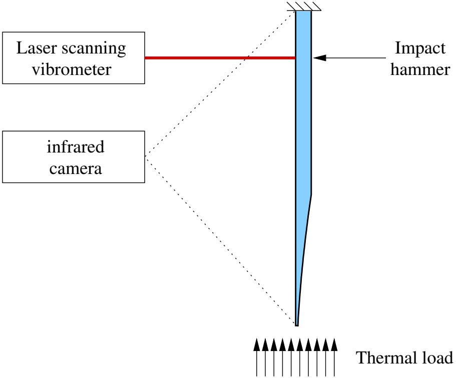

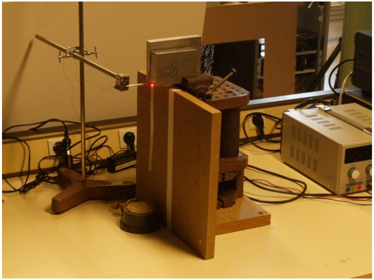

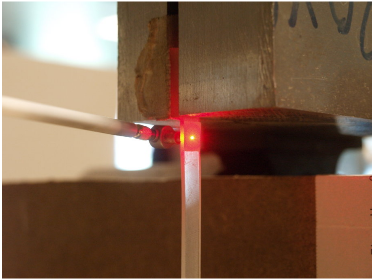

Simultaneous measurement of
input mobility and **temperature**

Black-hole effect by a thermal gradient: Measurements

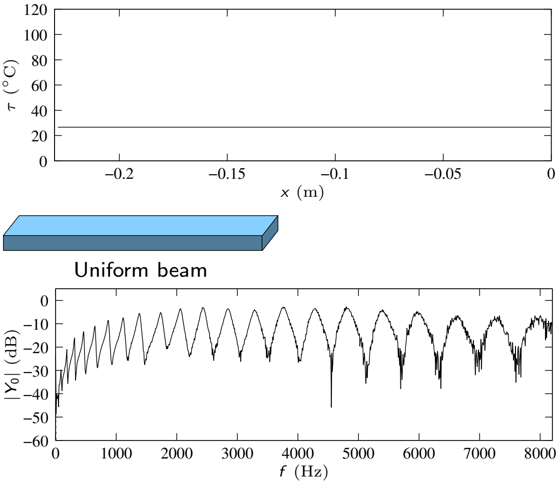

Black-hole effect by a thermal gradient: Measurements

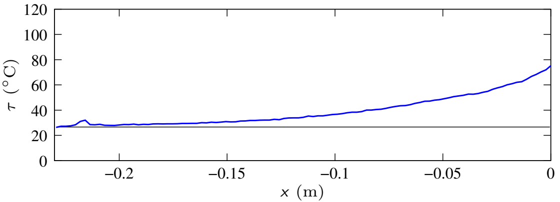

Uniform beam

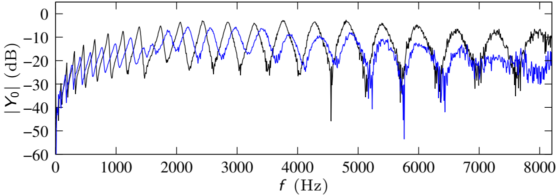

Black-hole effect by a thermal gradient: Measurements

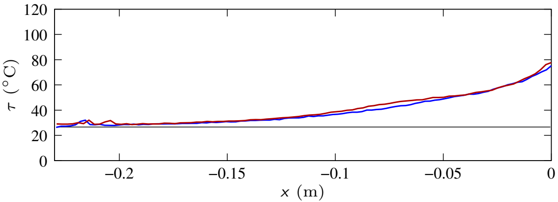

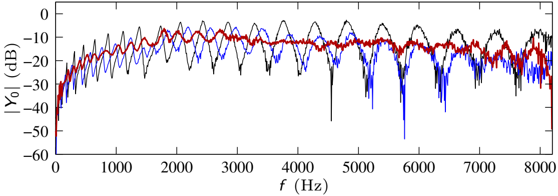

The combined geometrical and thermal effects reduce the resonant behaviour of the structure.

Conclusion: Image source method

The developed method is applicable to...

- Polygonal plates arbitrary convex polygonal shape, arbitrary linear boundary conditions
- Plate assemblies
- The measurement of material properties of damped panels

Summary of the approximations

In the general case:

- **Diffraction** by the plate corners is ignored
- **Evanescent waves** are ignored from the 2nd reflection and transmission
- The image source series has to be **truncated**

Results

- Closed form of the Green's function for 4 particular plate shapes
- Good accuracy outside the nearfield of edges
- Convergence with **modal overlap** (frequency or damping)
- Precision control with the **number of sources**

Cuenca, Gautier, Simon. *J. Sound. Vib. 322* (2009)
Cuenca, Gautier, Simon. Submitted to J. Sound. Vib. (September 2009)

Conclusion: Image source method

The developed method is applicable to...

- **Polygonal plates** arbitrary convex polygonal shape, arbitrary linear boundary conditions
- Plate assemblies
- The measurement of material properties of damped panels

Summary of the approximations

In the general case:

- **Diffraction** by the plate corners is ignored
- **Evanescent waves** are ignored from the 2nd reflection and transmission
- The image source series has to be **truncated**

Results

- Closed form of the Green's function for 4 particular plate shapes
- Good accuracy outside the nearfield of edges
- Convergence with **modal overlap** (frequency or damping)
- Precision control with the **number of sources**

Cuenca, Gautier, Simon. *J. Sound. Vib. 322* (2009)
Cuenca, Gautier, Simon. Submitted to J. Sound. Vib. (September 2009)

Conclusion: Image source method

The developed method is applicable to...

- Polygonal plates arbitrary convex polygonal shape, arbitrary linear boundary conditions
- Plate assemblies
- The measurement of material properties of damped panels

Summary of the approximations

In the general case:

- **Diffraction** by the plate corners is ignored
- **Evanescent waves** are ignored from the 2nd reflection and transmission
- The image source series has to be **truncated**

Results

- Closed form of the Green's function for 4 particular plate shapes
- Good accuracy outside the nearfield of edges
- Convergence with **modal overlap** (frequency or damping)
- Precision control with the **number of sources**

Cuenca, Gautier, Simon. *J. Sound. Vib. 322* (2009)
Cuenca, Gautier, Simon. Submitted to J. Sound. Vib. (September 2009)

Conclusion: Acoustic black hole effect

Work done

- Model of the complete flexural wave field in inhomogeneous beams
- Optimisation of the parameters for efficient vibration damping
- Experiments on polygonal and elliptical plates
- Experiments on a shape-memory polymer

Results

- Simulated and measured responses show up to 20 dB of level reduction
- Efficient wave focusing towards a black hole pit improves the effect
- Geometrical and thermal effects can be combined for improving the effect

Georgiev, Cuenca, Gautier, Simon, Krylov. Submitted to J. Acoust. Soc. Am. (July 2009)
Georgiev, Cuenca, Gautier, Simon. (In preparation)

Conclusion: Acoustic black hole effect

Work done

- Model of the complete flexural wave field in inhomogeneous beams
- Optimisation of the parameters for efficient vibration damping
- Experiments on polygonal and elliptical plates
- Experiments on a shape-memory polymer

Results

- Simulated and measured responses show up to 20 dB of level reduction
- Efficient wave focusing towards a black hole pit improves the effect
- Geometrical and thermal effects can be combined for improving the effect

---

Georgiev, Cuenca, Gautier, Simon, Krylov. Submitted to J. Acoust. Soc. Am. (July 2009)
Georgiev, Cuenca, Gautier, Simon. (In preparation)

Prospects

Image source method

- Validate the image source approach for different junctions (internal support, stiffener, . . .)
- Non-planar assemblies: Include in-plane motion in the model
- **Open questions:**
  - How to include diffraction effects? (Useful for concave plates)
  - How to include all evanescent terms?

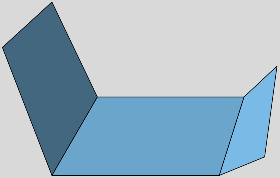

Acoustic black hole effect

- Other **focusing possibilities**: parabolic stiffener reflectors
- Application to satellite reflector vibration damping in colaboration with Thales Alenia Space $\Rightarrow$ prevent damage during satellite launch

Prospects

Image source method

- Validate the image source approach for different junctions (internal support, stiffener, . . .)
- Non-planar assemblies: Include in-plane motion in the model
- **Open questions:**
  - How to include diffraction effects? (Useful for concave plates)
  - How to include all evanescent terms?

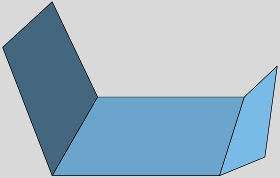

Acoustic black hole effect

- Other **focusing possibilities**: parabolic stiffener reflectors
- Application to **satellite reflector vibration damping**
  in colaboration with Thales Alenia Space
  $\Rightarrow$ prevent damage during satellite launch

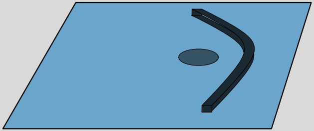

Prospects

Image source method

- Validate the image source approach for different junctions (internal support, stiffener, . . .)
- Non-planar assemblies: Include in-plane motion in the model
- **Open questions:**
  - How to include diffraction effects? (Useful for concave plates)
  - How to include all evanescent terms?

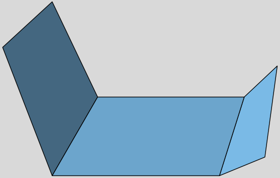

Acoustic black hole effect

- Other **focusing possibilities**:
  parabolic stiffener reflectors
- Application to **satellite reflector vibration damping**
  in colaboration with Thales Alenia Space
  $\Rightarrow$ prevent damage during satellite launch

Prospects

Image source method

- Validate the image source approach for different junctions (internal support, stiffener, . . .)
- Non-planar assemblies: Include in-plane motion in the model
- **Open questions:**
  - How to include diffraction effects? (Useful for concave plates)
  - How to include all evanescent terms?

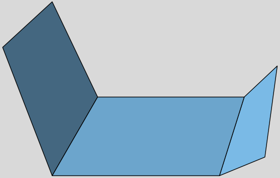

Acoustic black hole effect

- Other **focusing possibilities**:
  parabolic stiffener reflectors
- Application to **satellite reflector vibration damping**
  in colaboration with Thales Alenia Space
  $\Rightarrow$ prevent damage during satellite launch

Special thanks to

François Gautier, Laurent Simon, Vasil Georgiev, Miguel Molerón, Hervé Mézière

Stanislas Renard, Alain Aragot, Serge Collin, Yves Carbonnel (IUT Le Mans)

Sylvain Germès, Christophe Chaut, Jean-Luc Vojtovicki (Henkel Adhesive Technologies)

Victor Krylov, Emmanuel Foltête, Jan Klesa, Vincent Martin, Charles Pézerat, Laurent Maxit

Yves Aurégan, Jean-Michel Génevaux, Rachid El Guerjouma, Adrien Pelat, Anne Degroot, Stéphane Griffiths, Benoît Mérit, Tony Valier-Brasier, Frédéric Ablitzer, Ygaäl Renou, Guillaume Nief, Jean-Loïc Le Carrou, Marcos Pinho, Mathias Rémy, Antonin Novák, Olivier Doutres, Axis Kolorbarov, Mourad Bentahar, Simon Félix, Bertrand Lihoreau, Bruno Brouard, Annie Versaire, Olivier Dazel, Catherine Potel, Michel Bruneau, Christophe Ayrault, Nicolas Dauchez, Vincent Tournat, Olivier Richoux, Jean-Pierre Dalmont, Joël Gilbert, Bernard Castagnède, Claude Depollier, . . .

Wave models for the flexural vibrations of thin plates

—

Image source method for polygonal plates
&
Vibration damping using the acoustic black hole effect

Jacques Cuenca

supervised by Prof. **François Gautier** and Prof. **Laurent Simon**

Laboratoire d'Acoustique de l'Université du Maine – UMR CNRS 6613

Le Mans, France, 20th October 2009

Convergence with the truncation radius

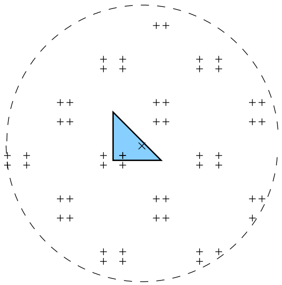

Isosceles right triangular plate
steel; thickness = 2mm; $\eta = 0.03$
L = 1m; r_c = 0.39m

$\gamma = \mathbf{6}$

$\Rightarrow r_t$ = 2.4m (52 sources)

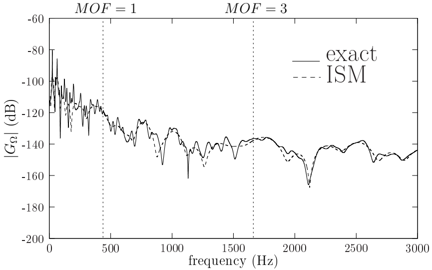

Modulus of G_Ω

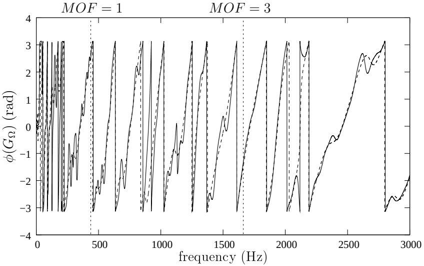

Phase of G_Ω

Convergence with the truncation radius

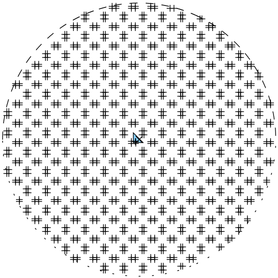

Isosceles right triangular plate
steel; thickness = 2mm; η = 0.03
L = 1m; r_c = 0.39m

$\gamma = \mathbf{30}$

$\Rightarrow r_t$ = 12m (1255 sources)

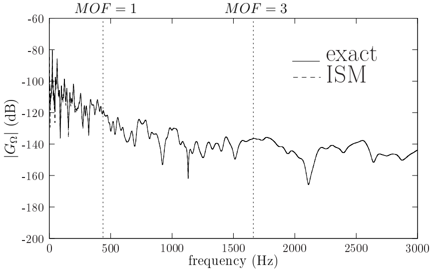

Modulus of G_Ω

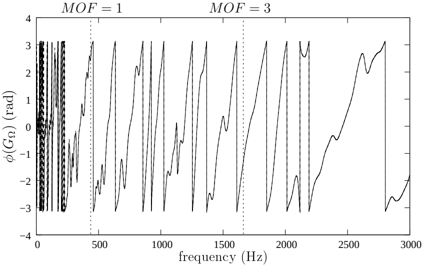

Phase of G_Ω

Convergence with the truncation radius

Mean error in HF

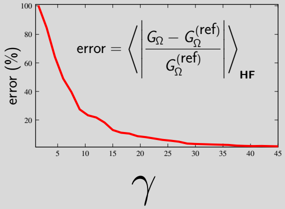

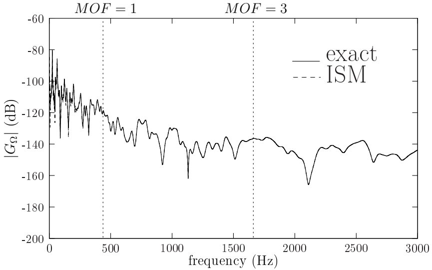

Modulus of G_Ω

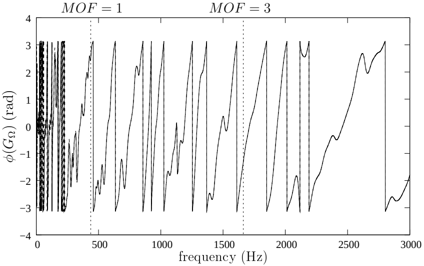

Phase of G_Ω

Variable separation in different coordinate systems

In coordinate system (ξ, μ), separated-variable wave field:

$$w(\xi,\mu) = e^{\kappa_\xi \xi} e^{\kappa_\mu \mu}, \quad \kappa_\xi \in \mathbb{I} \text{ or } \mathbb{R}, \quad \kappa_\mu \in \mathbb{I} \text{ or } \mathbb{R}$$

$$\text{Coordinate change} \quad \begin{cases} \xi = x\cos(\alpha) + y\sin(\alpha) \\ \mu = -x\sin(\alpha) + y\cos(\alpha) \end{cases}$$

In coordinate system (x, y):

$$\begin{aligned} w(x,y) &= e^{(\kappa_\xi \cos(\alpha) - \kappa_\mu \sin(\alpha))x} e^{(\kappa_\xi \sin(\alpha) + \kappa_\mu \cos(\alpha))y} \\ &= e^{\kappa_x x} e^{\kappa_y y} \end{aligned}$$

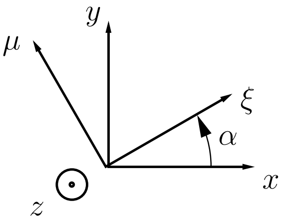

If
$\kappa_\xi \in \mathbb{I}$ and $\kappa_\mu \in \mathbb{R}$
then
~~$\kappa_x \in \mathbb{I}$ and $\kappa_y \in \mathbb{R}$~~

and

If
$\kappa_\xi \in \mathbb{R}$ and $\kappa_\mu \in \mathbb{I}$
then
~~$\kappa_x \in \mathbb{R}$ and $\kappa_y \in \mathbb{I}$~~

A wave field that is propagating in one direction of space and attenuating in another **cannot be written in a separated-variable form in two different coordinate systems** in the general case.

Model of boundary conditions: State vector formalism

Infinite plate

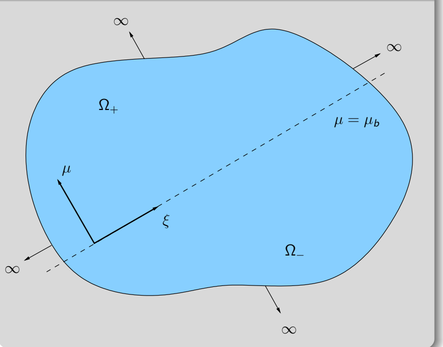

State vector:

$$\mathbf{W}(\xi,\mu) = \begin{bmatrix} w(\xi,\mu) \\ \theta_\mu(\xi,\mu) \\ M_\mu(\xi,\mu) \\ V_\mu(\xi,\mu) \end{bmatrix} = \mathbf{W}(k_\xi,\mu)e^{jk_\xi \xi}$$

State equation:

$$\frac{\partial \mathbf{W}}{\partial \mu} = \mathbf{HW}$$

In the eigenspace of matrix **H**:

$$\mathbf{HE} = \mathbf{\Lambda E} \qquad \begin{cases} (\mathbf{E}\text{: eigenvectors}) \\ (\mathbf{\Lambda}\text{: eigenvalues}) \end{cases}$$

$$\Rightarrow \mathbf{W} = \mathbf{EV} \qquad \text{where } \mathbf{V} = \begin{bmatrix} \mathbf{V}_- \\ \mathbf{V}_+ \end{bmatrix}$$

- Boundary conditions: requirements on **W**
- Reflection and transmission matrices of discontinuities: link between $\mathbf{V}_-$ and $\mathbf{V}_+$

Model of boundary conditions: Reflection matrix of an edge

Semi-infinite plate

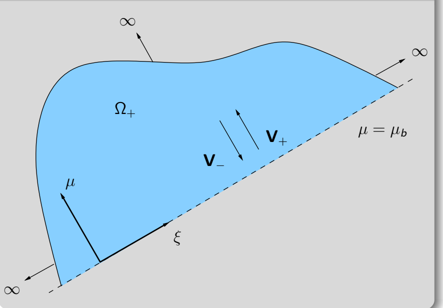

Boundary conditions: 2 equations:

$$\begin{bmatrix} \bullet & \bullet & \bullet & \bullet \\ \bullet & \bullet & \bullet & \bullet \end{bmatrix} \begin{bmatrix} w(\xi,\mu_b) \\ \theta_\mu(\xi,\mu_b) \\ M_\mu(\xi,\mu_b) \\ V_\mu(\xi,\mu_b) \end{bmatrix} = \mathbf{0}$$

$$\Updownarrow$$

$$\mathbf{BW} = \mathbf{0}$$

Basis change:

$$\mathbf{W} = \mathbf{EV} = \begin{bmatrix} \mathbf{E}_- & \mathbf{E}_+ \end{bmatrix} \begin{bmatrix} \mathbf{V}_- \\ \mathbf{V}_+ \end{bmatrix}$$

$$\mathbf{V}_+ = \mathbf{R}\mathbf{V}_-$$

$$\mathbf{R} = \begin{bmatrix} R_{pp} & R_{ep} \\ R_{pe} & R_{ee} \end{bmatrix}$$

(p: propagating; e: evanescent)

Model of boundary conditions: Scattering matrix of a junction

Infinite plate $\Omega = \Omega_1 \cup \Omega_2$

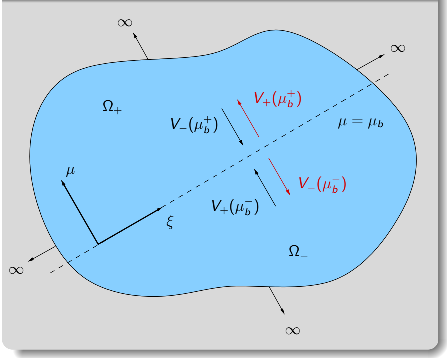

Boundary conditions: 4 equations:

$$\begin{bmatrix} \bullet & \bullet & \bullet & \bullet & \bullet & \bullet & \bullet & \bullet \\ \bullet & \bullet & \bullet & \bullet & \bullet & \bullet & \bullet & \bullet \\ \bullet & \bullet & \bullet & \bullet & \bullet & \bullet & \bullet & \bullet \\ \bullet & \bullet & \bullet & \bullet & \bullet & \bullet & \bullet & \bullet \end{bmatrix} \begin{bmatrix} \begin{bmatrix} w(\mu_b^-) \\ \theta_\mu(\mu_b^-) \\ M_\mu(\mu_b^-) \\ V_\mu(\mu_b^-) \end{bmatrix} \\ \begin{bmatrix} w(\mu_b^+) \\ \theta_\mu(\mu_b^+) \\ M_\mu(\mu_b^+) \\ V_\mu(\mu_b^+) \end{bmatrix} \end{bmatrix} = \mathbf{0}$$

$$\mathbf{J} \begin{bmatrix} \mathbf{W}(\mu_b^-) \\ \mathbf{W}(\mu_b^+) \end{bmatrix} = \mathbf{0}$$

Ingoing and outgoing waves at the junction:

$$\mathbf{V}^{\text{in}}(\mu_b) = \begin{bmatrix} V_+(\mu_b^-) \\ V_-(\mu_b^+) \end{bmatrix}, \quad \mathbf{V}^{\text{out}}(\mu_b) = \begin{bmatrix} V_+(\mu_b^+) \\ V_-(\mu_b^-) \end{bmatrix}$$

$$\mathbf{V}^{\text{out}} = \mathbf{S}\mathbf{V}^{\text{in}}$$

$$\mathbf{S} = \begin{bmatrix} \mathbf{T}_{-+} & \mathbf{R}_{++} \\ \mathbf{R}_{--} & \mathbf{T}_{+-} \end{bmatrix}, \quad \text{where} \quad \mathbf{R} = \begin{bmatrix} R_{pp} & R_{ep} \\ R_{pe} & R_{ee} \end{bmatrix} \text{ and } \mathbf{T} = \begin{bmatrix} T_{pp} & T_{ep} \\ T_{pe} & T_{ee} \end{bmatrix}$$

(p: propagating; e: evanescent)

Measurement of the flexural rigidity of damped panels

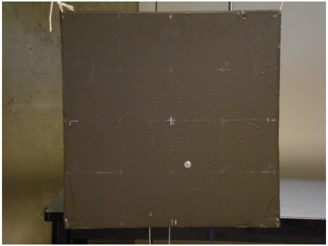

Car floor panel sample
(3 mm steel, 2 mm damping material)

$$D = \frac{E_0(1 - j\eta)h^3}{12\,(1 - \nu^2)}$$

How to measure the Young's modulus and structural damping ratio of highly damped panels?

Measurement of the flexural rigidity of damped panels

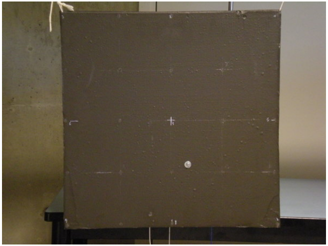

Car floor panel sample
(3 mm steel, 2 mm damping material)

$$D = \frac{E_0(1 - j\eta)h^3}{12\,(1-\nu^2)}$$

How to measure the Young's modulus and structural damping ratio of highly damped panels?

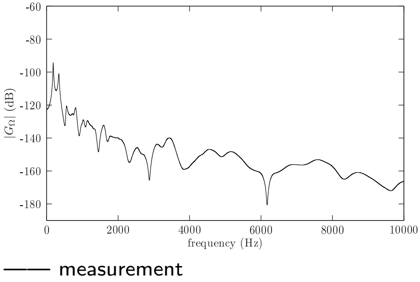

Measurement of the flexural rigidity of damped panels

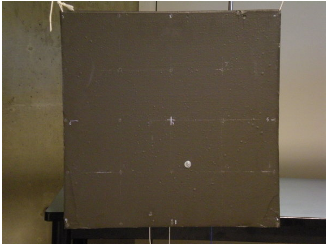

Car floor panel sample
(3 mm steel, 2 mm damping material)

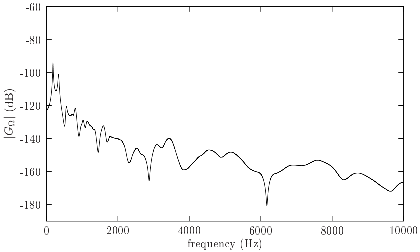

—— measurement

$$D = \frac{E_0(1 - j\eta)h^3}{12\,(1-\nu^2)}$$

How to measure the Young's modulus and structural damping ratio of highly damped panels?

Common measurement technique:
Oberst method
(restricted to relatively high Q)

Measurement of the flexural rigidity of damped panels

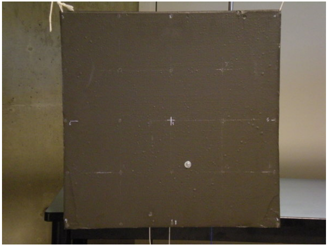

Car floor panel sample
(3 mm steel, 2 mm damping material)

$$D = \frac{E_0(1 - j\eta)h^3}{12\,(1 - \nu^2)}$$

How to measure the Young's modulus and structural damping ratio of highly damped panels?

Alternative technique: **image source formalism** as an inverse method (suitable for low Q)

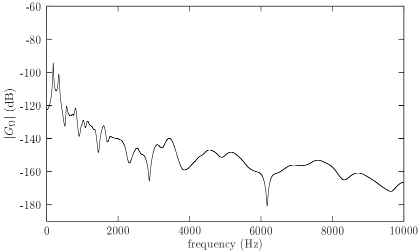

Measurement of the flexural rigidity of damped panels

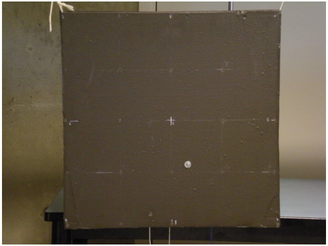

Car floor panel sample
(3 mm steel, 2 mm damping material)

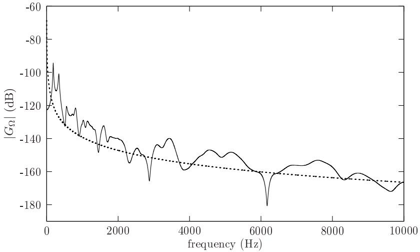

—— measurement ---- simulation

- mean line of the response: direct field **(original source)**
- variance of the response: interferences between successive reflections **(image sources)**

Measurement of the flexural rigidity of damped panels

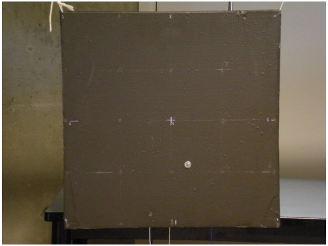

Car floor panel sample
(3 mm steel, 2 mm damping material)

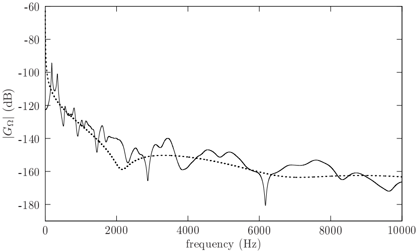

—— measurement ---- simulation

- mean line of the response: direct field **(original source)**
- variance of the response: interferences between successive reflections **(image sources)**

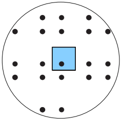

Measurement of the flexural rigidity of damped panels

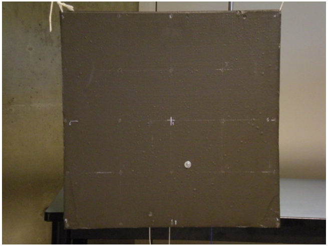

Car floor panel sample
(3 mm steel, 2 mm damping material)

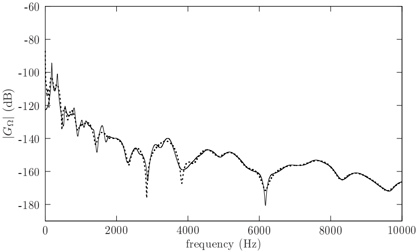

—— measurement ---- simulation

- mean line of the response: direct field **(original source)**
- variance of the response: interferences between successive reflections **(image sources)**

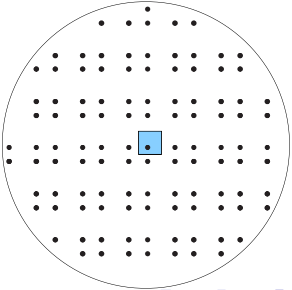

Measurement of the flexural rigidity of damped panels

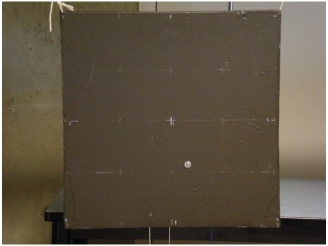

Car floor panel sample
(3 mm steel, 2 mm damping material)

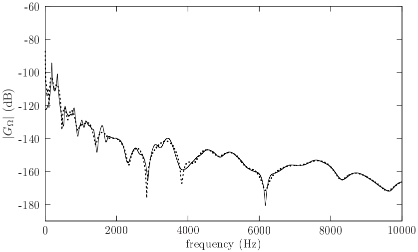

—— measurement ---- simulation

- mean line of the response: direct field **(original source)** Stiffness
- variance of the response: interferences between successive reflections **(image sources)** Damping

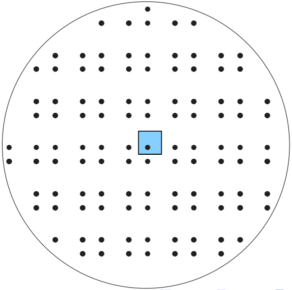

Measurement of the flexural rigidity of damped panels: Method

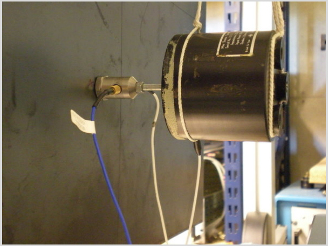

1. Measure the **input mobility**
2. Extract the **mean line** of the response per 1/3-octave bands $\Rightarrow |D|$

$$|Y_\infty(\mathbf{r}_0, \mathbf{r}_0; k_f)| = |j\omega \lim_{\mathbf{r}\longrightarrow\mathbf{r}_0} G_\infty(\mathbf{r}, \mathbf{r}_0; k_f)| = \frac{1}{8\sqrt{\rho h}|D^{1/2}|}$$

$$\left(|D| = \frac{E_0\sqrt{1+\eta^2}h^3}{12(1-\nu^2)}\right) \Rightarrow \infty \text{ possible combinations of } (E_0, \eta)$$

3. Best fit of **image source simulation** $\Rightarrow (E_0, \eta)$ for each 1/3 octave band

Measurement of the flexural rigidity of damped panels: Method

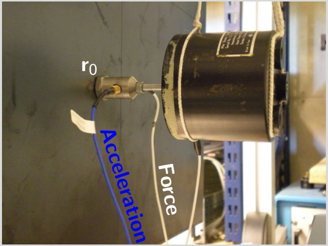

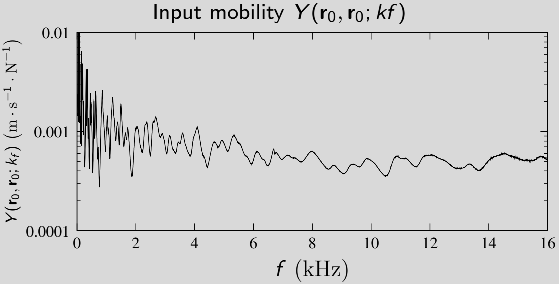

1. Measure the **input mobility**
2. Extract the **mean line** of the response per 1/3-octave bands $\Rightarrow |D|$

$$|Y_\infty(\mathbf{r}_0, \mathbf{r}_0; k_f)| = |j\omega \lim_{\mathbf{r} \to \mathbf{r}_0} G_\infty(\mathbf{r}, \mathbf{r}_0; k_f)| = \frac{1}{8\sqrt{\rho h}|D^{1/2}|}$$

$$\left(|D| = \frac{E_0\sqrt{1+\eta^2}h^3}{12(1-\nu^2)}\right) \Rightarrow \infty \text{ possible combinations of } (E_0, \eta)$$

3. Best fit of **image source simulation** $\Rightarrow (E_0, \eta)$ for each 1/3 octave band

Measurement of the flexural rigidity of damped panels: Method

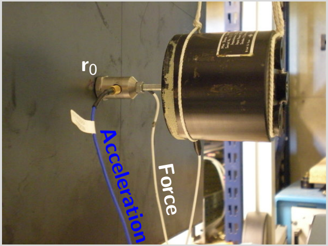

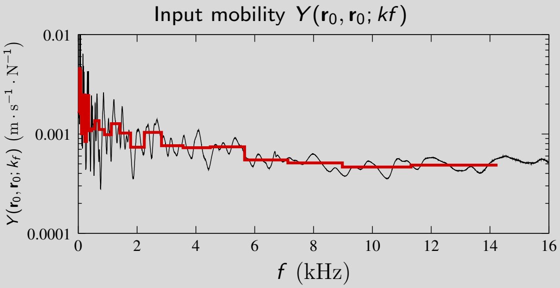

1. Measure the **input mobility**
2. Extract the **mean line** of the response per 1/3-octave bands $\Rightarrow |D|$

$$|Y_\infty(\mathbf{r}_0, \mathbf{r}_0; k_f)| = |j\omega \lim_{\mathbf{r}\to\mathbf{r}_0} G_\infty(\mathbf{r}, \mathbf{r}_0; k_f)| = \frac{1}{8\sqrt{\rho h}|D^{1/2}|}$$

$$\left(|D| = \frac{E_0\sqrt{1+\eta^2}h^3}{12(1-\nu^2)}\right) \Rightarrow \infty \text{ possible combinations of } (E_0, \eta)$$

3. Best fit of **image source simulation** $\Rightarrow (E_0, \eta)$ for each 1/3 octave band

Measurement of the flexural rigidity of damped panels: Method

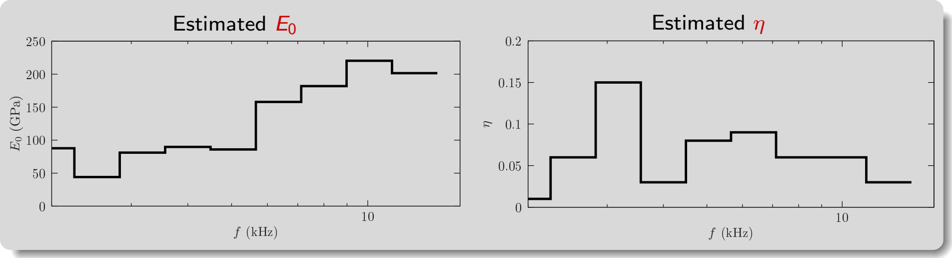

1. Measure the **input mobility**
2. Extract the **mean line** of the response per 1/3-octave bands $\Rightarrow |D|$

$$|Y_\infty(\mathbf{r}_0, \mathbf{r}_0; k_f)| = |j\omega \lim_{\mathbf{r}\to\mathbf{r}_0} G_\infty(\mathbf{r}, \mathbf{r}_0; k_f)| = \frac{1}{8\sqrt{\rho h}|D^{1/2}|}$$

$$\left(|D| = \frac{E_0\sqrt{1+\eta^2}h^3}{12(1-\nu^2)}\right) \Rightarrow \infty \text{ possible combinations of } (E_0, \eta)$$

3. Best fit of **image source simulation** $\Rightarrow (E_0, \eta)$ for each 1/3 octave band

Measurement of the flexural rigidity of damped panels: Method

Advantages of the method

- High frequency measurement method
- Applicable to convex polygonal panels
- Only **one input mobility measurement** is needed
- Free boundaries can be used

1. Measure the **input mobility**
2. Extract the **mean line** of the response per 1/3-octave bands $\Rightarrow |D|$

$$|Y_\infty(\mathbf{r}_0, \mathbf{r}_0; k_f)| = |j\omega \lim_{\mathbf{r}\longrightarrow\mathbf{r}_0} G_\infty(\mathbf{r}, \mathbf{r}_0; k_f)| = \frac{1}{8\sqrt{\rho h}|D^{1/2}|}$$

$$\left(|D| = \frac{E_0\sqrt{1+\eta^2}h^3}{12(1-\nu^2)}\right) \Rightarrow \infty \text{ possible combinations of } (E_0, \eta)$$

3. Best fit of **image source simulation** $\Rightarrow (E_0, \eta)$ for each 1/3 octave band